

# **The Role of Intervertebral Disc Cartilage Catabolites in Modic Type 1 Changes**

---

**Dissertation**

zur

**Erlangung der naturwissenschaftlichen Doktorwürde  
(Dr. sc. nat.)**

vorgelegt der

**Mathematisch-naturwissenschaftlichen Fakultät**

der

**Universität Zürich**

von

**Tamara Mengis**

von

**Rapperswil, BE**

**Promotionskommission**

Prof. Dr. Oliver Distler (Vorsitz)

PD Dr. Stefan Dudli (Leitung der Dissertation)

Prof. Dr. Christian Stockmann

PD. Dr. Sibylle Grad

**Zürich, 2024**

# Contents

List of abbreviations .....	5
Summary.....	7
Zusammenfassung .....	9
<b>Chapter 1: General Introduction .....</b>	<b>11</b>
1.1 Modic changes .....	<b>Error! Bookmark not defined.</b>
1.2 Disc-endplate-bone marrow in the context of Modic changes.....	<b>Error! Bookmark not defined.</b>
1.3 Relevance of danger associated molecular patterns and TLRs in Modic changes	<b>Error! Bookmark not defined.</b>
1.4 References chapter 1 .....	<b>Error! Bookmark not defined.</b>
<b>Chapter 2: Aims and Relevance.....</b>	<b>33</b>
<b>Chapter 3: Bone marrow stromal cells in Modic type 1 changes promote neurite outgrowth.....</b>	<b>37</b>
3.1 Abstract.....	38
3.2 Introduction.....	38
3.3 Materials and Methods.....	39
3.4 Results.....	43
3.5 Discussion.....	47
3.6 Conflict of Interest .....	50
3.7 Author Contributions .....	50
3.8 Funding .....	50
3.9 Acknowledgments.....	50
3.10 Supplementary Material.....	50
3.11 Data Availability Statement .....	52
3.12 References chapter 3 .....	52
<b>Chapter 4: Intervertebral disc microbiome in Modic Changes: lack of result replication underscores the need for a consensus in low-biomass microbiome analysis.....</b>	<b>55</b>
4.1 Abstract.....	56
4.2 Introduction.....	56
4.3 Methods .....	58
3.4 Results.....	61
3.5 Discussion.....	67
3.6 Ethics Statement.....	69
3.7 Author Contributions .....	69
3.8 Funding .....	69

3.9 Conflicts of Interest.....	69
3.10 Acknowledgements.....	69
3.11 References chapter 4.....	70
<b>Chapter 5: Pro-inflammatory and catabolic gene expression in cartilage endplate cells after stimulation of toll-like receptor 2 .....</b>	<b>73</b>
5.1 Abstract.....	74
5.2 Introduction.....	<b>Error! Bookmark not defined.</b>
5.3 Methods .....	74
5.4 Results.....	78
5.5 Discussion.....	78
5.6 Ethics Statement.....	84
5.7 Author Contributions .....	85
5.8 Funding .....	86
5.9 Conflicts of Interest.....	86
5.10 Acknowledgements.....	86
5.11 Supplementary .....	86
5.12 References chapter 5 .....	87
<b>Chapter 6: Elevated Abundance of HTRA1-Generated Fragments in MC1 Discs Induces Cartilage Endplate Degeneration.....</b>	<b>92</b>
6.1 Abstract.....	93
6.2 Introduction.....	94
6.3 Methods .....	95
6.4 Results.....	99
6.5 Discussion.....	108
6.6 Ethics Statement.....	112
6.7 Author Contributions .....	112
6.8 Funding .....	113
6.9 Conflicts of Interest.....	113
6.10 Acknowledgements.....	113
6.11 Supplementary .....	113
6.12 References chapter 6.....	114
<b>Chapter 7: General Discussion.....</b>	<b>117</b>
7.1 Complexity of neurite growth.....	118

7.2. Role of the disc’s microbiome .....	119
7.3 Cartilage endplate cells – important players in inflammation and degeneration .....	121
7.4 The role of the MC1 disc degradome.....	121
7.5 Conclusion .....	125
7.6 References chapter 7.....	126
Appendix .....	129
Acknowledgments.....	130
Curriculum Vitae .....	132

# List of abbreviations

ADAMTS5	A disintegrin and metalloproteinase with thrombospondin motifs 5
AF	Annulus fibrosus
ANOVA	Analysis of variance
ASV	Amplicon sequencing variants
BEP	Bony endplate
BMI	Body mass index
BMSC	Bone marrow stromal cells
BVNA	Basivertebral nerve ablation
C. Acnes	Cutibacterium Acnes
CCL2	Chemokine ligand 2
CD	Cluster of differentiation
CEP	Cartilage endplate
CEPC	Cartilage endplate cells
CIAA	Chloriodacetamid
CILP1	Cartilage intermediate layer protein 1
CLBP	Chronic low back pain
CLR	C-type lectin receptor
CNTF	Ciliary neurotrophic factor
COL1A1	Collagen alpha 1 chain
COMP	Cartilage oligomeric matrix protein
CT	Computed tomography
CXCL12	C-X-C motif chemokine ligand 12
DAMPS	Damage associated molecular pattern
DAPI	4',6-diamidino-2-phenylindole
DD	Disc degeneration
DMEM	Dulbecco's Modified Eagles Medium
DMMB	1,9-dimethylmethylene blue
ECM	Extracellular matrix
FCS	Fetal calf serum
FN	Fibronectin
FNf30	Fibronectin fragment 30 kDa
GABA	Gamma-aminobutyric acid
GAG	Glycosaminoglycan
GAPDH	Glyceraldehyde-3-phosphate dehydrogenase
GSEA	Gene set enrichment analysis
HEPES	4-(2-hydroxyethyl)-1-piperazineethanesulfonic acid
HMGB1	High mobility group box 1
HPG-ADLII	Hyperbranched polyaldehyde polymer
HPRT1	Hypoxanthine Phosphoribosyltransferase 1
HTRA1	High Temperature Requirement A serine peptidase 1
ICD-11	International Classification of Diseases 11th
IL13	Interleukin 13
IL1B	Interleukin 1 beta
IL6	Interleukin 6
IL8	Interleukin 8
IQR	Interquartile ratio

IVD	Intervertebral disc
LAMB1	Laminin Subunit Beta 1
LEPR	Leptin receptor
LPS	Lipopolysaccharide
MC	Modic changes
MC1	Modic type 1 changes
MC2	Modic type 2 changes
MC3	Modic type 3 changes
MMP1	Matrix metalloproteinase 1
MMP13	Matrix metalloproteinase 13
MMP2	Matrix metalloproteinase 2
MMP9	Matrix metalloproteinase 9
MRI	Magnetic resonance image
MWCO	Molecular weight cut off
NES	Nestin
NET	Neutrophil extracellular traps
NEUROD1	Neurogenic differentiation 1
NFkB	Nuclear factor 'kappa-light-chain-enhancer'
NGF	Neurite growth factor
NGFR	Neurite growth factor receptor
NGS	Next generation sequencing
NLR	Nod-like receptor
nonMC	Non Modic
NP	Nucleus pulposus
NT3	Neurotrophin 3
ODI	Oswestry disability index
OTU	Operational taxonomic unit
Pam2csk4	Pam2CysSerLys4
Pam3csk4	Pam3CysSerLys4
PAMP	Pathogen associated molecular pattern
PBS	Phosphate buffered saline
PCR	Polymerase chain reaction
PRR	Pattern recognition receptor
RAGE	Receptor for advanced glycation endproducts
SEMA3a	Semaphorin 3a
SORT	Sortilin
STIR	Short Tau Inversion Recovery
T1w	T1 weighted
T2w	T2 weighted
TAILS	N-Terminal Amine Isotopic Labeling of Substrates
TCEP	Tris (2-carboxyethyl)phosphine hydrochloride
TLR	Toll like receptor
TMT	Tandem mass tag
TNF-a	Tumor necrosis factor alpha
TRKA	Tyrosine kinase A
TRKB	Tyrosine kinsae B
TRKC	Tyrosine kinase C
TUBB3	Tubulin 3
VAS	Visual analog scale

# Summary

The thesis investigates the pathobiology of Modic changes (MCs), specifically focusing on Modic type 1 changes (MC1), emphasizing the complexity of the disease. Although MCs manifest as vertebral bone marrow lesions, the inflammation and degeneration observed in the neighboring intervertebral disc and cartilage endplate (CEP) are also closely linked to MCs. However, the underlying mechanisms and how the tissues crosstalk to induce MC development are unclear to this point. Yet, comprehending these pathobiological mechanisms is crucial for the development of targeted therapies, which are currently nonexistent. The thesis explores various aspects of MC1 addressing pathologic processes seen within the MC1 bone marrow, the CEP and the disc. Finally, the project's findings suggest a new disease mechanism for MC1 development initiated through MC1 specific disc degeneration.

Chapter three investigated the impact of bone marrow stromal cells (BMSC) from MC1 on neurite outgrowth, using an in-vitro co-culture system. Multiple studies have reported an elevated presence of nerve fibers in the MC1 bone marrow and endplate, a definitive connection to the underlying cause has not been established. For the first time, the dysregulated MC1 BMSCs were directly linked to increased neurite outgrowth. With this knowledge, an important treatment target has been identified, paving the way for further studies to explore how to mitigate this effect.

The fourth chapter explores the concept of a disc microbiome, particularly focusing on the MC1 and MC2 microbiomes, using metagenomic analysis. The disc microbiome challenges the conventional notion of disc sterility, necessitating clear methodological definitions for further investigation. Although our analysis confirmed the presence of a disc microbiome, the findings deviated from those of previous studies on degenerated MC discs, even after aligning the parameters of bioinformatic analysis to the previous studies. This study underscores the importance of not only standardizing bioinformatic analysis approaches but also further investigating factors that influence the bacterial composition of the disc microbiome. Differences could stem from sample preparation techniques or variations in the geographical and ethnic backgrounds of patients. Once clarified, the exploration of the disc microbiome will unlock numerous opportunities for diagnostic and treatment applications.

The fifth chapter of the thesis highlights the to this point overlooked biological role of CEP cells. The experiments were able to confirm the presence of Toll-like receptors (TLRs) on CEP cells and particularly emphasized the presence of TLR2 as it was the only TLR that was upregulated through direct stimulation. The discovery of TLRs on CEP cells is noteworthy due to their high density compared to the cells in the adjacent disc and their ability to induce inflammation and promote the production of catabolic enzymes, potentially leading to endplate degeneration. This not only enhances our understanding of CEP cells but also reveals novel treatment targets.

The sixth chapter presents the main project of the thesis, which focuses on understanding MC1 pathobiology and proposes a new mechanism for MC1 development beginning with MC1-specific disc degeneration. It is

grounded in the fact that although disc degeneration is often observed in the disc adjacent to MC1, not all degenerated discs progress to MC1. The proposed MC1-specific disc degeneration is hypothesized to generate more fragments, triggering inflammation in the adjacent endplate, causing endplate destruction. This ultimately breaches the CEP barrier between the disc and bone marrow, allowing pro-inflammatory fragments (damage associated molecular patterns (DAMPs)) and inflammatory cytokines to spill over into the bone marrow, inducing MC1. Although the study is ongoing, significant discoveries have been made. MC1 discs were found to have a higher abundance of extracellular matrix derived fragments as well a greater abundance of the protease high temperature requirement serine protease 1 (HTRA1) than degenerated nonMC discs. In a subsequent phase, the abundant cartilage intermediate layer protein 1 (CILP1) fragments were successfully replicated by exposure to HTRA1 and were demonstrated to possess pro-inflammatory properties via TLR4 signaling activation, thereby classifying them as DAMPs. A CEP explant model was used to show that TLR activation can induce CEP tissue destruction, connecting the DAMP abundance in the disc to CEP damage. However, further experiments are necessary to address the gaps within the proposed mechanism.

MC1 is a pathology associated with distinct inflammatory and pain-related processes, suggesting it could and should be treated specifically. This thesis demonstrates this and thus marks an important step towards targeted therapy for MC1.



# Zusammenfassung

Die Dissertation untersucht die Pathobiologie von Modic Changes (MCs), wobei der Fokus speziell auf Modic-Typ-1-Changes (MC1) liegt. Obwohl MCs sich als Läsionen im Wirbelknochenmark manifestieren, ist eine Entzündung und Degeneration in der benachbarten Bandscheiben- und Endplatte (EP) ebenfalls eng mit MCs verbunden. Bisher sind die Mechanismen für die Entstehung von MCs noch nicht geklärt, jedoch ist das Verstehen dieser Mechanismen entscheidend für die Entwicklung von zielgerichteten Therapien. Die Dissertation untersucht verschiedene Aspekte von MC1 im Knochenmark aber vor allem auch die Beteiligung der Bandscheibe und der Endplatte. Letztendlich führen die Projektergebnisse zur Vorstellung eines neuen Krankheitsmechanismus für die Entstehung von MC1, der durch die MC1-spezifische Bandscheibendegeneration initiiert wird.

Im Kapitel 1 wurden die Auswirkungen von MC1 Knochenmarksstromazellen (BMSCs) auf das Nervenwachstum mithilfe eines *in-vitro* Ko-Kultur-Systems untersucht. Es wurden zum ersten Mal die veränderten MC1-BMSCs direkt mit einem erhöhten Nervenwachstum in Verbindung gebracht. Mit diesem Wissen wurde ein wichtiger Behandlungsansatz identifiziert. Dies eröffnet die Möglichkeit für weitere Untersuchungen, um zu erforschen, wie dieser Effekt abgemildert werden kann.

Das zweite Kapitel konzentrierte sich auf die Erkundung des Konzepts eines Mikrobioms in der Bandscheibe, wobei insbesondere die Mikrobiome von MC1 und MC2 Bandscheiben durch einen Metagenomics Ansatz analysiert wurden. Das Bandscheibenmikrobiom hinterfragt das herkömmliche Konzept der Sterilität der Bandscheibe und erfordert daher eine klare methodische Herangehensweise, um es weiter zu erforschen. Obwohl unsere Analyse die Existenz eines Bandscheibenmikrobioms bestätigte, wich das Ergebnis von vorherigen Studien zu degenerierten MC Bandscheiben ab, auch nach der Angleichung der bioinformatischen Parameter. Diese Studie unterstreicht, dass es wichtig ist die bioinformatische Analyse des Bandscheibenmikrobioms zu standardisieren, aber auch weitere Faktoren zu untersuchen, die die bakterielle Zusammensetzung des Bandscheibenmikrobioms beeinflussen. Variationen könnten auf Unterschiede in den Probenvorbereitungstechniken oder auf Variationen in den geografischen und ethnischen Hintergründen der Patienten zurückzuführen sein. Wenn dies geklärt ist, wird die Erkundung des Bandscheibenmikrobioms zahlreiche Möglichkeiten für diagnostische und therapeutische Anwendungen eröffnen.

Das dritte Kapitel der Dissertation konzentrierte sich darauf, die bislang übersehene biologische Rolle der EP-Zellen hervorzuheben. Die Experimente konnten das Vorhandensein von Toll-like-Rezeptoren (TLRs) auf EP-Zellen bestätigen und betonten insbesondere das Vorhandensein von TLR2, da es der einzige TLR war, welcher durch direkte Stimulation hochreguliert wurde. Die Entdeckung von TLRs auf EP-Zellen ist bemerkenswert aufgrund ihrer hohen Dichte im Vergleich zu den Zellen in der benachbarten Bandscheibe und ihrer Fähigkeit, Entzündungen auszulösen und die Produktion kataboler Enzyme zu fördern. Dies könnte potenziell massgebend zur Endplattendegeneration beitragen und somit auch eine biologische Art der Endplattendegeneration vorweisen.

Das letzte Kapitel der Dissertation konzentriert sich auf das Hauptprojekt, das sich mit dem Verständnis der MC1-Pathobiologie befasst und einen neuen Mechanismus für die Entwicklung von MC1 vorschlägt, der mit der MC1-spezifischen Bandscheibendegeneration beginnt. Es basiert auf der Tatsache, dass zwar eine Bandscheibendegeneration fast immer neben MC1 beobachtet wird, jedoch nicht alle degenerierten Bandscheiben MC1 im benachbarten Knochenmark aufweisen. Es wird vermutet, dass die vorgeschlagene MC1-spezifische Bandscheibendegeneration zu mehr Fragmenten führt, welche Entzündungen in der benachbarten Endplatte auslösen und zu deren Zerstörung führen. Dies durchbricht die EP-Barriere zwischen der Bandscheibe und dem Knochenmark, was proinflammatorische Fragmente (danger associated molecular patterns (DAMPs)) und entzündliche Zytokine in das Knochenmark freisetzt und MC1 induzieren kann. Obwohl die Studie noch läuft, wurden bereits bedeutende Entdeckungen gemacht. MC1-Discs wiesen eine höhere Anzahl an Matrixfragmenten sowie eine höhere Konzentration der Protease HTRA1 auf als degenerierte Bandscheiben ohne MC1. In einer nachfolgenden Phase wurden die zahlreichen CILP1-Fragmente erfolgreich durch Exposition gegenüber HTRA1 repliziert und konnten durch Aktivierung des TLR4-Signalwegs proinflammatorische Eigenschaften nachgewiesen werden, wodurch sie als DAMPs klassifiziert werden können. Ein EP-Modell wurde verwendet, um zu zeigen, dass TLR-Aktivierung eine Zerstörung des EP-Gewebes induzieren kann, was den Zusammenhang zwischen der DAMP-Abundanz in der Bandscheibe und der EP-Schädigung herstellt. Weitere Experimente sind jedoch erforderlich, um die Lücken im vorgeschlagenen Mechanismus zu klären und diesen Mechanismus zu festigen. Dieses Wissen hat das Verständnis von MC1 deutlich vorangetrieben und könnte zahlreiche Therapiemöglichkeiten eröffnen, um in der Zukunft eine gezielte Behandlung zu ermöglichen.

Insgesamt zeigt diese Dissertation auf, dass MC1 eine Pathologie ist, welche mit deutlichen entzündlichen und schmerzbedingten Prozessen verbunden ist, was darauf hindeutet, dass sie spezifisch behandelt werden könnte und sollte. Dies markiert somit einen wichtigen Schritt hin zu einer gezielten Therapie für MC1.

# **Chapter 1: General Introduction**

## Modic changes

### 1.1.1 Definition

Modic changes (MCs) are vertebral bone marrow lesions defined as magnetic resonance imaging (MRI) signal intensity changes. In 1988, the nomenclature "Modic changes" was adopted following the publication by Modic et al. in 1988<sup>1</sup>. However, MCs were already described one year earlier by Assheuer and De Roos et al., 1987 and were then referred to as abnormal bone marrow signal intensity changes<sup>2,3</sup>. Three types of MCs were defined based on their appearance on T1 and T2 weighted MRI (Figure 1). Type 1 Modic Changes (MC1) are characterized by a hypointense signal on T1-weighted images and a hyperintense signal on T2-weighted images (Figure 1, left panel). In contrast, Type 2 Modic Changes (MC2) are characterized by hyperintensity on both T1 and T2 weighted images (Figure 1, middle panel). The third type is hypointense on both T1 and T2 weighted images (Figure 1, right panel)<sup>1,1</sup>. The three subtypes were found to be interconvertible over time and can also occur as mixed types<sup>4,5</sup>. Approximately 20 % of the MCs identified are of a mixed-type nature, either MC1/MC2 or MC2/MC3<sup>5,6</sup>.

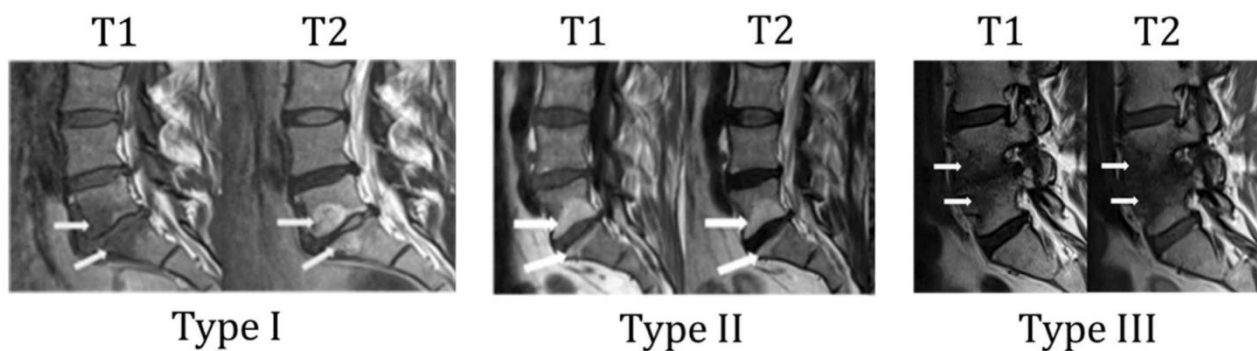


**Figure 1.** Subtypes of Modic changes (MCs) on magnetic resonance images (MRI) with T1 weighted (T1w) and T2 weighted images (T2w). Type 1 MC (left panel) are hyperintense on T1w images and hypointense on T2. Type 2 MCs (middle panel) are characterized by hypointense T1w and T2w image. Type 3 MCs (right panel) are hyperintense on both T1w and T2w images. Adapted from Li et al., (2022)<sup>19</sup>.

### 1.1.2 Subtypes

The representation of MC1 on MRI reveals a distinctive signal pattern descriptive of bone marrow edema, a characteristic feature of inflammation<sup>1</sup>. Examination of MC1 bone marrow through histologic analysis revealed the presence of fibrovascular granulation tissue, displacing the typical bone marrow<sup>7</sup>. Moreover, the infiltration of plasma cells, lymphocytes, and neutrophils further underscores the inflammatory nature of these processes. The identification of Cluster of Differentiation 90 (CD90) positive cells serves as an indicator of the presence of bone marrow stromal cells<sup>7</sup>.

An examination of gene expression in bone marrow aspirates revealed heightened levels of granulocyte progenitors, increased neurotrophic receptors (tyrosine kinase receptor A and C (TrkA and C)) and the increased presence of pro-fibrotic genes. Intriguingly, the study conducted by Dudli et al. in 2016 reported no

significant elevation in inflammatory genes such as interleukin 6 (IL6) or C-C chemokine ligand 2 (CCL2)<sup>8</sup>. This and other research revealed the absence of elevated pro-inflammatory genes, which at first seem contradictory to previous connections that linked MC1 to inflammation<sup>8-10</sup>. However, it actually may suggest a dynamic nature of the disease, wherein phases of inflammation and fibrosis may alternate over time<sup>11</sup>. Micro-computed tomography (CT) revealed a large bone turnover in MC1 which authors linked to inflammation<sup>12</sup>. The adjacent endplates to the MC1 bone marrow displayed signs of damage as well as a high presence of PGP 9.5 positive nerve fibers. In essence, the three primary characteristics defining MC1 are fibrosis, inflammation, and heightened bone turnover<sup>11</sup>.

MC2 MRI signals reveal the substitution of bone marrow with fatty tissue. Histologically, an increase in CD90 positive cells, as observed in MC1, is evident<sup>7</sup>. Evaluation of gene expression in MC2 bone marrow aspirates suggests the presence of fibrosis and the absence of active inflammation<sup>8</sup>. Proteomic analysis of MC2 bone marrow indicates an activated complement system which correlates with the endplate degeneration scores<sup>13</sup>. The disc adjacent to MC2 exhibits elevated IL6 and CCL2 levels, signifying inflammation<sup>8,13</sup>. Micro-CT analysis of bone marrow biopsies reveals a significant reduction in the osteoid surface to bone surface ratio in MC2, indicating decreased bone reformation and remodeling<sup>12</sup>. Unlike MC1, there is no indication of high bone turnover in MC2<sup>12</sup>. These findings led to MC2 being most recently described as fibroinflammatory changes with complement system involvement<sup>13</sup>.

The third subtype, MC3, has received the least research attention, likely attributed to its low prevalence and minimal association with pain<sup>5</sup>. The MRI of MC3, characterized by T1 and T2 weighted hyperintense signals, suggests the presence of sclerotic bone formation in MC3. This is backed by the micro-CT analysis which found a high volume of trabecular bone formation<sup>12</sup>. Currently, there are no existing pathomechanistic studies for MC3.

Mixed-type MCs are predominantly observed as MC1/2 or MC2/3<sup>14,15</sup>. The mixed types were shown to have endplate edema and endplate sclerosis<sup>15</sup>. The ability of MCs to undergo interconversion suggests that all three types are integral components of the same pathology at varying stages. Initially, the belief was that MC1 progresses towards MC3, but this hypothesis was challenged by a longitudinal study which found that MC1 and MC2 can change to a different type or even revert to MC0, signifying the interconvertibility of MCs<sup>16-18</sup>.

### *1.1.3 Prevalence of Modic changes*

While the prevalence of MCs in the general and asymptomatic population is found to be around 6 %<sup>19</sup>, it significantly rises among individuals experiencing chronic low back pain with a reported prevalence ranging from 20 % to 50 %<sup>14,20</sup>. MC2 is most often reported as the most prevalent type, while MC3 is considered the rarest<sup>5,21-23</sup>. Notably, MCs are most frequently observed at the L4/5 and L5/S1 spine levels<sup>5,19</sup>. Across various age groups, the prevalence of MCs tends to increase with advancing age<sup>5,19,21,23</sup>. Associations with male gender, high body mass index (BMI), increased height and weight, as well as certain lifestyle factors such as smoking and high workload, have been identified in relation to MC occurrence<sup>5,21,23</sup>.

### *1.1.3 Low Back Pain and Modic changes*

Globally, low back pain stands as the leading cause of years lived with disability and represents the most prevalent musculoskeletal disorder <sup>24-26</sup>. Given the aging demographic, it is expected that the global number of individuals affected by low back pain will increase from 619 million to over 843 million, an increase of nearly 35 % <sup>27</sup>. This not only poses a challenge for the affected individuals, causing pain and discomfort, but it also places a significant burden on the economic systems in both high-income and middle to low-income countries <sup>26,28-30</sup>. This is attributed to not only the substantial medical expenses, but also the inability of these individuals to go to work <sup>31,32</sup>.

In respect to MCs there have been inconsistent findings reported on whether MCs are more closely linked to pain compared to general disc degeneration <sup>33,34</sup>. Exploring the causes behind these disparities revealed a combination of factors, including varied study designs, diverse participant demographics, and discrepancies in the definition of MCs, all of which contribute to potentially bias the study and lead to different results <sup>33,34</sup>. Upon re-analysis with a more homogenous patient population, the connection between MCs and low back pain became more apparent, revealing a clear association <sup>35</sup>. Additionally, it was found that MC1 are the most painful type of MCs, followed by MC2 <sup>35-38</sup>. The pain associated with MCs is referred to as vertebral endplate pain. Notably, in 2022 an addition to the ICD-11 classifies "low back vertebral endplate pain" (DM54.51) for patients experiencing low back pain due to MCs, providing a diagnostic code for reimbursement purposes.

The sensation of low back pain in general is frequently associated with sensory nerves within the vertebrae and the vertebral endplate, and the compression of nerve roots by the lumbar disc is a common contributing factor <sup>39</sup>. In the context of low back pain due to MCs, the precise mechanism that triggers pain is not clearly defined, but the increased density of nerve fibers in MC-affected vertebral bodies and endplates may heighten pain perception <sup>40</sup>.

The primary innervation of the vertebral body occurs through gray rami communicantes, which distributes sensory fibers known as basivertebral nerve fibers originating from sinuvertebral nerves <sup>41,42</sup>. In contrast to the disc, the bone marrow is rich in capillaries and nerves. These capillaries derive from blood vessels entering the bone through the basivertebral foramen, converging in the central part of the vertebral bone and then spreading into the bony endplate <sup>43</sup>. Accompanying these vessels are nerve fibers from the basivertebral nerve <sup>43-45</sup>. Aspirates from Modic change (MC) type 1 bone marrow revealed an elevation in tyrosine receptor kinase B (TRKB), suggesting a potential association for these nerve fibers in pain generation. Additionally, MC type 2 showed significant increases in both TRKB and TRKC <sup>8</sup>. Moreover, more PGP9.5-positive sensory nerve fibers as well as increased tumor necrosis factor-alpha (TNF- $\alpha$ ) were observed in endplates with adjacent MC1 <sup>40,46</sup>.

Components and cytokines of the disc adjacent to MCs also need to be considered as potential contributors to pain generation due to possible diffusion between the disc and bone marrow due to the impaired endplate. A degenerated disc releases proinflammatory cytokines like interleukin-1 $\beta$  (IL-1 $\beta$ ), TNF- $\alpha$ , nerve growth factor (NGF), and brain-derived neurotrophic factor (BDNF), all known to promote neurite outgrowth and promote

firing of neurons through e.g. transient receptor potential vanilloid 1 (TRPV1) <sup>47-49</sup>. Moreover, in Modic Change Type 1 (MC1), there is an elevated expression of TRKA compared to an equally degenerated disc <sup>8</sup>. This heightened expression indicates increased neurotrophic activity, which may be one of the reasons for more aberrant nerve growth and potentially exacerbate pain sensation.

Overall, there is limited knowledge about the factors contributing to heightened pain perception in patients with MCs. Consequently, it is essential to investigate the underlying reasons for the intensified pain associated with MCs. Such exploration is crucial, as only with the comprehension of the factors which lead to increased innervation will the development of effective prevention strategies be possible. This will not only alleviate the burden on patients but also contributes to reduction of the substantial socio-economic costs associated with this condition.

#### *1.1.4 Etiologies*

Adjacent to MCs, the disc displays degeneration, and the endplate exhibits damage. Nevertheless, the underlying reasons why some degenerated discs develop adjacent MCs, while others do not, remains unclear. Three potential models are under consideration for the development of MCs. The first posits an autoinflammatory response of the bone marrow against disc components that have spilled over from the disc. The second focuses on the mechanical stress on the endplate due to the degenerating disc which induces damages to the endplate again allowing spillover of disc components to the adjacent bone marrow. In some cases, these two etiologies are combined and termed mechano-immunological etiology. Third, an etiology of bacterial origin is suggested, indicating the possibility of a low-grade bacterial infection of the disc <sup>11,50,51</sup>.

Examining the proposed autoinflammatory etiology more closely, the concept revolves around the notion that the disc, once formed embryologically, loses contact with the immune system, rendering it immune privileged. The nucleus pulposus (NP) cells express Fas ligands that induce apoptosis in lymphocytes, establishing immune privilege <sup>52</sup>. When introducing NP tissue into immune-active surroundings, this triggers an immune response, as evident from cytokine release, macrophage infiltration, and activation of B and T-cells <sup>53-55</sup>. A further study revealed the presence of IgG antibodies against typical NP extracellular matrix (ECM) proteins, such as collagen type I, II and V as well as aggrecan, in both degenerated and post-traumatic discs <sup>56</sup>.

Similar to the autoinflammatory model, Albert et al. (2008) proposed a mechanical mechanism. She described it as the loss of disc material which results in a diminished disc height and loss of hydrostatic pressure, consequently leading to increased shear forces on the endplate, inducing microfractures <sup>50</sup>. Subsequently, these microfractures may lead to edema as well as allowing material of the immune privileged NP to seep through initiating inflammation in the adjacent bone marrow <sup>50</sup>.

Thirdly, the bacterial origin is attributed to a low-virulent infection of the disc. In 2001, Stirling et al. identified *Cutibacterium Acnes* (*C. Acnes*) in the disc <sup>57</sup>. A few years later Alber et al. (2008), suggested the passage of this bacterium through the disrupted endplate into the disc and linked it to MC development <sup>50</sup>. Subsequently, it was observed that individuals with disc herniation and MCs exhibit a significantly higher presence of low-virulence anaerobic bacteria <sup>58</sup>. The disc's low oxygen levels and acidic pH provide an ideal environment for

anaerobic bacteria to flourish and construct a protective biofilm<sup>59,60</sup>. The inflammatory response in the disc cells is then triggered by the bacteria<sup>61</sup>, causing tissue damage to both the disc and the endplate. With the damaged endplate, leukocytes can enter the disc resulting in an immune response to the bacteria which can involve TNF- $\alpha$ , IL-6 and IL-8 release<sup>62</sup>. Animal models demonstrated that the injection of *C. Acnes* into the disc led to disc degeneration, endplate damage, and eventually the formation of MCs. Interestingly, this effect was not replicated when *Staphylococcus aureus* was injected. Additionally, proteomic data analysis of 22 discs found an increase in bacterial specific proteins in degenerated discs<sup>63</sup>. However, the emergence of the bacterial etiology hypothesis sparked considerable debate and skepticism regarding the true presence of bacteria versus the possibility of contamination<sup>64,65</sup>. Fluorescence in situ hybridization (FISH), enabling the demonstration of *C. Acnes* in situ, has successfully identified the presence of this bacterium<sup>59</sup>.

In general, numerous uncertainties persist concerning the origins of MCs. It remains unclear whether diverse etiologies give rise to distinct subtypes of the disease or if these alleged etiologies rather represent different chronological stages of the same condition.

### *1.1.5 Treatment approaches of Modic changes*

Patients with MCs are currently not being treated as a separate group but are usually treated the same way other chronic low back pain patients are treated. This can be attributed to both the scarcity of specialized treatments and the inconsistent identification of motion segments causing pain. Consequently, many clinicians tend to diagnose non-specific low back pain rather than pinpointing MC1 specifically.

The challenge to develop a targeted therapy is multifaceted. Firstly, the lack of animal models that replicate MCs and would allow for in vivo investigations poses a significant obstacle. Furthermore, the acquisition of samples from patients relies on their undergoing spinal fusion surgery, wherein a bone marrow sample from the MC area can be obtained before screw insertion. However, this process presents challenges, including obtaining ethical approvals and ensuring proper sample collection. Additionally, these bone marrow biopsies only represent a singular moment in the progression of the disease. These limitations make it challenging to comprehensively study the development and the transitions between different types of MCs and with that the options for a successful treatment approach.

Treatment strategies for MCs have involved intradiscal steroid injections and the intravenous administration of TNF- $\alpha$  inhibitors and bisphosphonates. However, these approaches have demonstrated only short-term benefits<sup>66-69</sup>. A more targeted strategy to treat is the basivertebral nerve ablation (BVNA), a minimally invasive spinal procedure<sup>70,71</sup>. This method includes introducing a thin radiofrequency probe into the vertebral body to induce a heat lesion on the basivertebral nerve. It has demonstrated moderate-quality evidence in the effectiveness of pain reduction for MC patients, as confirmed by a 24-month follow-up<sup>72,73</sup>. However, beyond this period, it remains uncertain whether the sustained reduction in pain development persists making it a targeted but not disease modifying treatment approach. Another limitation is the contraindications to basivertebral nerve ablation (BVNA), including conditions like osteoporosis and morbid obesity. These contraindications would exclude a significant portion of the MC population, as MCs are associated with higher



BMI and are more prevalent with advancing age<sup>71</sup>. The most recent treatments for MCs that are being tested included platelet-rich plasma injection as well as the use of mesenchymal stromal cells (MSCs)<sup>74-77</sup>.

In the case of MC stemming from bacterial infection, the treatment with antibiotics would make most sense. However, the outcomes of such trials showed varying success rates. Some trials found a significantly positive impact on MC1 patients treated with antibiotics<sup>78-81</sup>, while others show no substantial difference compared to a placebo-treated group<sup>82</sup>. The discrepancies in findings may be attributed to the heterogeneity within the MC patient cohorts<sup>81,83</sup>. Recent discoveries have identified two distinct groups within the MC population, with one subgroup exhibiting high *C. Acnes* counts in the adjacent disc and the other demonstrating low counts<sup>84,85</sup>. Consequently, accurate treatment is only possible with the ability to differentiate patients into these two subgroups. A suggested serum biomarker for bacterial presence in MC1 discs includes interleukin (IL)-13, IL-12p70, and interferon gamma, which were found to be elevated in the subgroup with high *C. acnes* counts<sup>84</sup>.

In conclusion, a targeted disease-modifying treatment approach for MCs remains elusive. For this to be established a fundamental understanding of the underlying causes of the disease needs to be clarified.

## **Disc-endplate-bone marrow in the context of Modic changes**

### *1.2.1 Vertebral bone marrow*

The spine houses the body's largest reserve of bone marrow, which is entirely encased within bone within the cancellous part of the bone, presenting as a soft, spongy tissue<sup>86</sup>. It consists of two main types: red marrow, responsible for generating red blood cells, platelets, and some white blood cells, and yellow marrow, primarily composed of fat cells and acting as a reserve for nutrients. Within the bone marrow there is a hematopoietic compartment with hematopoietic stem cells and a stromal compartment with mesoderm-derived cells like mesenchymal stem cells, fibroblasts, endothelial cells, and adipocytes. Serving as a major hematopoietic organ and primary lymphoid tissue, the bone marrow is dynamic, undergoing continual changes with age and adapting to varying hematopoietic demands in diverse environmental and health conditions<sup>87</sup>. It also acts as a focal point for numerous pathological processes, resulting in altered signal intensity or a heterogeneous signal pattern on magnetic resonance imaging (MRI).

The evaluation of signal patterns in bone marrow is crucial in spinal MRI. MRI emerges as the preferred imaging modality for capturing bone marrow, given its inherent soft tissue contrast and non-ionizing nature<sup>88</sup>. Routine spine imaging protocols typically include a T1 weighted (T1w) and T2 weighted (T2W) image as well as in some institutes a short tau inversion recovery (STIR) sequence. The T1w image shows the red marrow as low signal due to its high water content, though still higher than within a very hydrated healthy disc. In case of inflammation and oedema the signal intensity will be even lower, as seen in MC1. However, if fat dominates the bone marrow, a higher signal intensity can be observed, as seen in MC2<sup>89</sup>. The T2w imaging display both water and fat with a high signal intensity, with fat and water alone giving even a more pronounced intensity, as observed in both MC1 and MC2, displaying hyperintensity in T2w<sup>90</sup>. Additionally, the STIR sequence allows for better visualization of non-fatty components such as water, which provides value for detection of

edema, as for example in MC1<sup>91</sup>. While this is not officially recognized for MC1 classification it does provide further insight into the bone marrows condition<sup>92</sup>.

### *1.2.2 Vertebral endplate*

Between the vertebral body and the disc is the vertebral endplate. The endplate is composed of the cartilage endplate (CEP) towards the side of the disc and the bony endplate (BEP) on the side of the vertebrae<sup>93</sup>. Experimental isolation of CEP from BEP is challenging, and clinically, distinguishing these tissues on medical images is difficult. This may be the reason why many studies do not specify and differentiate between the CEP and BEP despite acknowledging the bilayer composition<sup>94</sup>.

The BEP is made up of a dense, porous layer of fused trabecular bone containing osteocytes enclosed within saucer-shaped lamellar packets<sup>95</sup> and its thickness ranges from 0.2 to 0.8 mm dependent on the location. In contrast, the CEP is composed of chondrocytes dispersed within an extracellular matrix containing proteoglycans, collagen (types I and II), and water. The collagen fibers are found horizontally aligned parallel to the ends of the vertebrae. The thickness of the CEP typically ranges between 0.1 and 2.0 mm, being thinner centrally compared to the periphery<sup>96,97</sup>. The cell density of the CEP is approximately four times greater than in the NP of the disc and two time more than in the annulus fibrosus (AF)<sup>98</sup>.

The CEP plays a dual role, serving both mechanical and nutritional functions for the disc. Mechanically, it prevents the disc from protruding into the adjacent vertebral body under pressure<sup>99</sup> and provides anchorage for the disc fibers. Nutritionally, the CEP facilitates the diffusion of vital nutrients into the disc, crucial for maintaining homeostasis in the avascular disc<sup>100</sup>.

Instead of using the term MCs some authors have used “endplate changes” or “vertebral endplate signal changes (VESC)”<sup>46,94,101</sup>. While mechanical cues are thought to be the primary cause of endplate damage, understanding of biological processes leading to CEP damage remain limited. Several studies have suggested that changes in the biological composition of the cartilaginous endplate (CEP) can disrupt its ability to adequately supply the intervertebral disc with nutrients<sup>102</sup>. Subsequently this can have adverse effects on the disc, contributing to accelerated degeneration<sup>102-104</sup>. Additionally a high endplate score, signifying endplate damage, was found to be an independent risk factor for the progression of both disc degeneration and MCs in individuals experiencing low back pain<sup>105</sup>. It was found that immune responses in MC1 bone marrow can independently cause damage to the adjacent endplate, emphasizing that MC1 is not solely reactive to disc degeneration but can actively contribute to CEP damage. Recent studies further support the potential for activated immune cells, such as neutrophils, in MC1 bone marrow to induce CEP damage<sup>106</sup>.

Further research is essential to comprehensively unravel the role of the CEP in MC development. A particular emphasis should be put on the significance of MC CEP cells as with their high density relative to cells in the adjacent disc tissue their impact should not be underestimated<sup>107</sup>.

### *1.2.3 Intervertebral disc*

The intervertebral disc, a vital component of the human spine, is positioned between two vertebrae, forming part of the vertebral column. The disc's main functions are to serve as a critical shock absorber and enhance the spine's flexibility. The disc is not vascularized and is therefore the largest avascular organ in the body. The cells found within the disc get their nutrients through diffusion from the capillary endings entering only the the endplate and the outer AF <sup>108,109</sup>. The disc comprises two primary components, namely the AF, which envelops the disc and the NP which resides at the core of the disc.

The NP is a gel-like component situated centrally within the intervertebral disc, playing a pivotal role in imparting strength and flexibility to the spine. Comprising a substantial 66 % to 86 % water content, the remaining composition primarily consists of type II collagen, with possible inclusions of types VI, IX, and XI, alongside essential proteoglycans. Notable among these proteoglycans are the larger molecules, aggrecan and versican, which bind with hyaluronic acid, as well as various small leucine-rich proteoglycans <sup>110,111</sup>. Despite a low cellular density, the cells present in this structure play a crucial role in synthesizing ECM components, including aggrecan and type II collagen <sup>112,113</sup>. These ECM products collectively contribute to maintaining the structural integrity of the nucleus pulposus, reinforcing its vital function within the intervertebral disc.

The AF, encircling the NP, is an organized structure with 15 to 25 collagen-based lamellae. These sheets, interspersed with proteoglycans and other components, are aligned in a radial-ply formation, providing exceptional strength. Trans-lamellar bridges interconnect the lamellae to balance strength and flexibility. The AF's inner and outer portions differ in collagen composition, with predominantly type I in the outer annulus and mostly type II in the inner annulus, which also contains more proteoglycans responsible for the discs hydration <sup>114</sup>. The collagen ratio shifts gradually from type II to type I with increasing distance from the NP <sup>115</sup>. Cells in the inner annulus are round, while those in the outer annulus have an elongated fibroblast-like appearance <sup>113,116</sup>.

Maintaining the integrity of discs is crucial for overall spinal health. However, it is a natural aspect of the aging process for individuals to experience disc degeneration, with more than 90% of people having at least one degenerated disc by the age of 50, encompassing both painful and non-painful degeneration <sup>117</sup>. Disc degeneration is marked by a reduction in cellularity, breakdown of the extracellular matrix (ECM), and dehydration of the disc, resulting in a decrease in disc height. This process can trigger facet joint osteoarthritis, stenosis, or vertebral alterations such as sclerosis or Modic changes (MCs), ultimately compromising the biomechanical integrity of the spine and rendering it unable to adequately withstand loads <sup>118,119</sup>.

In the case of MCs, the observation of an adjacently lying degenerated discs suggests a potential pivotal role for the disc in the development of MCs. This is further supported by MCs frequently manifesting symmetrically, both cranially and caudally to the degenerated disc. This suggests a systemic involvement surrounding the disc region <sup>105</sup>, possibly implicating structural and biochemical alterations within the intervertebral disc and its adjacent tissues in the pathogenesis of MCs.

During the highly complex process of disc degeneration, disc cells specifically release a high level of proinflammatory cytokines. Additionally, while MMPs are important for physiological structural recombination, degenerating discs show increased expression of MMPs, specifically MMP-1, -2, -3, -7, -8, -10, and -13, as well as ADAMTS4/5 also found to be produced by disc cells. This is accompanied by a decrease in Tissue Inhibitors of Metalloproteinase-3 (TIMP-3), further shifting the balance towards catabolic processes<sup>120, 121</sup>. These factors promote the degradation of the ECM, resulting in the release of numerous ECM fragments<sup>120–123</sup>. This imbalance in catabolic and anabolic mechanisms has been shown to lead to increased levels of fibronectin, fibromodulin, biglycan, lumican, and decorin fragments<sup>123–128</sup>. Additionally, disc cells, particularly those in the nucleus pulposus, undergo increased apoptosis due to reduced nutrient supply from calcified endplates and decreased hydration from fewer water-binding molecules<sup>121,129,130</sup>. This leads to a reduction in NP cells, which are essential for producing key structural ECM proteins such as proteoglycans and collagens.

The disc resorption subsequent to the now outdated chemonucleolysis treatment was causally linked to MCs, underscoring the damaging potential of disc derived ECM fragments on surrounding structures<sup>131</sup>. Some of these fragments can trigger inflammation through the recognition of Toll-like Receptors (TLRs), classifying them as ECM-derived Damage-Associated Molecular Patterns<sup>124</sup>. Persistent activation of TLRs can lead to further degenerative changes<sup>132</sup>. Studies have demonstrated that inhibiting TLR4 in the disc results in reduced pain and disc degeneration in mice<sup>133,134</sup>. Additionally, ECM fragments, apart from activating TLRs on disc cells, have the potential to migrate into the adjacent bone marrow due to their small size and mobility, as they are no longer firmly bound to the matrix of the disc<sup>135</sup>. This is particularly important to consider in the case of MCs, where the damaged endplate has higher permeability potentially allowing even larger fragments to pass through.

## **Relevance of danger associated molecular patterns and TLRs in Modic changes**

### *1.3.1 Danger associated molecular patterns*

Damage associated molecular patterns (DAMPs), sometimes also known as Danger-Associated Molecular Patterns or Alarmins, are endogenous molecules released from damaged or dying cells or tissues. They possess the potential to activate the innate immune system through recognition by pattern recognition receptors such as toll-like receptors (TLRs) and the receptor for advanced glycation end products (RAGE). This leads to a non-infectious inflammation and should induce the initiation of tissue repair<sup>136</sup>. Polly Matzinger first described this concept in 1994<sup>137</sup>.

The origins of DAMPs are diverse, encompassing both extracellular and intracellular proteins. Among the extracellular proteins are ECM-derived DAMPs, including full-length biglycan, decorin, and fibronectin. Intracellular proteins originate from various compartments such as the cytosol, represented by S100 proteins

and uric acid, and nuclear components, including histones and high-mobility group box 1. Additionally, DAMPs can emerge from mitochondrial proteins and many other molecules which fall in this category <sup>137</sup>.

The DAMPs are recognized by pattern recognition receptors which are found both on the surface as well as within the cell on intracellular membranes. When a DAMP is recognized by a pattern recognition receptor (PRR) this initiates either phagocytosis or inflammation overall inducing innate immunity reactions. To the group of the PRRs belong TLR1 through TLR10, nod-like receptors (NLRs), C-type lectin receptors (CLRs) and many more.

Unfortunately, although the inflammatory reaction serves as a protective response, it can simultaneously contribute to the onset of various diseases, including autoimmune diseases, cardiovascular diseases, degenerative joint diseases, cancer and neurodegenerative diseases <sup>138-142</sup>. Hence, extensive research has been conducted on DAMPs to elucidate their mechanisms of action in various diseases with the goal of utilizing them as biomarkers or potential therapeutic targets.

### *1.3.2 TLRs*

TLRs, are a class of type 1 transmembrane glycoproteins crucial for the innate immune response and the main PRRs in humans <sup>143</sup>. Ten TLRs have been identified so far in humans. TLRs 1, 2, 4, 5, 6, and 10 are situated on the cell surface, while TLRs 3, 7, 8, and 9 are located within endosomal compartments <sup>144</sup>. Their primary function involves recognizing foreign structures, such as microbial components like lipopolysaccharide found in the cell walls of microbes but absent in humans. This concept, proposed by Janeway, highlights their pivotal role in immune defense <sup>145</sup>. Subsequently, with the recognition of DAMPs, it became evident that TLRs also play a role in the recognition of endogenous molecules associated with cellular and tissue damage <sup>137</sup>.

For DAMP recognition, TLR2 in conjunction with TLR1 or TLR6, as well as TLR4, have been listed as the most relevant ones. While TLR2 can create heterodimers with either TLR1 or TLR6, it's important to note that these heterodimers are pre-existing and are not induced based on ligand presence. The downstream signaling pathways of TLR initiated through endogenous molecules are not fully understood. However current research has found that distinct adaptor molecules can recognize various molecules, leading to the initiation of diverse downstream pathways. For example, the activation of TLR4 with LPS can initiate both TRIF and MyD88-dependent pathways. In contrast, the TLR4 agonist tenascin-C specifically triggers the MyD88 pathway and biglycan has been observed to activate signaling through both TLR2 and TLR4 in a MyD88-dependent manner <sup>146,147</sup>. The outcome of TLR signaling involves the activation of transcription factors, such as NFkB, AP-1, or IRF5, which in turn regulate the expression of specific genes. This process leads to the production of inflammatory cytokines.

While numerous DAMPs can induce TLR-dependent inflammation *in vivo*, it is essential to recognize that this alone may not establish their significance in disease progression. Nevertheless, research involving mice deficient in particular endogenous TLR activators or treated with DAMP inhibitory compounds has shown a reduction in inflammation *in vivo*, as demonstrated in studies which focused on inflammatory conditions such as atherosclerosis and arthritic joint diseases <sup>146,148,149</sup>.

### *1.3.3 DAMPs and TLR signaling in the disc*

Disc cells express TLRs and have been observed to upregulate their expression primarily through self-regulation which implies that the activation of TLRs results in an increased expression of TLRs within disc cells. Furthermore, stimulation with lipopolysaccharide (LPS) and tumor necrosis factor-alpha (TNF- $\alpha$ ), along with injurious loading, led to an elevation in the expression of TLR2 and TLR4 in disc cells<sup>133,150-152</sup>. Additionally, it was noted that in more advanced degenerative stages, there was an increased expression of TLR1, TLR2, TLR4, and TLR6<sup>133</sup>. This observation is intriguing as the activation of these TLRs can induce the upregulation of MMP1, MMP3, and MMP13 but also inflammatory cytokines such as IL6, IL8 or TNF-alpha to name only a few<sup>132,151,153</sup>. These MMPs are well-known for their involvement in disc degeneration, capable of cleaving a wide range of ECM molecules and the named cytokines are also strongly linked to the progression of disc degeneration. Moreover, TLR activation negatively influences the expression of collagen type II and aggrecan, crucial structural and organizational proteins in the disc<sup>151</sup>. This dual impact on MMPs and essential disc proteins suggests a potential role for TLR activation in promoting not only tissue remodeling but also contributing to destructive processes within the disc. Overall, this suggests the continuous activation of TLRs which induces tissue degeneration as illustrated in Figure 2.

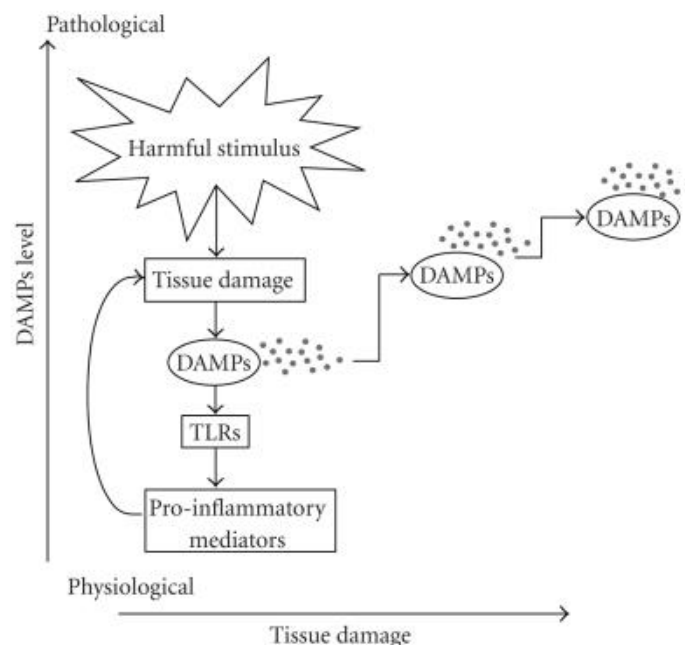


**Figure 2.** Proposed cascade of damage induction. Tissue injury generates DAMPs, activating TLRs and instigating inflammatory responses, thereby restarting the cycle. Figure adapted from Piccinini et al. (2010)<sup>128</sup>.

The activation of these TLRs through DAMPs in discs is a possible scenario as the disc has been shown to have an increased presence of HMGB1 and peroxiredoxin-5 which are both intracellular DAMPs<sup>154,155</sup>. Besides that, as the ECM undergoes degeneration, new fragments are generated such as aggrecan, fibronectin or hyaluronan<sup>123,156-159</sup>. While lots of research has been done on identifying such ECM-derived DAMPs, the list is far from complete, mainly focused on the compounds which are commercially available or easily producible. However, the significant quantity of fragments generated during the degeneration process could

also be biologically active, potentially exhibiting pro-inflammatory effects. Consequently, there is a need for further investigation and identification of these fragments.

## 1.4 References

1. Modic, M. T., Steinberg, P. M., Ross, J. S., Masaryk, T. J. & Carter, J. R. Degenerative disk disease: assessment of changes in vertebral body marrow with MR imaging. *Radiology* **166**, 193–199 (1988). doi:10.1148/radiology.166.1.3336678.
2. Assheuer G; Lenz W; Gottschlich K W; Schulitz K P, J. L. Fett-/Wassertrennung im Kernspintomogramm. *RöFo - Fortschritte auf dem Gebiet der Röntgenstrahlen und der bildgebenden Verfahren* **147**, 58–63 (1987). doi:10.1055/s-2008-1048590.
3. de Roos, A., Kressel, H., Spritzer, C. & Dalinka, M. MR imaging of marrow changes adjacent to end plates in degenerative lumbar disk disease. *American Journal of Roentgenology* **149**, 531–534 (1987). doi:10.2214/ajr.149.3.531.
4. Kääpä, E., Luoma, K., Pitkäniemi, J., Kerttula, L. & Grönblad, M. Correlation of Size and Type of Modic Types 1 and 2 Lesions With Clinical Symptoms: A Descriptive Study in a Subgroup of Patients With Chronic Low Back Pain on the Basis of a University Hospital Patient Sample. *Spine (Phila Pa 1976)* **37**, (2012).
5. Wang, Y., Videman, T. & Battié, M. Modic changes: Prevalence, distribution patterns, and association with age in white men. *Spine J* **12**, 411–416 (2012). doi:10.1016/j.spinee.2012.03.026.
6. Kuisma, M. *et al.* Modic changes in vertebral endplates: a comparison of MR imaging and multislice CT. *Skeletal Radiol* **38**, 141–147 (2009). doi:10.1007/s00256-008-0590-9.
7. Dudli, S. *et al.* CD90-positive stromal cells associate with inflammatory and fibrotic changes in modic changes. *Osteoarthr Cartil Open* **4**, (2022). doi:10.1016/j.ocarto.2022.100287.
8. Dudli, S. *et al.* ISSLS PRIZE IN BASIC SCIENCE 2017: Intervertebral disc/bone marrow cross-talk with Modic changes. *European Spine Journal* **26**, 1362–1373 (2017). doi:10.1007/s00586-017-4955-4.
9. Torkki, M. *et al.* Osteoclast activators are elevated in intervertebral disks with Modic changes among patients operated for herniated nucleus pulposus. *European Spine Journal* **25**, 207–216 (2016). doi:10.1007/s00586-015-3897-y.
10. Schroeder, G. D. *et al.* Are Modic changes associated with intervertebral disc cytokine profiles? *Spine Journal* **17**, 129–134 (2017). doi:10.1016/j.spinee.2016.08.006.
11. Dudli, S., Fields, A. J., Samartzis, D., Karppinen, J. & Lotz, J. C. Pathobiology of Modic changes. *European Spine Journal* vol. 25 3723–3734 Preprint at <https://doi.org/10.1007/s00586-016-4459-7> (2016). doi:10.1007/s00586-016-4459-7.
12. Perilli, E. *et al.* Modic (endplate) changes in the lumbar spine: bone micro-architecture and remodelling. *European Spine Journal* **24**, 1926–1934 (2015). doi:10.1007/s00586-014-3455-z.
13. Heggli, I. *et al.* Modic type 2 changes are fibroinflammatory changes with complement system involvement adjacent to degenerated vertebral endplates. *JOR Spine* **6**, (2023). doi:10.1002/jsp2.1237.



14. Rahme, R. & Moussa, R. The modic vertebral endplate and marrow changes: Pathologic significance and relation to low back pain and segmental instability of the lumbar spine. in *American Journal of Neuroradiology* vol. 29 838–842 (2008). doi:10.3174/ajnr.A0925.
15. Xu, L., Chu, B., Feng, Y., Xu, F. & Zou, Y.-F. Modic changes in lumbar spine: prevalence and distribution patterns of end plate oedema and end plate sclerosis. *British Journal of Radiology* **89**, 20150650 (2016). doi:10.1259/bjr.20150650.
16. Jensen, T. S. *et al.* Characteristics and natural course of vertebral endplate signal (Modic) changes in the Danish general population. *BMC Musculoskelet Disord* **10**, 81 (2009). doi:10.1186/1471-2474-10-81.
17. Tamai, H. *et al.* A Prospective, 3-year Longitudinal Study of Modic Changes of the Lumbar Spine in a Population-based Cohort: The Wakayama Spine Study. *Spine (Phila Pa 1976)* **47**, (2022).
18. Mitra, D., Cassar-Pullicino, V. N. & McCall, I. W. Longitudinal study of vertebral type-1 end-plate changes on MR of the lumbar spine. *Eur Radiol* **14**, 1574–1581 (2004). doi:10.1007/s00330-004-2314-4.
19. Mok, F. P. S. *et al.* Modic changes of the lumbar spine: prevalence, risk factors, and association with disc degeneration and low back pain in a large-scale population-based cohort. *The Spine Journal* **16**, 32–41 (2016). doi:https://doi.org/10.1016/j.spinee.2015.09.060.
20. Chen, Y. *et al.* Distribution of Modic changes in patients with low back pain and its related factors. *Eur J Med Res* **24**, 34 (2019). doi:10.1186/s40001-019-0393-6.
21. Chen, Y. *et al.* Distribution of Modic changes in patients with low back pain and its related factors. *Eur J Med Res* **24**, 34 (2019). doi:10.1186/s40001-019-0393-6.
22. Teraguchi, M. *et al.* Detailed Subphenotyping of Lumbar Modic Changes and Their Association with Low Back Pain in a Large Population-Based Study: The Wakayama Spine Study. *Pain Ther* **11**, 57–71 (2022). doi:10.1007/s40122-021-00337-x.
23. Han, C., Kuang, M. J., Ma, J. X. & Ma, X. L. Prevalence of Modic changes in the lumbar vertebrae and their associations with workload, smoking and weight in northern China. *Sci Rep* **7**, (2017). doi:10.1038/srep46341.
24. Buchbinder, R. *et al.* Low back pain: a call for action. *The Lancet* **391**, 2384–2388 (2018).
25. Hoy, D. *et al.* A systematic review of the global prevalence of low back pain. *Arthritis Rheum* **64**, 2028–2037 (2012).
26. Hartvigsen, J. *et al.* What low back pain is and why we need to pay attention. *The Lancet* **391**, 2356–2367 (2018).
27. Ferreira, M. L. *et al.* Global, regional, and national burden of low back pain, 1990–2020, its attributable risk factors, and projections to 2050: a systematic analysis of the Global Burden of Disease Study 2021. *Lancet Rheumatol* **5**, e316–e329 (2023). doi:10.1016/S2665-9913(23)00098-X.
28. Deyo, R. A., Cherkin, D., Conrad, D. & Volinn, E. Cost, controversy, crisis: low back pain and the health of the public. *Annu Rev Public Health* **12**, 141–156 (1991).
29. Fatoye, F., Gebrye, T., Ryan, C. G., Useh, U. & Mbada, C. Global and regional estimates of clinical and economic burden of low back pain in high-income countries: a systematic review and meta-analysis. *Front Public Health* **11**, 1098100 (2023).



30. Fatoye, F., Gebrye, T., Mbada, C. E. & Useh, U. Clinical and economic burden of low back pain in low- and middle-income countries: a systematic review. *BMJ Open* **13**, e064119 (2023). doi:10.1136/bmjopen-2022-064119.
31. Driscoll, T. *et al.* The global burden of occupationally related low back pain: estimates from the Global Burden of Disease 2010 study. *Ann Rheum Dis* **73**, 975–981 (2014).
32. Lee, H. *et al.* How does pain lead to disability? A systematic review and meta-analysis of mediation studies in people with back and neck pain. *Pain* **156**, 988–997 (2015).
33. Herlin, C. *et al.* Modic changes—Their associations with low back pain and activity limitation: A systematic literature review and meta-analysis. *PLoS One* **13**, e0200677- (2018).
34. Hopayian, K., Raslan, E. & Soliman, S. The association of modic changes and chronic low back pain: A systematic review. *J Orthop* **35**, 99–106 (2023). doi:https://doi.org/10.1016/j.jor.2022.11.003.
35. Czaplewski, L. G., Rimmer, O., McHale, D. & Laslett, M. Modic changes as seen on MRI are associated with nonspecific chronic lower back pain and disability. *J Orthop Surg Res* **18**, 351 (2023). doi:10.1186/s13018-023-03839-w.
36. Saukkonen, J. *et al.* Association Between Modic Changes and Low Back Pain in Middle Age: A Northern Finland Birth Cohort Study. *Spine (Phila Pa 1976)* **45**, (2020).
37. Järvinen, J. *et al.* Association between changes in lumbar Modic changes and low back symptoms over a two-year period. *BMC Musculoskelet Disord* **16**, 98 (2015). doi:10.1186/s12891-015-0540-3.
38. Thompson, K. J., Dagher, A. P., Eckel, T. S., Clark, M. & Reinig, J. W. Modic changes on MR images as studied with provocative diskography: clinical relevance—a retrospective study of 2457 disks. *Radiology* **250**, 849–855 (2009).
39. Baron, R. *et al.* Neuropathic low back pain in clinical practice. *European Journal of Pain (United Kingdom)* vol. 20 861–873 Preprint at <https://doi.org/10.1002/ejp.838> (2016). doi:10.1002/ejp.838.
40. Ohtori, S. *et al.* Tumor Necrosis Factor-Immunoreactive Cells and PGP 9.5-Immunoreactive Nerve Fibers in Vertebral Endplates of Patients With Discogenic Low Back Pain and Modic Type 1 or Type 2 Changes on MRI. *Spine (Phila Pa 1976)* **31**, (2006).
41. Antonacci MD, Mody DR & Heggeness MH. Innervation of the human vertebral body. *J Spinal Disord* **11**, 526–531 (1998).
42. Kim, H. S., Wu, P. H. & Jang, I. T. Lumbar degenerative disease part 1: Anatomy and pathophysiology of intervertebral discogenic pain and radiofrequency ablation of basivertebral and sinuvertebral nerve treatment for chronic discogenic back pain: A prospective case series and review of literature. *Int J Mol Sci* **21**, (2020). doi:10.3390/ijms21041483.
43. Bailey, J. F., Liebenberg, E., Degmetich, S. & Lotz, J. C. Innervation patterns of PGP 9.5-positive nerve fibers within the human lumbar vertebra. *J Anat* **218**, 263–270 (2011). doi:10.1111/j.1469-7580.2010.01332.x.
44. Calvo, W. The innervation of the bone marrow in laboratory animals. *American Journal of Anatomy* **123**, 315–328 (1968). doi:https://doi.org/10.1002/aja.1001230206.
45. Carmeliet, P. & Tessier-Lavigne, M. Common mechanisms of nerve and blood vessel wiring. *Nature* vol. 436 193–200 Preprint at <https://doi.org/10.1038/nature03875> (2005). doi:10.1038/nature03875.

46. Fields, A. J., Liebenberg, E. C. & Lotz, J. C. Innervation of pathologies in the lumbar vertebral end plate and intervertebral disc. *Spine Journal* **14**, 513–521 (2014). doi:10.1016/j.spinee.2013.06.075.
47. Capoor, M. N. *et al.* Pro-inflammatory and neurotrophic factor responses of cells derived from degenerative human intervertebral discs to the opportunistic pathogen cutibacterium acnes. *Int J Mol Sci* **22**, 1–16 (2021). doi:10.3390/ijms22052347.
48. Staszkiwicz, R. *et al.* Usefulness of Detecting Brain-Derived Neurotrophic Factor in Intervertebral Disc Degeneration of the Lumbosacral Spine. *Medical Science Monitor* **29**, 0 (2023). doi:https://dx.doi.org/10.12659/MSM.938663.
49. Zhang, Y. H., Chi, X. X. & Nicol, G. D. Brain-derived neurotrophic factor enhances the excitability of rat sensory neurons through activation of the p75 neurotrophin receptor and the sphingomyelin pathway. *J Physiol* **586**, 3113–3127 (2008). doi:https://doi.org/10.1113/jphysiol.2008.152439.
50. Albert, H. B. *et al.* Modic changes, possible causes and relation to low back pain. *Med Hypotheses* **70**, 361–368 (2008). doi:https://doi.org/10.1016/j.mehy.2007.05.014.
51. Crockett, M. T., Kelly, B. S., van Baarsel, S. & Kavanagh, E. C. Modic Type 1 Vertebral Endplate Changes: Injury, Inflammation, or Infection? *American Journal of Roentgenology* **209**, 167–170 (2017). doi:10.2214/AJR.16.17403.
52. Kaneyama, S. *et al.* Fas ligand expression on human nucleus pulposus cells decreases with disc degeneration processes. *Journal of Orthopaedic Science* **13**, 130–135 (2008).
53. Shamji, M. F. *et al.* Gait abnormalities and inflammatory cytokines in an autologous nucleus pulposus model of radiculopathy. *Spine (Phila Pa 1976)* **34**, 648–654 (2009).
54. Geiss, A., Larsson, K., Junevik, K., Rydevik, B. & Olmarker, K. Autologous nucleus pulposus primes T cells to develop into interleukin-4-producing effector cells: an experimental study on the autoimmune properties of nucleus pulposus. *Journal of Orthopaedic Research* **27**, 97–103 (2009).
55. Kanerva, A. *et al.* Inflammatory cells in experimental intervertebral disc injury. *Spine (Phila Pa 1976)* **22**, 2711–2715 (1997).
56. Capossela, S. *et al.* Degenerated human intervertebral discs contain autoantibodies against extracellular matrix proteins. *Eur Cell Mater* **27**, 251–263 (2014).
57. Stirling, A. , Worthington, T. , Rafiq, M. , Lambert, P. A. , & Elliott, T. S. Association between sciatica andPropionibacterium acnes. *The Lancet* **357**, 2024–2025 (2001).
58. Albert, H. B. *et al.* Does nuclear tissue infected with bacteria following disc herniations lead to Modic changes in the adjacent vertebrae? *European Spine Journal* **22**, 690–696 (2013). doi:10.1007/s00586-013-2674-z.
59. Ohrt-Nissen, S. *et al.* Bacterial biofilms: a possible mechanism for chronic infection in patients with lumbar disc herniation—a prospective proof-of-concept study using fluorescence in situ hybridization. *Apmis* **126**, 440–447 (2018).
60. Capoor, M. N. *et al.* Propionibacterium acnes biofilm is present in intervertebral discs of patients undergoing microdiscectomy. *PLoS One* **12**, e0174518 (2017).
61. Dudli, S., Miller, S., Demir-Deviren, S. & Lotz, J. C. Inflammatory response of disc cells against Propionibacterium acnes depends on the presence of lumbar Modic changes. *European spine journal* **27**, 1013–1020 (2018).

62. Lin, Y. *et al.* Propionibacterium acnes induces intervertebral disc degeneration by promoting nucleus pulposus cell apoptosis via the TLR2/JNK/mitochondrial-mediated pathway. *Emerg Microbes Infect* **7**, 1–8 (2018).
63. Rajasekaran, S. *et al.* ISSLS PRIZE IN CLINICAL SCIENCE 2017: Is infection the possible initiator of disc disease? An insight from proteomic analysis. *European Spine Journal* **26**, 1384–1400 (2017). doi:10.1007/s00586-017-4972-3.
64. Urquhart, D. M. *et al.* Could low grade bacterial infection contribute to low back pain? A systematic review. *BMC Med* **13**, 13 (2015). doi:10.1186/s12916-015-0267-x.
65. Ganko, R., Rao, P. J., Phan, K. & Mobbs, R. J. Can bacterial infection by low virulent organisms be a plausible cause for symptomatic disc degeneration? A systematic review. *Spine (Phila Pa 1976)* **40**, E587–E592 (2015).
66. Fayad, F. *et al.* Relation of inflammatory modic changes to intradiscal steroid injection outcome in chronic low back pain. *Eur Spine J* **16**, 925–931 (2007). doi:10.1007/s00586-006-0301-y.
67. Koivisto, K. *et al.* Efficacy of zoledronic acid for chronic low back pain associated with Modic changes in magnetic resonance imaging. *BMC Musculoskelet Disord* **15**, 64 (2014). doi:10.1186/1471-2474-15-64.
68. Beaudreuil, J., Dieude, P., Poiraudreau, S. & Revel, M. Disabling chronic low back pain with Modic type 1 MRI signal: Acute reduction in pain with intradiscal corticotherapy. *Ann Phys Rehabil Med* **55**, 139–147 (2012). doi:https://doi.org/10.1016/j.rehab.2012.01.004.
69. Cao, P. *et al.* Intradiscal injection therapy for degenerative chronic discogenic low back pain with end plate Modic changes. *Spine J* **11**, 100–106 (2011). doi:10.1016/j.spinee.2010.07.001.
70. Koreckij, T. *et al.* Prospective, randomized, multicenter study of intraosseous basivertebral nerve ablation for the treatment of chronic low back pain: 24-Month treatment arm results. *North American Spine Society Journal (NASSJ)* **8**, (2021). doi:10.1016/j.xnsj.2021.100089.
71. Schnapp, W., Martiatu, K. & Delcroix, G. J.-R. Basivertebral nerve ablation for the treatment of chronic low back pain in a community practice setting: 6 Months follow-up. *North American Spine Society Journal (NASSJ)* **14**, 100201 (2023). doi:https://doi.org/10.1016/j.xnsj.2023.100201.
72. Koreckij, T. *et al.* Prospective, randomized, multicenter study of intraosseous basivertebral nerve ablation for the treatment of chronic low back pain: 24-Month treatment arm results. *North American Spine Society Journal (NASSJ)* **8**, (2021). doi:10.1016/j.xnsj.2021.100089.
73. Conger, A., Burnham, T. R., Clark, T., Teramoto, M. & McCormick, Z. L. The Effectiveness of Intraosseous Basivertebral Nerve Radiofrequency Ablation for the Treatment of Vertebrogenic Low Back Pain: An Updated Systematic Review with Single-Arm Meta-analysis. *Pain Medicine* **23**, S50–S62 (2022). doi:10.1093/pm/pnac070.
74. Levy, O. *et al.* Shattering barriers toward clinically meaningful MSC therapies. *Sci Adv* **6**, eaba6884 (2024). doi:10.1126/sciadv.aba6884.
75. Akeda, K. *et al.* Intradiscal Injection of Autologous Platelet-Rich Plasma Releasate to Treat Discogenic Low Back Pain: A Preliminary Clinical Trial. *Asian Spine J* **11**, 380–389 (2017). doi:10.4184/asj.2017.11.3.380.
76. Comella, K., Silbert, R. & Parlo, M. Effects of the intradiscal implantation of stromal vascular fraction plus platelet rich plasma in patients with degenerative disc disease. *J Transl Med* **15**, 12 (2017). doi:10.1186/s12967-016-1109-0.

77. Dabrowska, S., Andrzejewska, A., Janowski, M. & Lukomska, B. Immunomodulatory and Regenerative Effects of Mesenchymal Stem Cells and Extracellular Vesicles: Therapeutic Outlook for Inflammatory and Degenerative Diseases. *Front Immunol* **11**, (2021).
78. Manniche, C., Morsø, L. & Kiertzner, L. Vertebral endplate changes/Modic changes: an audit study using antibiotics in 147 chronic low back pain patients. *Global Spine J* **6**, s-0036 (2016).
79. Albert, H. B., Manniche, C., Sorensen, J. S. & Deleuran, B. W. Antibiotic treatment in patients with low-back pain associated with Modic changes Type 1 (bone oedema): a pilot study. *Br J Sports Med* **42**, 969–973 (2008).
80. Albert, H. B., Sorensen, J. S., Christensen, B. S. & Manniche, C. Antibiotic treatment in patients with chronic low back pain and vertebral bone edema (Modic type 1 changes): a double-blind randomized clinical controlled trial of efficacy. *European Spine Journal* **22**, 697–707 (2013). doi:10.1007/s00586-013-2675-y.
81. Al-Falahi, M. A., Salal, M. H. & Abdul-Wahab, D. M. *Antibiotic Treatment in Patients with Chronic Low Back Pain and Vertebral Bone Edema (Modic Type I Changes): A Randomized Clinical Controlled Trial of Efficacy*. *THE IRAQI POSTGRADUATE MEDICAL JOURNAL* vol. 13 (2014).
82. Bråten, L. C. H. *et al.* Clinical effect modifiers of antibiotic treatment in patients with chronic low back pain and Modic changes - secondary analyses of a randomised, placebo-controlled trial (the AIM study). *BMC Musculoskelet Disord* **21**, 458 (2020). doi:10.1186/s12891-020-03422-y.
83. Kristoffersen, P. M. *et al.* Oedema on STIR modified the effect of amoxicillin as treatment for chronic low back pain with Modic changes—subgroup analysis of a randomized trial. *Eur Radiol* **31**, 4285–4297 (2021). doi:10.1007/s00330-020-07542-w.
84. Heggli, I. *et al.* Low back pain patients with Modic type 1 changes exhibit distinct bacterial and non-bacterial subtypes. *Osteoarthr Cartil Open* **6**, (2024). doi:10.1016/j.ocarto.2024.100434.
85. da Rocha, V. M. *et al.* Would Cutibacterium acnes Be the Villain for the Chronicity of Low Back Pain in Degenerative Disc Disease? Preliminary Results of an Analytical Cohort. *J Pers Med* **13**, 598 (2023).
86. Nouh, M. R. & Eid, A. F. Magnetic resonance imaging of the spinal marrow: basic understanding of the normal marrow pattern and its variant. *World J Radiol* **7**, 448 (2015).
87. Woods, K. & Guezguez, B. Dynamic Changes of the Bone Marrow Niche: Mesenchymal Stromal Cells and Their Progeny During Aging and Leukemia. *Front Cell Dev Biol* **9**, (2021).
88. Nouh, M. R. & Eid, A. F. Magnetic resonance imaging of the spinal marrow: Basic understanding of the normal marrow pattern and its variant. *World J Radiol* **7**, 448 (2015).
89. Carroll, K. W., Feller, J. F. & Tirman, P. F. J. Useful internal standards for distinguishing infiltrative marrow pathology from hematopoietic marrow at MRI. *Journal of Magnetic Resonance Imaging* **7**, 394–398 (1997). doi:https://doi.org/10.1002/jmri.1880070224.
90. Levine, C. D., Schweitzer, M. E. & Ehrlich, S. M. Pelvic marrow in adults. *Skeletal Radiol* **23**, 343–347 (1994).
91. Shah, L. M. & Hanrahan, C. J. MRI of spinal bone marrow: part 1, techniques and normal age-related appearances. *American journal of roentgenology* **197**, 1298–1308 (2011).
92. Kristoffersen, P. M. *et al.* Short tau inversion recovery MRI of Modic changes: a reliability study. *Acta Radiol Open* **9**, 2058460120902402 (2020). doi:10.1177/2058460120902402.

93. Tomaszewski, K. A., Saganiak, K., Gładysz, T. & Walocha, J. A. The biology behind the human intervertebral disc and its endplates. *Folia Morphol (Warsz)* **74**, 157–168 (2015).
94. Crump, K. B. *et al.* Cartilaginous endplates: A comprehensive review on a neglected structure in intervertebral disc research. *JOR Spine* **6**, e1294 (2023). doi:<https://doi.org/10.1002/jsp2.1294>.
95. Fields, A. J., Sahli, F., Rodriguez, A. G. & Lotz, J. C. Seeing double: a comparison of microstructure, biomechanical function, and adjacent disc health between double- and single-layer vertebral endplates. *Spine (Phila Pa 1976)* **37**, E1310–E1317 (2012).
96. Moon, S. M. *et al.* Evaluation of intervertebral disc cartilaginous endplate structure using magnetic resonance imaging. *European Spine Journal* **22**, 1820–1828 (2013). doi:[10.1007/s00586-013-2798-1](https://doi.org/10.1007/s00586-013-2798-1).
97. Roberts, S., Menage, J. & Urban, J. P. G. Biochemical and structural properties of the cartilage endplate and its relation to the intervertebral disc. *Spine (Phila Pa 1976)* **14**, 166–174 (1989).
98. Maroudas, A., Stockwell, R. A., Nachemson, A. & Urban, J. Factors involved in the nutrition of the human lumbar intervertebral disc: cellularity and diffusion of glucose in vitro. *J Anat* **120**, 113 (1975).
99. Roberts, S., Urban, J. P. G., Evans, H. & Eisenstein, S. M. Transport properties of the human cartilage endplate in relation to its composition and calcification. *Spine (Phila Pa 1976)* **21**, 415–420 (1996).
100. Oegema Jr, T. R. Biochemistry of the intervertebral disc. *Clin Sports Med* **12**, 419–438 (1993).
101. Jensen, T. S., Karppinen, J., Sorensen, J. S., Niinimäki, J. & Leboeuf-Yde, C. Vertebral endplate signal changes (Modic change): A systematic literature review of prevalence and association with non-specific low back pain. *European Spine Journal* vol. 17 1407–1422 Preprint at <https://doi.org/10.1007/s00586-008-0770-2> (2008). doi:[10.1007/s00586-008-0770-2](https://doi.org/10.1007/s00586-008-0770-2).
102. Dolor, A. *et al.* Matrix modification for enhancing the transport properties of the human cartilage endplate to improve disc nutrition. *PLoS One* **14**, e0215218 (2019).
103. Habib, M. *et al.* Intradiscal treatment of the cartilage endplate for improving solute transport and disc nutrition. *Front Bioeng Biotechnol* **11**, (2023).
104. Bonnheim, N. B. *et al.* The contributions of cartilage endplate composition and vertebral bone marrow fat to intervertebral disc degeneration in patients with chronic low back pain. *European Spine Journal* **31**, 1866–1872 (2022). doi:[10.1007/s00586-022-07206-x](https://doi.org/10.1007/s00586-022-07206-x).
105. Farshad-Amacker, N. A., Hughes, A., Herzog, R. J., Seifert, B. & Farshad, M. The intervertebral disc, the endplates and the vertebral bone marrow as a unit in the process of degeneration. *Eur Radiol* **27**, 2507–2520 (2017). doi:[10.1007/s00330-016-4584-z](https://doi.org/10.1007/s00330-016-4584-z).
106. Heggli, I. *et al.* POS0417 ACTIVATED NEUTROPHILS DEGRADE CARTILAGE ENDPLATES. *Ann Rheum Dis* **82**, 464–465 (2023). doi:[10.1136/annrheumdis-2023-eular.197](https://doi.org/10.1136/annrheumdis-2023-eular.197).
107. Liebscher, T., Haefeli, M., Wuertz, K., Nerlich, A. G. & Boos, N. Age-Related Variation in Cell Density of Human Lumbar Intervertebral Disc. *Spine (Phila Pa 1976)* **36**, (2011).
108. De Geer, C. M. Intervertebral Disk Nutrients and Transport Mechanisms in Relation to Disk Degeneration: A Narrative Literature Review. *J Chiropr Med* **17**, 97–105 (2018). doi:<https://doi.org/10.1016/j.jcm.2017.11.006>.

109. Grunhagen, T., Wilde, G., Soukane, D. M., Shirazi-Adl, S. A. & Urban, J. P. G. Nutrient Supply and Intervertebral Disc Metabolism. *JBJS* **88**, (2006).
110. Wei, Q., Zhang, X., Zhou, C., Ren, Q. & Zhang, Y. Roles of large aggregating proteoglycans in human intervertebral disc degeneration. *Connect Tissue Res* **60**, 209–218 (2019). doi:10.1080/03008207.2018.1499731.
111. INOUE, H. Three-dimensional architecture of lumbar intervertebral discs. *Spine (Phila Pa 1976)* **6**, 139–146 (1981).
112. Naqvi, S. M. & Buckley, C. T. Extracellular matrix production by nucleus pulposus and bone marrow stem cells in response to altered oxygen and glucose microenvironments. *J Anat* **227**, 757–766 (2015). doi:https://doi.org/10.1111/joa.12305.
113. Pattappa, G. *et al.* Diversity of intervertebral disc cells: phenotype and function. *J Anat* **221**, 480–496 (2012).
114. Iatridis, J. C., MacLean, J. J., O'Brien, M. & Stokes, I. A. F. Measurements of proteoglycan and water content distribution in human lumbar intervertebral discs. *Spine (Phila Pa 1976)* **32**, 1493 (2007).
115. Eyre, D. R. & Muir, H. Types I and II collagens in intervertebral disc. Interchanging radial distributions in annulus fibrosus. *Biochemical Journal* **157**, 267 (1976).
116. Sakai, D., Nakai, T., Mochida, J., Alini, M. & Grad, S. Differential phenotype of intervertebral disc cells: microarray and immunohistochemical analysis of canine nucleus pulposus and anulus fibrosus. *Spine (Phila Pa 1976)* **34**, 1448–1456 (2009).
117. Teraguchi, M. *et al.* Prevalence and distribution of intervertebral disc degeneration over the entire spine in a population-based cohort: the Wakayama Spine Study. *Osteoarthritis Cartilage* **22**, 104–110 (2014). doi:10.1016/j.joca.2013.10.019.
118. Urban, J. P. G. & Roberts, S. Degeneration of the intervertebral disc. *Arthritis Res Ther* **5**, 1–11 (2003).
119. Lyons, G., Eisenstein, S. M. & Sweet, M. B. E. Biochemical changes in intervertebral disc degeneration. *Biochimica et Biophysica Acta (BBA)-General Subjects* **673**, 443–453 (1981).
120. Yamamoto, J. *et al.* Fas ligand plays an important role for the production of pro-inflammatory cytokines in intervertebral disc nucleus pulposus cells. *Journal of Orthopaedic Research* **31**, 608–615 (2013).
121. Risbud, M. V & Shapiro, I. M. Role of cytokines in intervertebral disc degeneration: pain and disc content. *Nat Rev Rheumatol* **10**, 44–56 (2014). doi:10.1038/nrrheum.2013.160.
122. Kang, J. D. *et al.* Herniated lumbar intervertebral discs spontaneously produce matrix metalloproteinases, nitric oxide, interleukin-6, and prostaglandin E2. *Spine (Phila Pa 1976)* **21**, 271–277 (1996).
123. Oegema, T. R. J., Johnson, S. L., Aguiar, D. J. & Ogilvie, J. W. Fibronectin and Its Fragments Increase With Degeneration in the Human Intervertebral Disc. *Spine (Phila Pa 1976)* **25**, (2000).
124. Bisson, D. G., Mannarino, M., Racine, R. & Haglund, L. For whom the disc tolls: Intervertebral disc degeneration, back pain and toll-like receptors. *Eur Cell Mater* **41**, 355–369 (2021). doi:10.22203/eCM.v041a23.

125. Ruel, N. *et al.* Fibronectin Fragments and the Cleaving Enzyme ADAM-8 in the Degenerative Human Intervertebral Disc. *Spine (Phila Pa 1976)* **39**, 1274–1279 (2014). doi:10.1097/BRS.0000000000000397.
126. Melrose, J. *et al.* Biglycan and fibromodulin fragmentation correlates with temporal and spatial annular remodelling in experimentally injured ovine intervertebral discs. *Eur Spine J* **16**, 2193–2205 (2007).
127. Erwin, W. M. *et al.* The biological basis of degenerative disc disease: proteomic and biomechanical analysis of the canine intervertebral disc. *Arthritis Res Ther* **17**, 240 (2015). doi:10.1186/s13075-015-0733-z.
128. Piccinini, A. M. & Midwood, K. S. DAMPening Inflammation by Modulating TLR Signalling. *Mediators Inflamm* **2010**, 672395 (2010). doi:10.1155/2010/672395.
129. Vasiliadis, E. S., Pneumaticos, S. G., Evangelopoulos, D. S. & Papavassiliou, A. G. Biologic treatment of mild and moderate intervertebral disc degeneration. *Molecular Medicine* **20**, 400–409 (2014).
130. Trout, J. J., Buckwalter, J. A. & Moore, K. C. Ultrastructure of the human intervertebral disc: II. Cells of the nucleus pulposus. *Anat Rec* **204**, 307–314 (1982).
131. Masaryk, T. J. *et al.* Effects of chemonucleolysis demonstrated by MR imaging. *J Comput Assist Tomogr* **10**, 917–923 (1986).
132. Krock, E. *et al.* Toll-like receptor activation induces degeneration of human intervertebral discs. *Sci Rep* **7**, (2017). doi:10.1038/s41598-017-17472-1.
133. Klawitter, M. *et al.* Expression and regulation of toll-like receptors (TLRs) in human intervertebral disc cells. *European Spine Journal* **23**, 1878–1891 (2014). doi:10.1007/s00586-014-3442-4.
134. Krock, E., Millecamps, M., Currie, J. B., Stone, L. S. & Haglund, L. Low back pain and disc degeneration are decreased following chronic toll-like receptor 4 inhibition in a mouse model. *Osteoarthritis Cartilage* **26**, 1236–1246 (2018). doi:10.1016/j.joca.2018.06.002.
135. SZTROLOVICS, R., RECKLIES, A., Roughley, P. & MORT, J. Hyaluronate degradation as an alternative mechanism for proteoglycan release from cartilage during interleukin-1 $\beta$ -stimulated catabolism. *Biochemical Journal - BIOCHEM J* **362**, (2002). doi:10.1042/0264-6021:3620473.
136. Chen, G. Y. & Nuñez, G. Sterile inflammation: sensing and reacting to damage. *Nat Rev Immunol* **10**, 826–837 (2010).
137. Matzinger, P. Tolerance, danger, and the extended family. *Annu Rev Immunol* **12**, 991–1045 (1994).
138. McInnes, I. B. & Schett, G. The pathogenesis of rheumatoid arthritis. *New England Journal of Medicine* **365**, 2205–2219 (2011).
139. Hansson, G. K. & Hermansson, A. The immune system in atherosclerosis. *Nat Immunol* **12**, 204–212 (2011).
140. Sohn, D. H. *et al.* Plasma proteins present in osteoarthritic synovial fluid can stimulate cytokine production via Toll-like receptor 4. *Arthritis Res Ther* **14**, 1–13 (2012).
141. Hernandez, C., Huebener, P. & Schwabe, R. F. Damage-associated molecular patterns in cancer: a double-edged sword. *Oncogene* **35**, 5931–5941 (2016).

142. Venegas, C. & Heneka, M. T. Danger-associated molecular patterns in Alzheimer's disease. *Journal of Leucocyte Biology* **101**, 87–98 (2017).
143. Newton, K. & Dixit, V. M. Signaling in innate immunity and inflammation. *Cold Spring Harb Perspect Biol* **4**, a006049 (2012).
144. Akira, S. TLR signaling. *From innate immunity to immunological memory* 1–16 (2006).
145. Janeway, C. A. Approaching the asymptote? Evolution and revolution in immunology. in *Cold Spring Harbor symposia on quantitative biology* vol. 54 1–13 (Cold Spring Harbor Laboratory Press, 1989).
146. Midwood, K. *et al.* Tenascin-C is an endogenous activator of Toll-like receptor 4 that is essential for maintaining inflammation in arthritic joint disease. *Nat Med* **15**, 774–780 (2009).
147. Schaefer, L. *et al.* The matrix component biglycan is proinflammatory and signals through Toll-like receptors 4 and 2 in macrophages. *J Clin Invest* **115**, 2223–2233 (2005).
148. Babelova, A. *et al.* Biglycan, a danger signal that activates the NLRP3 inflammasome via toll-like and P2X receptors. *Journal of Biological Chemistry* **284**, 24035–24048 (2009).
149. Tan, M. H. *et al.* Deletion of the alternatively spliced fibronectin EIIIA domain in mice reduces atherosclerosis. *Blood* **104**, 11–18 (2004).
150. Ellman, M. B. *et al.* Toll-like receptor adaptor signaling molecule MyD88 on intervertebral disk homeostasis: in vitro, ex vivo studies. *Gene* **505**, 283–290 (2012).
151. Rajan, N. E. *et al.* Toll-Like Receptor 4 (TLR4) expression and stimulation in a model of intervertebral disc inflammation and degeneration. *Spine (Phila Pa 1976)* **38**, 1343–1351 (2013).
152. Gawri, R. *et al.* High mechanical strain of primary intervertebral disc cells promotes secretion of inflammatory factors associated with disc degeneration and pain. *Arthritis Res Ther* **16**, 1–14 (2014).
153. Quero, L. *et al.* Hyaluronic acid fragments enhance the inflammatory and catabolic response in human intervertebral disc cells through modulation of toll-like receptor 2 signalling pathways. *Arthritis Res Ther* **15**, 1–13 (2013).
154. Rajasekaran, S. *et al.* Inflammaging determines health and disease in lumbar discs—evidence from differing proteomic signatures of healthy, aging, and degenerating discs. *The Spine Journal* **20**, 48–59 (2020).
155. Gruber, H. E. *et al.* High-mobility group box-1 gene, a potent proinflammatory mediators, is upregulated in more degenerated human discs in vivo and its receptor upregulated by TNF- $\alpha$  exposure in vitro. *Exp Mol Pathol* **98**, 427–430 (2015).
156. Miller, R. E. *et al.* An aggrecan fragment drives osteoarthritis pain through Toll-like receptor 2. *JCI Insight* **3**, (2018). doi:10.1172/jci.insight.95704.
157. Lees, S. *et al.* Bioactivity in an aggrecan 32-mer fragment is mediated via Toll-like receptor 2. *Arthritis & rheumatology* **67**, 1240–1249 (2015).
158. Greg Anderson, D., Li, X., Tannoury, T., Beck, G. & Balian, G. A Fibronectin Fragment Stimulates Intervertebral Disc Degeneration In Vivo. *Spine (Phila Pa 1976)* **28**, (2003).
159. Schmidli, M. R. *et al.* Fibronectin Fragments and Inflammation During Canine Intervertebral Disc Disease. *Front Vet Sci* **7**, (2020). doi:10.3389/fvets.2020.547644.



## **Chapter 2: Aims and Relevance**

Despite the growing evidence implicating Modic changes (MC) as significant contributors to low back pain, there remains a limited understanding of the underlying pathomechanisms associated with this condition. While MCs manifest as vertebral bone marrow lesions, the pathology also strongly involves the endplate and the disc. This multi-tissue involvement makes the disease very complex to investigate. To be able to develop targeted treatments for MCs, it is crucial to unravel the processes occurring in each of these tissues but also to understand how it all connects and ultimately leads to the formation of MCs. Therefore, the primary goal of this thesis was to gain a deeper understanding of the pathobiology of MCs, with a particular focus on the intervertebral disc.

The diverse aspects covered in this thesis are categorized into the following chapters, each with specific aims and hypotheses:

### **Chapter 3: Bone marrow Stromal Cells in Modic type 1 changes promote neurite outgrowth**

#### Motivation and Relevance:

The project's significance lies in addressing the gap in understanding the mechanisms behind the heightened innervation of the MC1 vertebral body via the basivertebral nerve, as well as increases in neurite growth in MC1 endplates. Currently, the drivers behind these phenomena remain unclear. Notably, bone marrow stromal cells (BMSCs) have been identified as dysregulated in MC1 bone marrow and are prominently located alongside blood and nerve vessels. Consequently, BMSCs emerge as prime candidates for potentially driving the increased innervation observed, suggesting a pivotal role in this process. Understanding the underlying factors driving the condition will enable the development of more precise pain treatments for MC1 patients, potentially involving direct targeting of the BMSCs population.

#### Aim:

Determine whether MC1 bone marrow stromal cells can enhance nerve growth.

#### Hypothesis:

We hypothesize that the dysregulated MC1 BMSCs contribute significantly to the increased innervation of the MC1 bone marrow.

### **Chapter 4: Intervertebral disc microbiome in Modic Changes: lack of result replication underscores the need for a consensus in low-biomass microbiome analysis**

#### Motivation and Relevance:

The project's significance lies in the emerging field of the disc microbiome, which challenges traditional views of disc sterility and offers new clinical insights. However, methodological inconsistencies in disc microbiome studies create discrepancies. Harmonized protocols are crucial to advancing understanding and clinical implications.

### Aim:

- i) To compare our methods and results with previous disc microbiome studies and to identify the differences in the bioinformatic pipeline
- ii) to demonstrate, based on our data, how variations in the previously identified bioinformatic parameters can yield distinct outcomes
- iii) to gain insights into the differences in microbiome profiles among non-Modic change (nonMC) discs, Modic type 1 change (MC1) discs, and Modic type 2 change (MC2) discs.

### Hypothesis:

We hypothesize that i.) a comprehensive comparison of our methods and findings with prior disc microbiome studies will reveal variations in the applied methodologies, ii) that manipulating key bioinformatic parameters will result in variations in outcomes, thereby emphasizing the importance of methodological nuances, and iii) that an exploration of microbiome profiles among nonMC discs, MC1 discs, and MC2 discs will reveal distinctive microbial compositions.

## **Chapter 5: Pro-inflammatory and catabolic gene expression in cartilage endplate cells after stimulation of toll-like receptor 2**

### Motivation and Relevance:

This project focuses on the currently overlooked biological functions of cartilage endplate cells (CEPCs), focusing on their capacity to exacerbate inflammation in degenerating discs found adjacent to them. CEPCs are examined for their ability to detect Damage-Associated Molecular Patterns (DAMPs) and Pathogen-Associated Molecular Patterns (PAMPs) originating from neighboring discs through Toll-like receptors (TLRs). Activation of Toll-like receptors (TLRs) on cartilage endplate cells (CEPCs) has the potential to heighten inflammation and trigger the release of catabolic cytokines, particularly given their notably higher density compared to cells within the disc itself. This would highlight potential therapeutic targets for mitigating inflammation by selectively inhibiting these receptors on CEPCs.

### Aim:

To first investigate the expression of TLRs in CEPCs, and then to show that TLR2 signaling causes pro-inflammatory and pro-catabolic changes in CEPC.

### Hypothesis:

We hypothesize that CEPCs express TLRs, especially the TLRs involved in DAMP and PAMP recognition (TLR1, 2, 4, 6) and that their activation can induce pro-inflammatory and catabolic cytokine release.

## **Chapter 6: Increased HTRA1 Generated Fragment Abundance in the Degradome of Modic Type 1 Discs**

(main project of this doctoral thesis)

### Motivation and Relevance:

This chapter constitutes the main project within this doctoral thesis, centered on the premise that while degenerated discs are a prerequisite for MC development, not all degenerating discs progress to MCs. Consequently, this work proposes and investigates a specific disc degeneration mechanism unique to MC1 which triggers a sequence of events ultimately leading to MC1 in the adjacent bone marrow. The pathobiology of MCs remains largely unknown, and to develop targeted and disease modifying therapies, a deeper comprehension of the biological mechanisms is imperative. This study of a newly proposed MC1 disease mechanism will further uncover the biological processes underlying MC1, thus presenting new targets for treatment.

### Aim:

Investigate whether the degradome of the MC1 disc is different and assess whether fragments found more abundant in the MC1 disc have the potential to induce tissue damage in the adjacent cartilage endplate by functioning as damage associated molecular patterns.

### Hypothesis:

We hypothesize i.) that the MC1 discs contain more ECM-derived fragments which are generated through a MC1-specific mechanism and ii.) that these fragments act as pro-inflammatory DAMPs, activating not only TLRs in the disc but also in the adjacent CEP and inducing tissue destruction.

# **Chapter 3: Bone marrow stromal cells in Modic type 1 changes promote neurite outgrowth**

**Tamara Mengis<sup>1,2\*</sup>, Nick Herger<sup>1,2</sup>, Irina Heggli<sup>1,2</sup>, Jan Devan<sup>1,2</sup>, José Miguel Spirig<sup>3</sup>, Christoph J. Laux<sup>3</sup>, Florian Brunner<sup>2</sup>, Mazda Farshad<sup>3</sup>, Oliver Distler<sup>1</sup>, Stefan Dudli<sup>1</sup>**

<sup>1</sup>Center of Experimental Rheumatology, Department of Rheumatology, University Hospital Zurich, University of Zurich, Switzerland

<sup>2</sup>Department of Physical Medicine and Rheumatology, Balgrist University Hospital, Balgrist Campus, University of Zurich, Switzerland

<sup>3</sup>Department of Orthopedics, Balgrist University Hospital, University of Zurich, Switzerland

**Frontiers in Cell and Developmental Biology, 11**

(Reprinted with permission of “Frontiers in Cell and Developmental Biology”)

### 3.1 Abstract

The pain in patients with Modic type 1 changes (MC1) is often due to vertebral body endplate pain, which is linked to abnormal neurite outgrowth in the vertebral body and adjacent endplate. In this study, the aim was to understand the role of MC1 bone marrow stromal cells (BMSCs) in neurite outgrowth. BMSCs can produce neurotrophic factors, have been shown to be pro-fibrotic in MC1, and expand in the perivascular space where sensory vertebral nerves are located. The study involved the exploration of the BMSC transcriptome in MC1, co-culture of MC1 BMSCs with the neuroblastoma cell line SH-SY5Y, analysis of supernatant cytokines and analysis of gene expression changes in co-cultured SH-SY5Y. Transcriptomic analysis revealed upregulated brain-derived neurotrophic factor (BDNF) signaling-related pathways. Co-cultures of MC1 BMSCs with SH-SY5Y cells resulted in increased neurite sprouting compared to co-cultures with control BMSCs. The concentration of BDNF and other cytokines supporting neuron growth were increased in MC1 vs. control BMSCs co-cultures supernatants. Together, these findings show that MC1 BMSCs provide strong pro-neurotrophic cues to nearby neurons and could be a relevant disease-modifying treatment target.

Keywords: Low back pain, neurotrophic, stromal cells, Modic changes, neurite outgrowth, basivertebral nerve

### 3.2 Introduction

Low back pain (LBP) sensation can be caused by sensory nerves of the vertebra <sup>1</sup>. Often, LBP is attributed to nerve root compression by the lumbar intervertebral disc. Moreover, vertebral endplate bone marrow lesions, known as Modic changes (MC), are a source of vertebral body endplate pain and add to LBP <sup>2-4</sup>. The increased number of nerve fibers found within the vertebral bodies affected by MC can contribute to the experience of pain (Conger et al., 2022; Ohtori et al., 2006). “Low back vertebral endplate pain” (DM54.51) has recently been added to the International Classification of Diseases (ICD-11) as a subclassification of patients with LBP and MC.

The innervation of the vertebral body primarily arises from the gray rami communicantes, which are branches of the spinal nerves emerging from the sympathetic trunk <sup>6</sup>. From there, sensory fibers, which originate from the sinuvertebral nerves, are distributed to the vertebral body and are known as basivertebral nerve fibers <sup>7</sup>. The presence of vertebral body innervation has been shown in healthy individuals <sup>8-10</sup>. The ability of these nerve fibers to transmit nociceptive signals can be assumed due to the presence of substance P and S-100 in the basivertebral nerve <sup>8,9</sup>. Yet, the role of the vertebral body and endplate innervation by the basivertebral nerve in LBP remains poorly understood.

The best evidence for a role of the basivertebral nerve in LBP exists for MC. MC are lesions in the vertebral body visualized on T1- and T2-weighted magnetic resonance (MR) images and can be classified into three interconvertible subtypes: an inflammatory-fibrotic type 1 (MC1), a fatty type 2 (MC2), and a sclerotic type 3 (MC3) <sup>2,11</sup>. MC1 is most associated with pain <sup>12</sup>. Two studies report increased protein gene product 9.5 (PGP-9.5) nerve density in defective MC1 endplates (Fields et al., 2014; Ohtori et al., 2006), suggesting that the basivertebral nerve may play a significant role in the generation and transmission of pain in MC1.

Despite the evidence for endplate neo-innervation in MC, the drivers responsible for the enhanced innervation are unknown. Nerves primarily grow alongside blood vessels within the bone marrow<sup>9,15,16</sup>. Bone marrow stromal cells (BMSCs) surround blood vessels in the bone marrow and are found to participate in the formation and remodeling of blood vessels and nerves within the bone marrow microenvironment<sup>17,18</sup>. In MC1, BMSCs are dysregulated and perivascular BMSCs are increased in number<sup>19</sup>. Generally, various mesenchymal stromal cells have been shown to be pro-neurotrophic<sup>20</sup>, however, it is unknown if the dysregulated MC1 BMSCs have an increased neurotrophic capacity.

Due to its high prevalence and socio-economic burden, it is crucial to identify the drivers of the increased innervation of the vertebral body through the basivertebral nerve in order to understand and ultimately treat LBP with MC1. We hypothesize that the dysregulated MC1 BMSCs contribute significantly to the increased innervation of the MC1 bone marrow. The aim of this study was to determine if MC1 BMSCs can enhance nerve growth.

### 3.3 Materials and Methods

#### *Gene set enrichment analysis of existing MC1 BMSCs dataset*

The published RNA sequencing data set of MC1 vs. intra-patient control BMSCs (ENA PRJEB39993) was used to investigate enriched gene sets<sup>19</sup>. Gene set enrichment analysis (GSEA) was performed using GSEA software v.4.3.2 (University of California San Diego, CA, USA and Broad Institute, Cambridge, MA, USA) with signal-to-noise ratio as the gene ranking metric. Gene sets from Molecular Signatures Database, specifically c2.cp.wikipathways (v7.5.1) were investigated<sup>21</sup>.

#### *BMSCs isolation and culture*

The research followed the principles outlined in the Declaration of Helsinki and received approval from the local Ethics Commission (#2017-00761; approved on June 05, 2017). Bone marrow aspirates from MC1 lesions and intra-patient vertebral control areas were obtained and isolated from patients undergoing spinal fusion surgery as described previously (Figure 1A/B) (Heggli et al., 2021). Before the surgery was performed, the patient's back pain was recorded with the visual analog scale (VAS). Inclusion criteria for the selection of the six patients were the absence of current or chronic systemic inflammatory or infectious diseases, as well as no prior lumbar fusion. Two aspirates were taken per patient as described previously<sup>22</sup>. One aspirate was taken from an MC1 region and the other from a non-affected control region using a Jamshidi needle before screw insertion. BMSCs (CD73<sup>+</sup>, CD90<sup>+</sup>, and CD105<sup>+</sup> and CD14<sup>-</sup>, CD19<sup>-</sup>, CD34<sup>-</sup> and CD45<sup>-</sup> measured by flow cytometry) were isolated through plastic adherence from vertebral bone marrow aspirates. Aspirates were centrifuged at 4° C, 700g for 15 min, followed plasma and fat layer removal. The remaining aspirate was seeded in T75 flask and expanded to passage 2 in Minimum Essential Medium  $\alpha$  (MEM- $\alpha$ ) without nucleosides (Gibco, Reinach, Switzerland), 50 U/mL penicillin/streptomycin (P/S), (Gibco), 10 mM 4-(2-hydroxyethyl)-1-piperazineethanesulfonic acid (HEPES) (Gibco), 10% heat-inactivated fetal calf serum (FCS), and 2.5 ng/mL human basic fibroblast growth factor (bFGF) (PeproTech, London, UK)

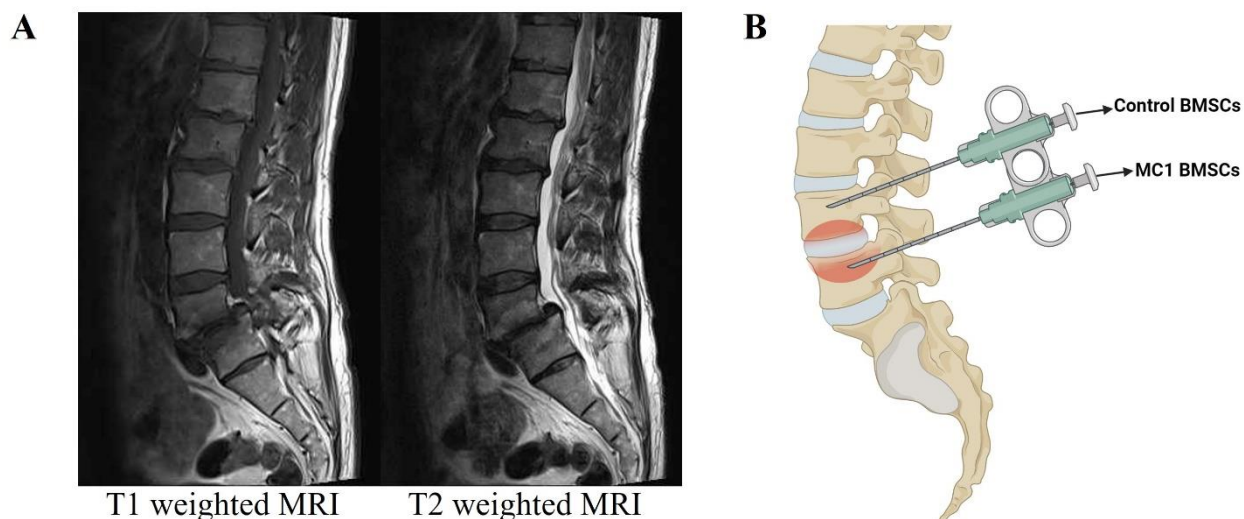


**Figure 1.** (A) Representative T1 and T2 weighted MRI of MC1 patient. (B) Schematic representation of regions used for aspirations. This allowed for isolation of control and MC1 BMSCs from the same patient.

### *Co-culture of BMSCs and SH-SY5Y*

To investigate the effect of MC1 BMSCs on neurite growth, MC1 and control BMSCs from 6 different patients ( $n = 6$  MC1 + 6 intra-patient controls) were co-cultured with passage 13-15 SH-SY5Y neuroblastoma cells (LuBioScience GmbH, Zurich, Switzerland) for 8 days. Preparation for co-culture consisted of SH-SY5Y cell expansion in SH-SY5Y growth medium (Dulbecco's Modified Eagle Medium (DMEM) (Gibco), 10% FCS, 5% L-Glutamine, 5% P/S, 5% HEPES) for 3-5 days as well as separate expansion of MC1 and control BMSCs in BMSCs growth medium. This was followed by pre-differentiation of SH-SY5Y for 48 h in SH-SY5Y differentiation media (DMEM, 2% B-27 without vitamin A (Gibco), 10  $\mu$ M retinoic acid). BMSCs (25'000 cells/insert) were seeded in Corning® transparent PET membrane cell culture inserts with 1  $\mu$ m pore size using BMSCs growth medium. SH-SY5Y cells were seeded separately into 6-well plates (75'000 cells/well) in SH-SY5Y differentiation medium. After 24 hours the cell culture inserts containing BMSCs were combined with the SH-SY5Y cells and cultured for 8 days in SH-SY5Y differentiation medium with media change on day 4. Three pre-defined regions of interest were imaged on days 1, 4, 6, and 8 at 4x magnification (Widefield Nikon Eclipse Ti2, inverted) using NIS-Elements with JOBS module (Nikon). Neurite outgrowths of SH-SY5Y cells were quantified on recorded images with the Fiji Image J Ridge Detection Plugin. Parameters for the Ridge Detection consisted of 2.7-line width, high contrast 100, low contrast 95, Sigma 1.00, lower threshold 4.20, upper threshold 6.00, and minimum line length 20.00. The sum of the neurite length from the three images was calculated. Fold changes to day 0 were calculated for each day. The significance was evaluated for each day between MC1 and intra-patient control using multiple paired t-tests of  $\log_2$  fold changes corrected for multiple comparisons using the Holm-Šidák method<sup>23</sup>.

To examine if brain-derived neurotrophic factor (BDNF) was responsible for the observed differences in neurite outgrowth, its receptor tyrosine kinase receptor B (TrkB) was inhibited. The same co-culture setup was used with the addition of either 10  $\mu$ M ANA-12 (Tocris Bioscience, Bristol, United Kingdom) dissolved in



dimethyl sulfoxide (DMSO) (Roth AG, Arlesheim, Switzerland), a small molecule that antagonizes TRKB, or DMSO only to the media. The media was changed on day 4 and the inhibitor freshly added. The chosen concentration of ANA-12 is the highest non-toxic dose based on pre-experiments. For the analysis, the fold change of ANA-12 dissolved in DMSO treated co-culture relative to DMSO treated co-culture was calculated for each group on each day individually. Significance was tested on log<sub>2</sub> fold changes by fitting a mixed effects model followed by multiple comparisons by two-stage linear step-up procedure of Benjamini, Krieger and Yekutieli<sup>24</sup>.

### *Cytokine Array*

A total of 30 neurotrophic cytokines were analyzed using C-Series Human Neuro Discovery Array C2 (RayBiotech, Georgia, USA) in the conditioned media of BMSCs/SH-SY5Y co-cultures from four patients (n = 4 MC1 + 4 intra-patient controls). Images were analyzed using the Protein Array Analyzer Plugin for ImageJ 1.53q. The negative control spot was subtracted from each spot and then presented as the ratio of the signal intensity of the positive control spot. Cytokines with a minimum intensity of 10 % of the positive control spot in at least one measurement were included. Significance was tested on detected cytokines with multiple paired t-tests corrected for multiple comparisons by two-stage linear step-up procedure of Benjamini, Krieger and Yekutieli<sup>24</sup>.

### *Quantitative real-time polymerase chain reaction (qPCR)*

The gene expression of both BMSCs and their co-cultured SH-SY5Y cells was analyzed for changes between control and MC1. RNA isolation was performed according to the RNeasy Mini Kit (Qiagen, Hilden, Germany) manufacturer protocol with cell lysis performed in RLT buffer containing 1% β-mercaptoethanol (Gibco) including the optional DNase digestion step. Reverse transcription of 100 ng RNA was performed using the SensiFast cDNA synthesis kit (Meridian Bioscience, USA).

**Table 1 Primer pairs for qPCR**

<b>Gene</b>	<b>Forward</b>	<b>Reverse</b>
BDNF	5'-CTA CGA GAC CAA GTG CAA TCC-3'	5'-AAT CGC CAG CCA ATT CTC TTT-3'
GAPD	5'- ATTCCACCCATGGCAAATTC-3'	5'-GGGATTTCATTGATGACAAGC-3'
HPRT1	5'-AGA ATG TCT TGA TTG TGG AAG A-3'	5'-ACC TTG ACC ATC TTT GGA TTA-3'
LAMB1	5'-TCA CCT CCC CTT ATC CCT GT-3'	5'-GGC AGC CAG CAC GCT TAG-3'
NES	5'-CCT CAA GAT GTC CCT CAG CC-3'	5'CCA GCT TGG GGT CCT GAA AG-3'
NEUROD1	5'-CCG TCC GCC GAG TTT G-3'	5'-GCG GTG CCT GAG AAG ATT G-3'
NGF	5'-GAG CGC AGC GGT GCA TAG-3'	5'-CTC TC T GAG TGT GGT TCC GC-3'
NGFR	5'-CCT CAT CCC TGT CTA TTG CTC-3'	5'-GTT GGC TCC TTG CTT GTT CTG-3'
NT3	5'-TTA CCT TGG ATG CCA CGG AG-3'	5'-CGC GTC CAC CTT TCT CTT CAT-3'
TRKA	5'-CAT CGT GAA GAG TGG TCT CCG-3'	5'-GAG AGA GAC TCC AGA GCG TTG AA-3'
TRKB	5'-TCT GCT CAC TTC ATG GGC TG-3'	5'-GTG GTG TCC CCG ATG TCA TT-3'
TRKC	5'-TTA CCT TGG ATG CCA CGG AG-3'	5'-CGC GTC CAC CTT TCT CTT CAT-3'
TUBB3	5'-GGC CTC TTC TCA CAA GTA CG-3'	5'-CCA CTC TGA CCA AAG ATG AAA-3'

Relative mRNA levels were quantified with use of the SensiFAST SYBR No-Rox kit (Labgene, Châtel-Saint-Denis, Switzerland) on a magnetic induction real-time qPCR cycler (Labgene). Cycle conditions after initial

denaturation at 95°C for 300s were as follows: 40 cycles of 5 seconds at 95 °C, 20 seconds at 60 °C, 10 seconds at 72 °C, followed by melting curve analysis. Analysis was done with the  $\Delta\Delta Cq$  method and with normalization to the housekeeping genes Hypoxanthine-guanine phosphoribosyltransferase (HPRT1) or Glyceraldehyde-3-Phosphate Dehydrogenase (GADPH) for BMSCs and SH-SY5Y cells, respectively. All used primer sequences are listed in Table 1. Paired t-test of MC1 vs. control  $\log_2$  fold change values was done to test for significance.

### *RNA sequencing and analysis of SH-SY5Y*

RNA was isolated from the 8-day co-cultured SH-SY5Y cells as described above. RNA fraction was enriched using Poly(A) selection. For library preparation, Illumina TruSeq Stranded mRNA library preparation protocol was used and subsequently sequenced on an Illumina NovaSeq 6000 instrument with a total of 200 million reads and the use of a single-read configuration of 100 base pairs.

The reference genome GRCh38.p13 was utilized to align the reads to the genome. Transcript quantification was performed with Kallisto. The transcriptome reference used for this step is based on GENCODE, GRCh38.p13 Release 42. Finally, differential expression analysis to compare gene expression profiles between two groups was performed using the EdgeR package in R. TMM was used for count normalization within EdgeR. The differential expression was calculated with the GLM method using the QL test. Differentially expressed genes were defined as  $FDR < 25\%$ .

GSEA was performed with WEB-based GEne SeT AnaLysis Toolkit (WebGestalt) on the Reactome gene sets with use of a cut-off false discovery rate ( $FDR < 25\%$ ) to prevent overlook of enriched gene sets due to the lack of coherence by most expression datasets.  $\log_2$  fold change was used as input with 1000 permutations<sup>25</sup>.

### *Statistical Analysis*

All statistical analyses were performed with GraphPad Prism V9.5.1. The significance level was  $\alpha = 0.05$  if not stated otherwise.

## 3.4 Results

### *Patients*

BMSCs of patients 1-6 were used for co-culture while 1-4 were used for TRKB inhibition experiments. The co-culture supernatants of patients 1-4 were analyzed for their cytokines and the co-cultured SH-SY5Y cells of these patients were used for qPCR and bulk RNA sequencing. The patients had a mean age of  $65.5 \pm 16.5$  years with an average body mass index (BMI) of  $24.6 \pm 3.9$ . The reported VAS had a median score of 7 (interquartile range (IQR) = 3) for back pain (Table 2).

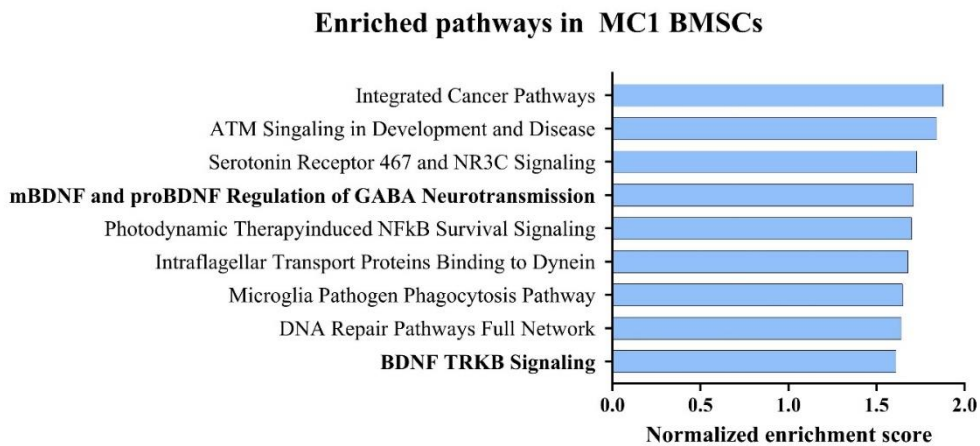
**Table 2** Patient characteristics

Patient	Age	Gender	BMI	Smoker	VAS back pain	Control Level	MC1 Level
1	83	female	26.0	yes	7	L4	L5
2	54	male	22.3	no	3	L4	S1
3	83	female	31.5	no	8	L3	L4
4	56	female	20.6	no	NA	L4	L5
5	73	male	24.3	yes	7	L4	L5
6	44	female	22.8	yes	8	L4	L5
	Mean = 65.5		Mean = 24.6		Median = 6.6		
	SD = 16.5		SD = 3.86		IQR = 3		

### *Neurotrophic signaling of MC1 BMSCs*

GSEA of MC1 vs. control BMSCs identified gene sets associated with BDNF signaling among the top 10 enriched pathways. Notably, the gene set related to BDNF TRKB signaling was significantly enriched in MC1 BMSCs (normalized enrichment score (NES) = 1.71, p-value < 0.001, FDR q-value = 0.198) (Figure 2A). Additionally, the gene sets involving the regulation of gamma-aminobutyric acid (GABA) neurotransmission by mature BDNF (mBDNF) and pro-BDNF were among the top enriched data sets (NES = 1.61, p-value < 0.001, FDR q-value = 0.346).

Next, the gene expression of neurotrophic factors and their receptors were measured (neurotrophic growth factor (NGF), BDNF, neurotrophic growth factor receptor (NGFR), neurotrophin 3 (NTF3), TRKA, TRKB) of MC1 and intra-patient control BMSCs. A significant difference was found for TRKB (p = 0.009, fold change =  $2.20 \pm 0.91$ ) and a non-significant upregulation of NGF (p = 0.055, fold change =  $1.53 \pm 0.76$ ) (Figure 2B). Taken together, pathways related to neurotrophic signaling are enriched in MC1 BMSCs.

**A****B**

**Gene expression of neurotrophins and their receptors in MC1 BMSCs**

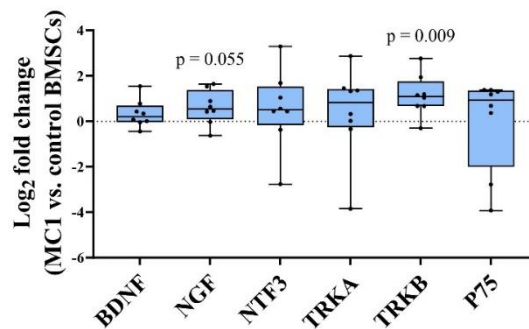


**Figure 2.** MC1 compared to intra-patient control BMSCs neurotrophic gene expression. **(A)** Gene set enrichment (GSEA) analysis of BMSCs bulk RNA sequencing indicated enrichment of BDNF signaling related pathways in MC1 BMSCs compared to control. **(B)** Gene expression of neurotrophic cytokines and respective receptors (n = 6 MC1 + 6 intra-patient controls). Significance was tested using paired t-test of MC1 compared to control log<sub>2</sub> fold change values and presented as log<sub>2</sub> fold change of MC1 vs. control BMSCs gene expression ± standard deviation.

### *Increased sprouting induced by MC1 BMSCs*

SH-SY5Y cells sprouted significantly more when co-cultured with MC1 compared to intra-patient control BMSCs (Figure 3A/B). After 4 days of co-culture, the sum of neurite outgrowths relative to day 0 was significantly greater in MC1 co-culture ( $2.88 \pm 0.80$  vs.  $1.79 \pm 0.27$ ,  $p = 0.028$ ) and persisted on day 6 ( $6.55 \pm 3.64$  vs.  $3.44 \pm 1.98$ ,  $p = 0.027$ ) and day 8 ( $7.67 \pm 3.07$  vs.  $4.18 \pm 1.29$ ,  $p = 0.028$ ) (Figure 3A and supplementary table 3).

Cytokine array analysis detected 17 out of 30 cytokines. Two of the detected cytokines were significantly different in the co-culture supernatant. Concentrations of BDNF ( $21.5 \% \pm 4.8 \%$  vs.  $29.5 \% \pm 3.5 \%$ ,  $p = 0.021$ , FDR q-value = 0.27) and of ciliary neurotrophic factor (CNTF) ( $9.3 \% \pm 2.4 \%$  vs.  $11.5 \% \pm 2.7 \%$ ,  $p = 0.030$ , FDR q-value = 0.272) were significantly higher in conditioned media of MC1 vs. control BMSCs (Figure 3C). All other cytokines were not significantly differently abundant (Table S1).

Next, the BDNF receptor TrkB was inhibited to determine if this reduced the additional outgrowth in the MC1 BMSCs co-culture. On day 8, there was a significantly lower outgrowth in the no BMSC group with TrkB inhibitor than the no BMSCs group with DMSO ( $\log_2$  fold change = -0.721,  $p = 0.042$ ) (data not shown) resulting in a significant decrease compared to control ( $p = 0.015$ ) and MC1 BMSC ( $p = 0.015$ ) co-cultures (Figure 3D). This shows the ability of the 10  $\mu\text{M}$  TrkB inhibitor ANA-12 to inhibit neurite outgrowth. The control and MC1 co-cultured SH-SY5Y did not show any decrease in neurite outgrowth when the TrkB inhibitor was added to the medium (Figure 3D).

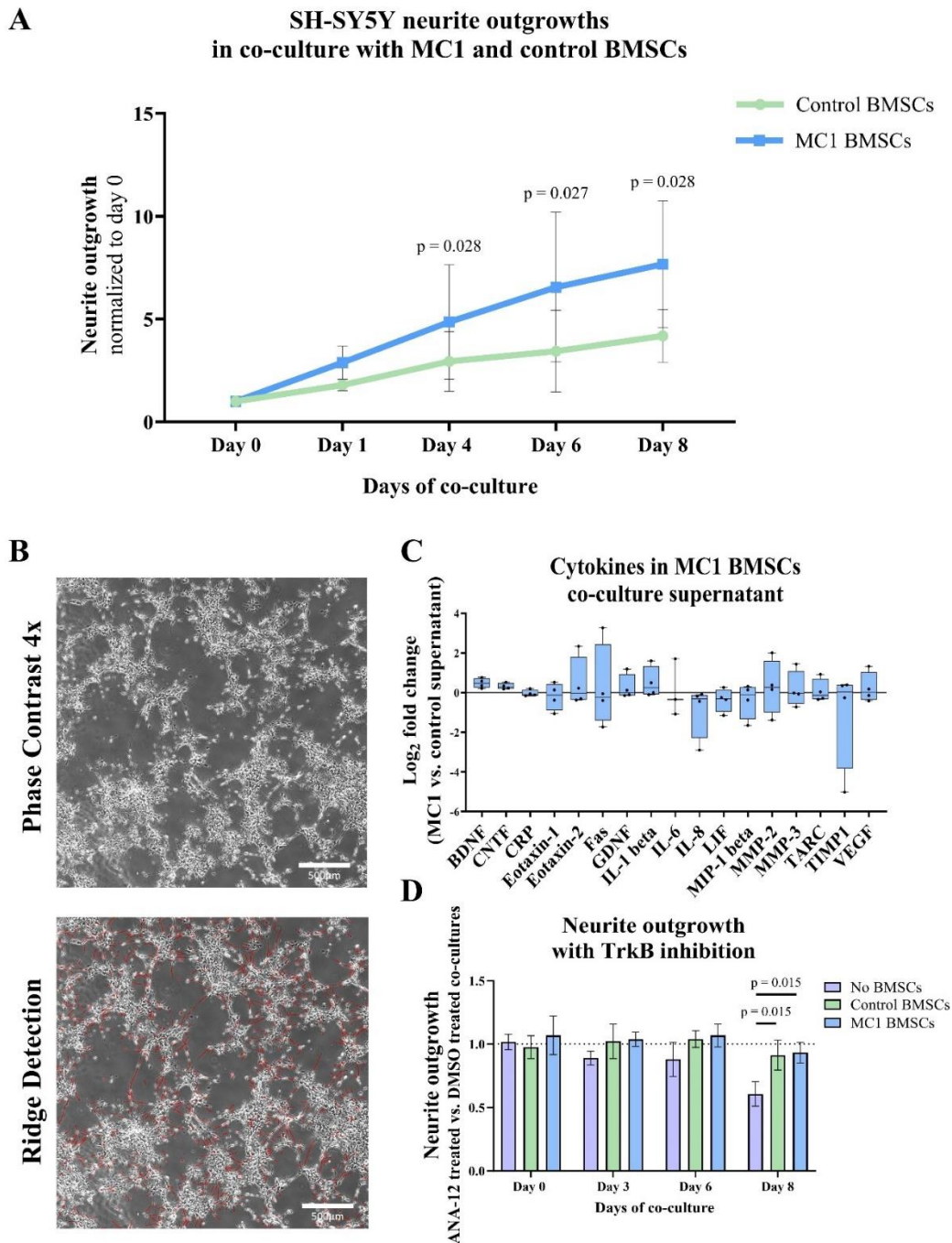


**Figure 3.** Co-culture of BMSCs with SH-SY5Y cells. **(A)** Total neurite length. Data shown as fold change to day 0 of co-culture. The significance of the difference between groups was tested on each day individually by paired t-tests of  $\log_2$  fold change to day 0 and shown as mean  $\pm$  standard deviation. **(B)** Representative image

of neurite outgrowth after 8 days of co-culture (top) and the same image after applied ridge detection (bottom) shown at 4x magnification. **(C)** Cytokines in co-culture supernatant on day 8. Data are shown as  $\log_2$  fold change of MC1 co-culture supernatant compared to control  $\pm$  standard error of mean. **(D)** Neurite outgrowth of SH-SY5Y with TrkB inhibitor ANA-12 in co-culture with either MC1 BMSCs, control BMSCs or no BMSCs over 8 days. Data shown as fold change of total neurite outgrowth in each group treated with ANA-12 dissolved in DMSO compared to their respective DMSO control  $\pm$  standard deviation.

### *MC1 BMSCs affect SH-SY5Y transcriptome*

Next, the transcriptome of the co-cultured neuroblastoma cells was investigated to determine if their gene expression was differently affected by exposure to MC1 or control BMSCs. First, commonly used differentiation markers (laminin subunit beta 1 (LAMB1), nestin (NES), neuronal differentiation 1 (NEUROD1), and tubulin beta 3 class III (TUBB3)), as well as neurotrophins (BDNF, NGF and the neurotrophic receptors (Sortilin (SORT), NGFR, TRKA, TRKB, TRKC) were measured on day 1, 4 and 8<sup>26,27</sup>. Two-way analysis of variance (ANOVA) calculated all measured differentiation markers, as well as BDNF and the TRKA to be significantly different between the measurement timepoints (day 1 vs. day 4 vs. day 8) but with no difference between the groups MC1 and control (Table S2). The exception to this was NEURDO1 which was also significantly different between the groups. This is in accordance with the microscopic images that show the neuroblastoma cells in both MC1, and control co-culture sprouted over the 8-day co-culture period.

**Table 3.** Significant dysregulated proteins (FDR < 0.25) identified by bulk RNA sequencing of co-cultured SH-SY5Y cells.

Gene Name	Description	Log <sub>2</sub> Ratio	Fold change	p-value	FDR
SEMA3A	semaphorin 3A	-0.339	0.790	0.000	0.043
RGPD5	RANBP2 like and GRIP domain containing 5	1.435	2.704	0.000	0.043
CEMIP2	cell migration inducing hyaluronidase 2	-0.647	0.639	0.000	0.043
SERF1A	small EDRK-rich factor 1A	-1.363	0.389	0.000	0.043
TFPI2	tissue factor pathway inhibitor 2	-0.409	0.753	0.000	0.043
FAM156B	family with sequence similarity 156 member B	-0.833	0.561	0.000	0.131
ENSG00000256349	novel protein	0.865	1.822	0.000	0.133
GNG11	G protein subunit gamma 11	-0.354	0.782	0.000	0.180
FAM156A	family with sequence similarity 156 member A	0.567	1.482	0.000	0.180
ASDURF	ASNSD1 upstream open reading frame	-1.389	0.382	0.000	0.196
LGR5	leucine rich repeat containing G protein-coupled receptor 5	-0.245	0.844	0.000	0.196
UPK3BL1	uroplakin 3B like 1	0.503	1.417	0.000	0.196
CORO7-PAM16	CORO7-PAM16 readthrough	-0.833	0.561	0.000	0.225
ELK3	ETS transcription factor ELK3	-0.256	0.837	0.000	0.225

As no obvious differences were observed in the most commonly investigated and measured neurotrophic genes to explain the observed phenotype, the neuroblastoma cells were subjected to bulk RNA sequencing to identify the neurotrophic mechanism mediated by MC1 BMSCs. Bulk RNA sequencing revealed 12 significantly differentially expressed genes (FDR < 0.25) (Table 3). The gene most significantly dysregulated was semaphorin 3a (SEMA3A) and downregulated in the MC1 co-cultured SH-SY5Y cells ( $\log_2$  ratio = -0.339, p



< 0.001, FDR = 0.043) (Figure 4A). SEMA3A is a gene involved in axonal guidance, specifically growth cone collapse. GSEA analysis of the co-cultured neuroblastoma transcriptome showed significant enrichment in the ECM reformation-related pathways such as activation of matrix metalloproteinases, degradation of ECM, and collagen chain trimerization. In addition, potassium channel signaling pathway, related to neuronal activity, was amongst the top enriched pathways (Figure 4B).

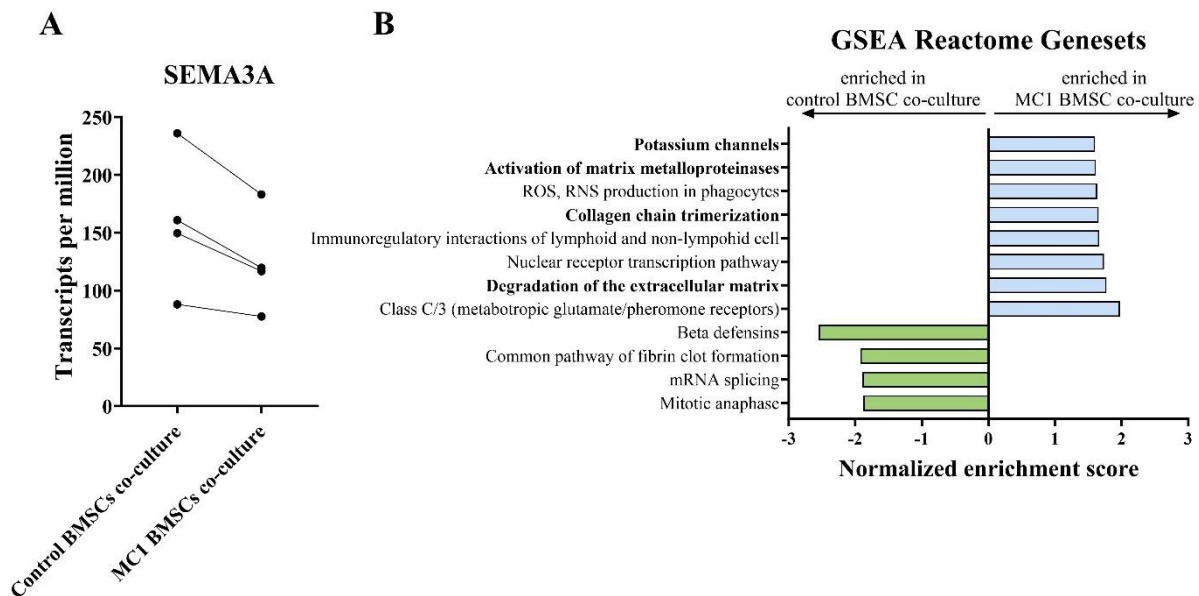


**Figure 4.** Bulk RNA sequencing of SH-SY5Y cells co-cultured with MC1 or control BMSCs for 8 days. **(A)** SEMA3A, the most dysregulated gene detected and shown as transcript per millions ( $\log_2$  ratio = -0.339,  $p = 0.00$ , FDR = 0.043). **(B)** GSEA analysis of SH-SY5Y transcriptome on Reactome database of all terms with FDR < 25%. Results shown as values of normalized enrichment score (NES).

### 3.5 Discussion

We investigated the neurotrophic function of BMSC in MC1. We found that MC1 BMSCs promote neurite growth *in-vitro*. The neurotrophic mechanisms seem to be multifactorial. Therefore, therapeutics targeting neurotropism in MC1 might be more effective by targeting the BMSC population than blocking individual neurotrophic factors.

With our model, we were able to show that MC1 BMSCs have a significant effect on neurite outgrowth. This underscores the important pathophysiological role of BMSCs in MC1. The BMSC population in MC1 has been shown to be pro-fibrotic, expanded, and associated with inflammatory changes<sup>19,28</sup>. A perivascular BMSCs population characterized as leptin receptor positive (LEPR)<sup>+</sup> and C-X-C motif chemokine ligand 12 (CXCL12)<sup>+</sup> is enriched (Heggli et al., 2021). CXCL12 is a neurotrophic factor, that supports neuronal growth, survival, and maintenance, as well as guidance for neuronal migration. Hence, the expanded CXCL12<sup>+</sup> BMSC

population in MC1 neoinnervation may lead to local accumulation of neurotrophic factors and to increased nerve growth. Our co-culture system showed that additional mechanisms are important, because the same cell numbers were used in MC1 and control co-cultures. Transcriptional analysis revealed increased expression of TRKB and NGF and enrichment of in BDNF TRKB signaling pathway activity. Consequently, despite enhanced neurotrophic signaling of MC1 BMSC, our co-culture model may even underestimate the impact of BMSC on nerve growth in MC1.

To understand what factors are produced by MC1 BMSCs that induce increased outgrowth the conditioned media of MC1 BMSCs co-cultures were investigated for neurotrophic factors. Only BDNF and CNTF were consistently increased in all four patients and BDNF had a larger effect size than CNTF. All other cytokines were highly variable. BDNF as well as CNTF are known to play a crucial role in the promotion of neuronal survival, differentiation, and neurite outgrowth. SH-SY5Y cells are particularly responsive to BDNF <sup>29,30</sup>. Therefore, we tested if inhibiting BDNF signaling in the co-culture system with the selective TrkB antagonist ANA-12 diminishes the increased sprouting seen in MC1 co-cultures <sup>29,31</sup>. Despite transcriptomic and proteomic evidence for a role of BDNF, inhibition of the BDNF receptor TrkB did not decrease neurite outgrowth. This is in accordance with previous studies reporting an increase in BDNF in the BMSCs/SH-SY5Y cells co-culture supernatant with no decrease upon inhibition of TrkB <sup>20</sup>. Since ANA-12 reduced the sprouting in SH-SY5Y in the absence of BMSCs, we concluded that TrkB signaling is important in sprouting of SH-SY5Y and can be inhibited. Yet, the inability to inhibit neurite outgrowth by TrkB inhibition in BMSC co-cultures indicates that BDNF is not the sole decisive factor. The increased neurite growth is more probable the result from a combination of growth factors and cytokines produced or activated by MC1 BMSCs.

If a single cytokine or mechanism is responsible for the increased sprouting efficiency, relevant pathways should be enriched in transcriptomic analysis of SH-SY5Y. However, the transcriptomic profile of SH-SY5Y cells co-cultured with MC1 BMSCs showed minimal differentially expressed genes compared to SH-SY5Y co-cultured with control BMSCs. Hence, increased nerve fiber growth in MC1 cultures is unlikely mediated by a dominant mechanism but rather the sum of multiple factors. Previous studies support the notion that several cellular cascades act in concert and drive neurite outgrowth, with minimal changes having significant effects <sup>27</sup>. One notable difference was the lower expression of SEMA3A in the SH-SY5Y cells co-cultured with MC1 BMSCs co-culture. SEMA3A is known for its ability to induce growth cone collapse in dorsal root ganglion (DRG) neurons and is primarily involved in the repulsive guidance of neurons which aids in preventing the growth of neurons into certain areas <sup>32</sup>. Hence, the downregulation of SEMA3A in MC1 cultures may present part of the complex mechanism involved in the increased neurite outgrowth. However, what transcriptionally regulates SEMA3A in SH-SY5Y cells and could be secreted by MC1 BMSC remains unknown. Pathway analysis of SH-SY5Y showed enrichment in gene sets involved in the degradation of ECM in SH-SY5Y co-cultured with MC1 BMSCs. Proteases such as matrix metalloproteinases (MMPs) and a disintegrin and metalloproteinase with thrombospondin motifs (ADAMTs) remove physical barriers in the extracellular space to make room for the neurites to grow. MMP expression is an important neurite growth mechanism in SH-SY5Y cells (Hearst et al., 2021; Kuzniewska et al., 2013;). Therefore, activation of matrix



degradation in SH-SY5Y may be another mechanism by which MC1 BMSCs enhance neurite outgrowth. Yet, upstream regulators of protease expression in SH-SY5Y that could be secreted by BMSCs remain unknown. Together, transcriptome analysis of SY-SY5Y confirms the concept that multiple factors are involved in creation of the pronounced increase in neurite outgrowth in the MC1 BMSC co-culture.

A novel treatment method for chronic LBP caused by MC1 is basivertebral nerve ablation (BVNA), also known as the Intracept® procedure by Relieva®. The branches of the basivertebral nerves in the center of the vertebra are ablated with radiofrequency energy. The procedure has shown positive results in pain relief and improved the quality of life for patients<sup>34</sup>. However, BVNA is not disease-modifying. It treats the pain but does not suppress neurotrophism. Hence, it potentially allows the nerves to grow back because the pro-neurotrophic MC1 BMSCs are still present. Therefore, for a more comprehensive approach, the neurotrophic activity of BMSCs should be blocked. Ways to reprogram or reverse dysregulation in MC1 BMSCs will need to be investigated in order to create a more sustainable improvement and allow for overall disease management, especially for younger patients.

### *Limitations*

SH-SY5Y cells are frequently used as a dopaminergic neuronal model *in vitro*, which provides an extensive amount of background data regarding the intrinsic mechanisms of differentiation and neurite outgrowth. Nevertheless, several limitations should be considered. First, although SH-SY5Y and DRG cells have been shown to react very similarly when co-cultured with BMSCs, the use of the neuroblastoma cell line as a model for the basivertebral nerve cells may not be fully accurate. Previous transcriptomic analysis of differentiating SH-SY5Y concluded that although the same molecular machinery is activated for differentiation initiation, they also exhibit many features commonly attributed to tumor cells, which are not representative of the nerve cells found in MC1<sup>27</sup>. Overall, it is however accepted to compare the behavior and reactions of SH-SY5Y cells to DRG cells which makes this finding highly relevant<sup>35</sup>.

Second, an important aspect that was not addressed in this study was the measure of apoptotic cells in the co-culture system. The total sum of the length of neurite outgrowth can also be influenced by the presence of apoptotic cells no longer in the differentiation state. The control co-culture condition may have contained a higher proportion of dying cells, which could potentially affect the overall neurite outgrowth. The lack of assessment for apoptosis levels or the quantification of neuroblastoma cells at each timepoint presents makes it difficult to determine whether the effects are primarily due to the enhanced neurotrophic factor production or to greater neuroprotective properties of MC1 BMSCs or even both. Either way, exposure to MC1 BMSCs leads to higher nerve fiber density *in-vitro* and can explain the clinically increased nerve fiber density.

### *Conclusion*

In conclusion, our study reveals that MC1 BMSCs exhibit neurotrophic activity, which likely contributes to the increased endplate innervation in MC1. This finding underscores the significance of BMSCs dysfunction in MC1-related vertebrogenic LBP and highlights BMSCs as a potential treatment target in MC1. These insights help pave the way for improved therapeutic treatments for MC1.

### 3.6 Conflict of Interest

SD: Aclarion

### 3.7 Author Contributions

TM: method establishment, all data acquisition, analysis, interpretation, drafting of manuscript. NH: data acquisition microscopy, method establishment. IH: data acquisition microscopy, manuscript review. JD: data interpretation, manuscript review. FB: manuscript review and funding. JS/CL/MF: surgeons. OD: funding and manuscript review. SD: supervised and funded study.

### 3.8 Funding

This study was supported by a Career Research grant from the Foundation for Research in Rheumatology (FOREUM) (SD, OD.), by a grant from the Center of Applied Biotechnology and Molecular Medicine of the University of Zurich (SD), and by a grant from the Swiss National Fond (SD, grant no 207989).

### 3.9 Acknowledgments

We would like to thank Ramona Büchel and Livia Stucki for conducting the pre-experiments and optimizing the protocols for SH-SY5Y cell culture.

### 3.10 Supplementary Material

S1: Cytokine array measurements of co-culture supernatant

	p value	Mean of MC1 BMSCs co-culture	Mean of control BMSCs co-culture	Difference	SE difference	of q value
<b>BDNF</b>	<b>0.021</b>	29.53	21.50	8.031	1.809	0.272
<b>CNTF</b>	<b>0.030</b>	11.52	9.283	2.233	0.5767	0.272
<b>CRP</b>	0.949	32.73	32.88	-0.1499	2.163	0.997
<b>Eotaxin-1</b>	0.554	15.26	17.71	-2.453	3.694	0.827
<b>Eotaxin-2</b>	0.503	14.78	10.40	4.378	5.770	0.827
<b>Fas</b>	0.550	12.81	14.52	-1.715	2.551	0.827
<b>GDNF</b>	0.535	15.96	14.24	1.722	2.465	0.827
<b>IL-1 beta</b>	0.293	19.48	13.17	6.308	4.962	0.827
<b>IL-6</b>	0.699	52.80	38.70	14.09	33.10	0.827
<b>IL-8</b>	0.067	164.6	212.5	-47.92	17.03	0.399
<b>LIF</b>	0.369	14.33	18.29	-3.969	3.767	0.827
<b>MIP-1 beta</b>	0.305	46.47	61.04	-14.57	11.82	0.827

<b>MMP-2</b>	0.432	9.751	6.867	2.884	3.187	0.827
<b>MMP-3</b>	0.701	24.98	21.93	3.049	7.200	0.827
<b>TARC</b>	0.741	17.58	16.17	1.406	3.883	0.827
<b>TIMP1</b>	0.709	329.3	374.9	-45.65	111.2	0.827
<b>VEGF</b>	0.562	20.68	16.33	4.347	6.684	0.827

**Supplementary 2: Neurotrophin gene expression in SH-SY5Y**

<b>Neurotrophic Receptors</b>												
<b>TRKA</b>												
Fixed effects (type III)		P value	P value summary	F (DFn, DFd)	Random Effects		SD	Variance	Difference group means	Difference between predicted means	SE of difference	95% CI of difference
	Day	0.0276 *		F (1.157, 6.943) = 7.3		Patient	0.4356	0.1897				
	Group	0.707 ns		F (1, 6) = 0.1554		Residual	0.4615	0.213				
	Day x Grc	0.3918 ns		F (2, 12) = 1.014								
										-0.1423	0.3611	-1.026 to 0.7411
<b>TRKB</b>												
Fixed effects (type III)		P value	P value summary	F (DFn, DFd)	Random Effects		SD	Variance	Difference group means	Difference between predicted means	SE of difference	95% CI of difference
	Day	0.5265 ns		F (2, 18) = 0.6650		Patient	0	0				
	Group	0.9913 ns		F (1, 18) = 0.000121		Residual	2.57	6.606				
	Day x Grc	0.9715 ns		F (2, 18) = 0.02894								
										0.01156	1.049	-2.193 to 2.216
<b>TRKC</b>												
Fixed effects (type III)		P value	P value summary	F (DFn, DFd)	Random Effects		SD	Variance	Difference group means	Difference between predicted means	SE of difference	95% CI of difference
	Day	0.3593 ns		F (1.230, 7.381) = 1.0		Patient	0.954	0.9101				
	Group	0.7231 ns		F (1, 6) = 0.1380		Residual	1.365	1.864				
	Day x Grc	0.8414 ns		F (2, 12) = 0.1751								
										0.3251	0.8751	-1.816 to 2.466
<b>NGFR</b>												
Fixed effects (type III)		P value	P value summary	F (DFn, DFd)	Random Effects		SD	Variance	Difference group means	Difference between predicted means	SE of difference	95% CI of difference
	Day	0.3497 ns		F (2, 12) = 1.148		Patient	0.8278	0.6852				
	Group	0.9451 ns		F (1, 6) = 0.005154		Residual	1.433	2.055				
	Day x Grc	0.7844 ns		F (2, 12) = 0.2479								
										-0.05942	0.8277	-2.085 to 1.966
<b>Neurotrophic Factors</b>												
<b>BDNF</b>												
Fixed effects (type III)		P value	P value summary	F (DFn, DFd)	Random Effects		SD	Variance	Difference group means	Difference between predicted means	SE of difference	95% CI of difference
	Day	0.001 **		F (2, 12) = 12.96		Patient	0.4495	0.202				
	Group	0.8381 ns		F (1, 6) = 0.04553		Residual	0.4847	0.235				
	Day x Grc	0.776 ns		F (2, 12) = 0.2591								
										0.07989	0.3744	-0.8363 to 0.9960
<b>NGF</b>												
Fixed effects (type III)		P value	P value summary	F (DFn, DFd)	Random Effects		SD	Variance	Difference group means	Difference between predicted means	SE of difference	95% CI of difference
	Day	0.1858 ns		F (2, 10) = 2.001		Patient	0.5644	0.3186				
	Group	0.2134 ns		F (1, 6) = 1.937		Residual	0.6934	0.4808				
	Day x Grc	0.1304 ns		F (2, 10) = 2.515								
										-0.7034	0.5054	-1.940 to 0.5332

Neurotrophins													
Sortilin													
Fixed effects (type III)		P value	P value summary	F (DFn, DFd)	Random Effects		SD	Variance	Difference group means	Difference between predicted means	SE of difference	95% CI of difference	
	Day		0.0456 *			F (2, 12) = 4.038	Patient	0.2281					0.05201
	Group		0.9933 ns			F (1, 6) = 7.645e-0	Residual	0.25					0.06249
	Day x Group		0.1574 ns			F (2, 12) = 2.165							
LAMB													
Fixed effects (type III)		P value	P value summary	F (DFn, DFd)	Random Effects		SD	Variance	Difference group means	Difference between predicted means	SE of difference	95% CI of difference	
	Day		0.0301 *			F (2, 4) = 9.536	Patient	0.08808					0.007758
	Group		0.2422 ns			F (1, 6) = 1.683	Residual	0.2191					0.048
	Day x Group		0.487 ns			F (2, 4) = 0.8660							
NES													
Fixed effects (type III)		P value	P value summary	F (DFn, DFd)	Random Effects		SD	Variance	Difference group means	Difference between predicted means	SE of difference	95% CI of difference	
	Day		0.0932 ns			F (2, 4) = 4.552	Patient	0.4931					0.2432
	Group		0.3694 ns			F (1, 6) = 0.9415	Residual	0.7577					0.574
	Day x Group		0.6337 ns			F (2, 4) = 0.5124							
NEUROD1													
Fixed effects (type III)		P value	P value summary	F (DFn, DFd)	Random Effects		SD	Variance	Difference group means	Difference between predicted means	SE of difference	95% CI of difference	
	Day		<0.0001 ****			F (2, 10) = 29.67	Patient	0					0
	Group		0.0084 **			F (1, 10) = 10.71	Residual	0.168					0.02823
	Day x Group		0.0669 ns			F (2, 10) = 3.587							
Sortilin													
Fixed effects (type III)		P value	P value summary	F (DFn, DFd)	Random Effects		SD	Variance	Difference group means	Difference between predicted means	SE of difference	95% CI of difference	
	Day		0.0456 *			F (2, 12) = 4.038	Patient	0.2281					0.05201
	Group		0.9933 ns			F (1, 6) = 7.645e-0	Residual	0.25					0.06249
	Day x Group		0.1574 ns			F (2, 12) = 2.165							
TUBB3													
Fixed effects (type III)		P value	P value summary	F (DFn, DFd)	Random Effects		SD	Variance	Difference group means	Difference between predicted means	SE of difference	95% CI of difference	
	Day		0.0018 **			F (2, 4) = 45.07	Patient	0.03679					0.001354
	Group		0.8072 ns			F (1, 6) = 0.06502	Residual	0.1327					0.01762
	Day x Group		0.9687 ns			F (2, 4) = 0.03200							

### Supplementary 3:

Normalized to day 0 (ratio)	Day 0						Day 1						Day 4						Day 6						day 8					
	88	98	122	103	138	126	88	98	122	103	138	126	88	98	122	103	138	126	88	98	122	103	138	126	88	98	122	103	138	126
Ctrl	1	1	1	1	1	1	1.42	1.78	1.72	cope	prc	2.0456	1.32	3.91	2.59	0.75	1.78	4.81	2.44	6.05	2.01	1.06	1.64	5.06	3.52	4.54	2.95	2.21	3.30	6.29
MCI	1	1	1	1	1	1	3.41	3.72	2.27	cope	prc	2.1318	1.97	8.05	3.19	1.01	3.45	7.63	6.86	9.91	2.72	1.13	2.95	10.29	7.80	10.68	3.94	2.24	5.26	10.66

## 3.11 Data Availability Statement

The raw data can be obtained upon request.

## 3.12 References chapter 3

1. Baron, R. *et al.* Neuropathic low back pain in clinical practice. *European Journal of Pain (United Kingdom)* vol. 20 861–873 Preprint at <https://doi.org/10.1002/ejp.838> (2016). doi:10.1002/ejp.838.
2. Dudli, S., Fields, A. J., Samartzis, D., Karppinen, J. & Lotz, J. C. Pathobiology of Modic changes. *European Spine Journal* vol. 25 3723–3734 Preprint at <https://doi.org/10.1007/s00586-016-4459-7> (2016). doi:10.1007/s00586-016-4459-7.
3. Lotz, J. C., Fields, A. J. & Liebenberg, E. C. The Role of the Vertebral End Plate in Low Back Pain. *Global Spine J* **3**, 153–163 (2013). doi:10.1055/s-0033-1347298.
4. Määttä, J. H. *et al.* Strong association between vertebral endplate defect and Modic change in the general population. *Sci Rep* **8**, (2018). doi:10.1038/s41598-018-34933-3.

5. Conger, A. *et al.* Vertebrogenic Pain: A Paradigm Shift in Diagnosis and Treatment of Axial Low Back Pain. *Pain Medicine (United States)* vol. 23 S63–S71 Preprint at <https://doi.org/10.1093/pm/pnac081> (2022). doi: 10.1093/pm/pnac081.
6. Antonacci MD, Mody DR & Heggeness MH. Innervation of the human vertebral body. *J Spinal Disord* **11**, 526–531 (1998).
7. Kim, H. S., Wu, P. H. & Jang, I. T. Lumbar degenerative disease part 1: Anatomy and pathophysiology of intervertebral discogenic pain and radiofrequency ablation of basivertebral and sinuvertebral nerve treatment for chronic discogenic back pain: A prospective case series and review of literature. *Int J Mol Sci* **21**, (2020). doi: 10.3390/ijms21041483.
8. Fras Christian, Kravetz Philip, Mody R Dina & Heggeness H Michael. Substance P–containing nerves within the human vertebral body. *The Spine Journal* **3**, 63–67 (2003). doi: 10.1016/s1529-9430(02)00455-2.
9. Bailey, J. F., Liebenberg, E., Degmetich, S. & Lotz, J. C. Innervation patterns of PGP 9.5-positive nerve fibers within the human lumbar vertebra. *J Anat* **218**, 263–270 (2011). doi: 10.1111/j.1469-7580.2010.01332.x.
10. Brown, M. F. *et al.* SENSORY AND SYMPATHETIC INNERVATION OF THE VERTEBRAL ENDPLATE IN PATIENTS WITH DEGENERATIVE DISC DISEASE. *J Bone Joint Surg [Br]* vol. 79 (1997). doi: 10.1302/0301-620x.79b1.6814.
11. Modic, M. T., Steinberg, P. M., Ross, J. S., Masaryk, T. J. & Carter, J. R. Degenerative disk disease: assessment of changes in vertebral body marrow with MR imaging. *Radiology* **166**, 193–199 (1988). doi:10.1148/radiology.166.1.3336678.
12. Jensen, T. S., Karppinen, J., Sorensen, J. S., Niinimäki, J. & Leboeuf-Yde, C. Vertebral endplate signal changes (Modic change): A systematic literature review of prevalence and association with non-specific low back pain. *European Spine Journal* vol. 17 1407–1422 Preprint at <https://doi.org/10.1007/s00586-008-0770-2> (2008). doi:10.1007/s00586-008-0770-2.
13. Fields, A. J., Liebenberg, E. C. & Lotz, J. C. Innervation of pathologies in the lumbar vertebral end plate and intervertebral disc. *Spine Journal* **14**, 513–521 (2014). doi:10.1016/j.spinee.2013.06.075.
14. Ohtori, S. *et al.* Tumor Necrosis Factor-Immunoreactive Cells and PGP 9.5-Immunoreactive Nerve Fibers in Vertebral Endplates of Patients With Discogenic Low Back Pain and Modic Type 1 or Type 2 Changes on MRI. *SPINE* vol. 31. doi: 10.1097/01.brs.0000215027.87102.7c.
15. Calvo, W. The innervation of the bone marrow in laboratory animals. *American Journal of Anatomy* **123**, 315–328 (1968). doi: 10.1002/aja.1001230206.
16. Carmeliet, P. & Tessier-Lavigne, M. Common mechanisms of nerve and blood vessel wiring. *Nature* vol. 436 193–200 Preprint at <https://doi.org/10.1038/nature03875> (2005). doi: 10.1038/nature03875.
17. Shi, H. *et al.* Bone marrow-derived neural crest precursors improve nerve defect repair partially through secreted trophic factors. *Stem Cell Res Ther* **10**, (2019). doi: 10.1186/s13287-019-1517-1.
18. Zhou, B. O., Yue, R., Murphy, M. M., Peyer, J. G. & Morrison, S. J. Leptin-receptor-expressing mesenchymal stromal cells represent the main source of bone formed by adult bone marrow. *Cell Stem Cell* **15**, 154–168 (2014). doi: 10.1016/j.stem.2014.06.008.
19. Heggli, I. *et al.* Pro-fibrotic phenotype of bone marrow stromal cells in modic type 1 changes. *Eur Cell Mater* **41**, 648–667 (2021). doi: 10.22203/eCM.v041a42.

20. Brohlin, M., Kingham, P. J., Novikova, L. N., Novikov, L. N. & Wiberg, M. Aging Effect on Neurotrophic Activity of Human Mesenchymal Stem Cells. *PLoS One* **7**, (2012). doi: 10.1371/journal.pone.0045052.
21. Subramanian, A. *et al.* Gene Set Enrichment Analysis: A Knowledge-Based Approach for Interpreting Genome-Wide Expression Profiles. doi: 10.1073/pnas.0506580102.
22. Dudli, S. *et al.* ISSLS PRIZE IN BASIC SCIENCE 2017: Intervertebral disc/bone marrow cross-talk with Modic changes. *European Spine Journal* **26**, 1362–1373 (2017). doi: 10.1007/s00586-017-4955-4.
23. Holm, S. A Simple Sequentially Rejective Multiple Test Procedure. *Scandinavian Journal of Statistics* **6**, 65–70 (1979).
24. Benjamini, Y., Krieger, A. M. & Yekutieli, D. Adaptive linear step-up procedures that control the false discovery rate. *Biometrika* **93**, 491–507 (2006). doi: 10.1093/biomet/93.3.491.
25. Liao, Y., Wang, J., Jaehnig, E. J., Shi, Z. & Zhang, B. WebGestalt 2019: gene set analysis toolkit with revamped UIs and APIs. *Nucleic Acids Res* **47**, W199–W205 (2019). doi: 10.1093/nar/gkz401.
26. Murillo, J. R. *et al.* Quantitative proteomic analysis identifies proteins and pathways related to neuronal development in differentiated SH-SY5Y neuroblastoma cells. *EuPA Open Proteom* **16**, 1–11 (2017). doi: 10.1016/j.euprot.2017.06.001.
27. Pezzini, F. *et al.* Transcriptomic Profiling Discloses Molecular and Cellular Events Related to Neuronal Differentiation in SH-SY5Y Neuroblastoma Cells. *Cell Mol Neurobiol* **37**, 665–682 (2017). doi: 10.1007/s10571-016-0403-y.
28. Dudli, S. *et al.* CD90-positive stromal cells associate with inflammatory and fibrotic changes in modic changes. *Osteoarthr Cartil Open* **4**, (2022). doi: 10.1016/j.ocarto.2022.100287.
29. Hromadkova, L. *et al.* Brain-derived neurotrophic factor (BDNF) promotes molecular polarization and differentiation of immature neuroblastoma cells into definitive neurons. *Biochimica et Biophysica Acta (BBA) - Molecular Cell Research* **1867**, 118737 (2020). doi: 10.1016/j.bbamcr.2020.118737.
30. Shipley, M. M., Mangold, C. A. & Szpara, M. L. Differentiation of the SH-SY5Y human neuroblastoma cell line. *Journal of Visualized Experiments* **2016**, (2016). doi: 10.3791/53193.
31. Kim, J. H. Brain-derived neurotrophic factor exerts neuroprotective actions against amyloid  $\beta$ -induced apoptosis in neuroblastoma cells. *Exp Ther Med* **8**, 1891–1895 (2014). doi: 10.3892/etm.2014.2033.
32. Luo, Y., Raible, D. & Raper, J. A. *Collapsin: A Protein in Brain That Induces the Collapse and Paralysis of Neuronal Growth Cones.* *Cell* vol. 75 (1993). doi: 10.1016/0092-8674(93)80064-1.
33. Hearst, S. *et al.* Expression of Drosophila Matrix Metalloproteinases in Cultured Cell Lines Alters Neural and Glial Cell Morphology. *Front Cell Dev Biol* **9**, (2021). doi: 10.3389/fcell.2021.610887.
34. Fischgrund, J. S. *et al.* Long-term outcomes following intraosseous basivertebral nerve ablation for the treatment of chronic low back pain: 5-year treatment arm results from a prospective randomized double-blind sham-controlled multi-center study. *European Spine Journal* **29**, 1925–1934 (2020). doi: 10.1007/s00586-020-06448-x.
35. Gangras, P. *et al.* Investigating SH-SY5Y Neuroblastoma Cell Surfaceome as a Model for Neuronal-Targeted Novel Therapeutic Modalities. *Int J Mol Sci* **23**, (2022). doi: 10.3390/ijms232315062.

# **Chapter 4: Intervertebral disc microbiome in Modic Changes: lack of result replication underscores the need for a consensus in low-biomass microbiome analysis**

**Tamara Mengis<sup>1,2</sup>, Natalia Zajac<sup>3</sup>, Laura Bernhard<sup>1,2</sup>, Irina Heggli<sup>1,2</sup>, Nick Herger<sup>1,2</sup>, Jan Devan<sup>1,2</sup>, Roy Marcus<sup>4</sup>, Florian Brunner<sup>2</sup>, Christoph Laux<sup>5</sup>, Mazda Farshad<sup>5</sup>, Oliver Distler<sup>1,2</sup>, Stefan Dudli<sup>1,2</sup>**

<sup>1</sup>Center of Experimental Rheumatology, Department of Rheumatology, University Hospital, University of Zurich, Switzerland

<sup>2</sup>Department of Physical Medicine and Rheumatology, Balgrist University Hospital, University of Zurich, Switzerland

<sup>3</sup>Functional Genomics Center Zurich, University and ETH Zurich, Zurich, Switzerland

<sup>4</sup>Department of Radiology, Balgrist University Hospital, University of Zurich

<sup>5</sup>Department of Orthopedics, Balgrist University Hospital, University of Zurich, CH

**Journal of Orthopedic Research Spine. Accepted.**

## 4.1 Abstract

**Introduction:** The emerging field of the disc microbiome challenges traditional views of disc sterility, which opens new avenues for novel clinical insights. However, the lack of methodological consensus in disc microbiome studies introduces discrepancies. The aims of this study were to i) compare the disc microbiome of non-Modic (nonMC), Modic type 1 change (MC1), and MC2 discs to findings from prior disc microbiome studies, and ii) investigate if discrepancies to prior studies can be explained with bioinformatic variations.

**Methods:** Sequencing of 16S rRNA in 70 discs (24 nonMC, 25 MC1 and 21 MC2) for microbiome profiling. The experimental setup included buffer contamination controls and was performed under aseptic conditions. Methodology and results were contrasted with previous disc microbiome studies. Critical bioinformatic steps that were different in our best-practice approach and previous disc microbiome studies (taxonomic lineage assignment, prevalence cut-off) were varied and their effect on results were compared.

**Results:** There was limited overlap of results with a previous study on MC disc microbiome. No bacterial genera were shared using the same bioinformatic parameters. Taxonomic lineage assignment using “amplicon sequencing variants” was more sensitive and detected 48 genera compared to 22 with “operational taxonomic units” (previous study). Increasing filter cut-off from 4 % to 50 % (previous study) reduced genera from 48 to 4 genera. Despite these differences, both studies observed dysbiosis with an increased abundance of gram-negative bacteria in MC discs as well as a lower beta-diversity. *Cutibacterium* was persistently detected in all groups independent of the bioinformatic approach, emphasizing its prevalence.

**Conclusion:** There is dysbiosis in MC discs. Bioinformatic parameters impact results yet cannot explain the different findings from this and a previous study. Therefore, discrepancies are likely caused by different sample preparations or true biologic differences. Harmonized protocols are required to advance understanding of the disc microbiome and its clinical implications.

**Keywords:** Microbiome, Modic changes, Metagenomics, *Cutibacterium Acnes*

## 4.2 Introduction

The microbiome of intervertebral discs (IVD) has become a focal point of intense debates within the spine research community because it challenges the longstanding paradigm of the disc’s sterility and because its clinical relevance is unclear. Particularly in the context of Modic changes (MC), the presence of bacteria, specifically *Cutibacterium acnes* (*C. acnes*), within the disc has been a long-debated topic<sup>1-4</sup>. Reports of a disc microbiome challenge the paradigm of the sterile disc and raise the questions of what are commensals and what are pathogenic bacteria<sup>5,6</sup>.

Rapid technological advancements have revolutionized our ability to explore the microbiome in low-biomass samples with next-generation sequencing (NGS). This innovation allows us to get insight into the complete microbial DNA present within a sample, which marks a significant leap forward from the traditional approach of culturing bacteria *in vitro*. In particular, the significant constraint of selecting cultural conditions that favor



the proliferation of specific bacteria was overcome with NGS (Chen, Sun, and He 2020). In addition, certain bacteria have very slow growth or remain completely unculturable and have therefore never been considered as part of the disc's microbiome. While DNA sequencing is highly sensitive and comprehensive, it cannot differentiate between live and deceased bacteria. Skeptics often focus on this aspect, suggesting that the identified bacterial DNA could potentially result from contamination or dead bacteria rather than from live resident bacteria with the potential to have a functional impact on the disc.

Rajasekaran et al. and Astur et al. were the first to perform in-depth analysis of the disc's microbiome with NGS (Astur et al., 2022; Rajasekaran et al., 2023). However, the overlap between the detected bacteria was very small. The potential causes for this disparity could be attributed to one or a combination of the following factors: First, True biologic difference, e.g. geographic and ethnic differences in patients, Second, differences in sample preparation and the presence of differing contaminating bacteria in reagents<sup>9</sup>, which mask the number of true bacteria present. Third, the bioinformatic analysis. Since they used different methodologies (points 2 and 3), true biologic differences and their clinical relevance (point 1) cannot be answered, emphasizing the need to harmonize the procedures. For example, both studies handle the control for contamination differently, which greatly affects the amount and speciation of detected bacteria. Consequently, a consensus is needed on the sample preparation, bioinformatic pipeline, and the use of contamination controls to ensure the comparability, reliability, and reproducibility of the results.

Despite the lack of methodological consensus, bacteria and particularly *C. acnes* have been found in discs using different methods (Agarwal et al., 2011; Albert et al., 2013; Capoor et al., 2016; Rajasekaran et al., 2020, 2023). The discovery of a vast number of bacteria present within the disc questioned the importance of *C. acnes* and raised the possibility that other bacteria or a state of a dysbiosis may be clinically more relevant (Astur et al., 2022; Rajasekaran et al., 2020, 2023). In prior NGS studies of IVDs, Astur et al. (2022) did not detect *C. acnes* in any disc<sup>5</sup>. In contrast, Rajasekaran identified *C. acnes*, however it was not amongst the most abundant bacterial species nor was it different between MC and non-MC discs. Hence, the new paradigm of a disc microbiome challenges the conventional notion of disc sterility and emphasizes the urgent necessity for a harmonized methodology for disc microbiome analysis. Moreover, in the context of MCs, it is essential to determine whether *C. acnes* should persist as the predominant pathogen under investigation or if a critical reassessment is warranted to encompass a broader spectrum of bacterial species.

The study aimed: i) to compare our methods and results with previous disc microbiome studies and to identify the differences in the bioinformatic pipeline, ii) to demonstrate, based on our data, how variations in the previously identified bioinformatic parameters can yield distinct outcomes; and iii) to gain insights into the differences in microbiome profiles among non-Modic change (nonMC) discs, Modic type 1 change (MC1) discs, and Modic type 2 change (MC2) discs.

## 4.3 Methods

### *Disc collection*

Twenty-four nonMC, 25 MC1, and 21 MC2 IVDs were collected aseptically from patients undergoing lumbar spinal fusion surgery at the Balgrist University Hospital Zurich between 25.05.2021 and 06.10.2022. The research followed the principles outlined in the Declaration of Helsinki and discs were collected with informed consent and with approval from the local ethics commission. Exclusion criteria were previous lumbar spinal fusions and current or chronic systemic inflammatory or infectious diseases.

A board-certified radiologist specialized in musculoskeletal conditions graded disc degeneration according to Pfirrmann<sup>14</sup> and classified adjacent bone marrow changes according to Modic<sup>15</sup> based on pre-operative magnetic resonance imaging not older than 3 months. General demographic metrics such as age, gender and BMI were collected, and patients filled out the visual analog score (VAS) for back pain and the Oswestry disability index (ODI) before surgery. Friedman's test was used to determine significant differences in age, body mass index (BMI), ODI and VAS back pain score among the three groups. Wilcoxon test was used to test differences in Pfirrmann grade between the groups and the gender distribution differences between the three groups were examined with the use of a Fisher's exact test.

Once the disc was removed, it was immediately placed in sterile tubes. All subsequent steps were also conducted in a sterile environment. The entire procedure also involved an additional 10 contamination control samples, which included all the buffers but did not contain any tissue. Each disc was minced into small pieces and mixed. Finally, the discs were snap-frozen and stored at -80 °C until all samples were collected and processed for genomic DNA extraction, 16S rRNA DNA amplification, and amplicon sequencing.

### *DNA isolation*

All discs underwent genomic DNA extraction using the Qiagen Pathogen Kit, following the manufacturer's protocol with an initial overnight incubation step with Proteinase K.

### *16S rRNA PCR*

The 16s rRNA V3-V4 region was amplified using primers with MiSeq-overhang adapters (Fwd: 5'TCGTCGGCAGCGTCAGATGTGTATAAGAGACAGCCTACGGGNGGCWGCAG and Rev: 5'GTCTCGTGGGCTCGGAGATGTGTATAAGAGACAGGACTACHVGGGTATCTAATCC). The PCR reaction consisting of 7ul forward/reverse Primer Mix (2 uM), 12.5 ul 2x KAPA Hifi HotStart Ready Mix (Roche, Basel, Switzerland) and 5.5 ul DNA template was performed using the following cycle conditions: initial denaturation at 94 °C for 2 min, 35 cycles of denaturation at 94 °C for 20 seconds, annealing at 64 °C for 30 seconds, elongation at 68 °C for 30 seconds, final elongation step at 72°C for 5 min. PCR products were verified with an agarose gel.

## *Library Preparation and sequencing*

A 2-step PCR approach was used to generate libraries; the first PCR amplifies the specific region (Forward primer: CCTACGGGNGGCWGCAG, Reverse primer: GACTACHVGGGTATCTAATCC) and the second PCR adds Illumina adapters and 8bp barcodes to the amplicons. This approach employs Truseq tag sequences. The PCR products generated from the second PCR were purified with magnetic beads. The quality and quantity of the libraries were validated using the Agilent 4200 TapeStation system and the GloMax® Explorer System, Promega. After library quantification, libraries were normalized to 10nM in Tris-Cl 10 mM, pH 8.5 with 0.1% Tween 20 and pooled equimolarly.

The Miseq Sequencing Systems (Illumina, Inc, California, USA) was used for cluster generation and sequencing according to standard protocol. Sequencing was performed with a run configuration of pair end 250bp. The sequencing raw data was processed with Trimmomatic (0.39) by trimming the Illumina-specific adapters, removing reads below average quality of Q20 and shorter than 30bp. The reads were then mapped to GRCh38.p13 human reference genome using Bowtie2 (2.4.2) with a standard set of parameters, to check for contamination resulting from off-target amplification<sup>16</sup>. The reads that mapped to the human genome were filtered out from both the forward and the reverse reads using Seqtk (1.3).

## *16s rRNA data analysis*

The described bioinformatic workflow will be referred to as our best practice approach throughout the paper. Data analysis of the pre-processed 16S rRNA reads was performed with QIIME 2 next-generation microbiome bioinformatics pipeline (v2022.2). Raw reads were transformed into a QIIME 2 artifact format (.qza) and the amplicon sequencing variants (ASV)s were extracted from the data using Divisive Amplicon Denoising Algorithm 2 (DADA2) implemented in QIIME 2 as a plugin. DADA2 corrected amplicon errors, dereplicated and denoised the sequences, identified and removed chimeras and merged the paired end reads<sup>17</sup>. The extracted representative sequences were assigned a taxonomic lineage using a sklearn-based Naive Bayes classifier trained on the SILVA v138 99% 16S database narrowed down to the V3-V4 region. The taxonomic classification was compared with a classifier trained on the Greengenes v138 99% database. SILVA database was chosen as the preferred choice due to the close correspondence between the two but an outdated classification for a small set of bacterial genomes by the Greengenes database<sup>18,19</sup>. The phylogeny plugin in QIIME 2, which utilizes MAFFT and FastTree for alignment, was also used to estimate the rooted and the unrooted tree. The data was subsequently processed in Rstudio (version 4.3). First, bacterial contaminants in the experimental samples were identified and removed from the samples with Decontam (1.20.0), using the prevalence method, comparing the composition of the positive samples to the negative controls (threshold=0.5). Additionally, ASVs present in less than 4% of the samples and having a count of less than or equal to 1 were filtered out. The gram stain of each genus was determined using the AMR R package (v2.1.0). Phyloseq (1.44.0) was used to measure a set of standard alpha diversity metrics (Shannon, Simpson, Observed, Chao1, ACE and Pielou). The significance of the difference in Shannon diversity index between samples was tested using the all-group and pairwise Kruskal–Wallis test (a non-parametric version of ANOVA). Beta

diversity (Jaccard, Bray-Curtis and weighted Unifrac) was also estimated with the phyloseq package and it was performed on transformed counts (counts per taxon normalized by the total sum of counts per sample).

### *Comparison to other disc microbiome studies*

Our study's methods and bioinformatic pipeline were compared to the ones used by Astur et al. (2020) and Rajasekaran et al. (2023) who previously used metagenomics to investigate the disc microbiome. For comparison of the microbiome disc results only the study of Rajasekaran et al.'s study (2023) was used, given that Astur et al.'s (2021) research focused on herniated discs. The main difference between the groups of our study to that of Rajasekaran et al. (2023) lies in our study's additional division of the MC group into MC1 and MC2.

### *Comparison of different bioinformatic approaches*

Based on the comparison to Rajasekaran et al.'s study the most critical steps in the bioinformatic processing pipeline were identified and the data of this study were used to compare the results when applying the methodologies from Rajasekaran's study. The main result that was compared was the extracted bacterial genera. The bioinformatic methodologies compared were 1.) taxonomic lineage assignment: ASV vs. operational taxonomic unit (OTU) and 2.) different prevalence cut-offs: 4% vs. 50%. When the prevalence cut-off is mentioned, it consistently corresponds to the minimum percentage of samples in which a particular ASV or OTU, depending on the analysis, was detected.

OTU table was computed from the ASV table with the tip glom function from the phyloseq R package using agglomerative hierarchical clustering (agnes). The data was then subsequently agglomerated at a taxonomic level of interest (genus). For comparison of OTUs and ASVs, the analysis involved the assessment of the detected genera, their distribution within each group, and the median abundance of all ASVs/OTUs across the three MC groups, both overall as well as split into gram positive and negative genera. The significance of the difference in median abundance among the groups was evaluated with use of the Friedman's test, followed by multiple comparisons adjusted for false positives through Dunn's statistical hypothesis testing.

The different filter methods were based on the number of samples in which a specific OTU or ASV was detected. Three distinct cut-off criteria were assessed: the requirement for the ASV to be present in at least 4% of all patients, the presence of the ASV in at least 50% of patients within at least one group, or the presence of the ASV in at least 50% of all patients. Pie charts showing the genera distribution within each group based on their prevalence were used for comparison of the different filters.

Invariant results from the bioinformatic variations were compared between nonMC, MC1 and MC2 and compared to Rajasekaran et al.'s (2023) MC microbiome study.

### 3.4 Results

#### *Patient demographics*

Age and gender did not differ between groups (Table 1). Disc degeneration was not significantly different between the groups ( $p = 0.448$ ). The nonMC group had higher BMI compared to the MC1 group ( $p = 0.019$ ) (Table ).

**Table 1.** Patient demographics of the groups divided into no Modic change (nonMC), Modic type 1 change (MC1) and Modic type 2 change (MC2) discs. Age, body mass index (BMI), Oswestry disability index (ODI) and visual analog scale (VAS) are indicated as mean  $\pm$  standard deviation (SD). Gender distribution is described as percentage of females per group and Pfirrmann grade is indicated as the median and the interquartile ratio (IQR). Significant p-values are highlighted in bold.

	<b>nonMC</b> (n=24)	<b>MC1</b> (n=25)	<b>MC2</b> (n=21)	<b>P-value</b>
<b>Pfirrmann Grade</b> (Median [IQR])	4 [2, 4]	4 [3, 4]	4 [4, 4.5]	0.267
<b>Age</b> (Average $\pm$ SD)	63.5 $\pm$ 17.1	62.0 $\pm$ 15.6	64.2 $\pm$ 10.2	0.781
<b>BMI</b> (Average $\pm$ SD)	30.5 $\pm$ 6.2	26.3 $\pm$ 4.2	28.2 $\pm$ 4.2	<b>0.019</b>
<b>Female</b> (Percentage)	42 %	56 %	29 %	0.197
<b>ODI</b> (Average $\pm$ SD)	43.3 $\pm$ 17.8	42.9 $\pm$ 19.7	36.4 $\pm$ 15.4	0.848
<b>VAS back pain</b> (Average $\pm$ SD)	6.6 $\pm$ 2.2	6.1 $\pm$ 2.7	6.7 $\pm$ 1.9	0.708

#### *Comparison to previous disc microbiome studies*

The comparison of the sample preparation and bioinformatic methods of the three disc metagenomic studies is shown in Table . All three studies used the same variable 16s rRNA region, and the same sequencing machine. DNA extraction was the same for Astur et al. and Rajasekaran et al. For contamination controls, our study included 10 tubes with only the reagents. The other two studies did not mention any control samples. For sequencing analysis, the three studies all used very different approaches. Differences were seen in taxonomic lineage assignment, filtering strategies, and the database used to annotate the bacteria (Table 2). No information was provided for bioinformatic identification of potential contaminant reads in the other two studies.

**Table 2.** The methods for metagenomic sequencing and analysis of discs of this study were compared to two prior disc metagenomic studies of Rajasekaran et al. (2023) and Astur et al. (2021) study.

	<b>Our study</b>	<b>Rajasekaran et al. (2023)</b>	<b>Astur et al. (2021)</b>
<b>Patients</b>	70 (24 nonMC, 25 MC1, 21 MC2)	40 (20 non-Modic, 20 Modic, 20 Control)	17 (herniated discs)
<b>Variable region used</b>	V3-V4 (341F and 806R)	V3-V4 (341F and 806R)	V3-V4
<b>Filtered for human genome content</b>	Yes, with Bowtie2 (reference genome GRCh38p13)	No	No
<b>DNA extraction</b>	QIAmp UCP Pathogen Mini Kit	QIAmp DNA Microbiome Kit	QIAmp DNA Microbiome Kit
<b>Contamination controls</b>	10 tubes included	N/A	N/A
<b>Sequencing platform</b>	Illumina	Illumina NovoSeq 6000	Illumina
<b>Decontamination strategy</b>	Decontam R package	N/A	N/A
<b>Database</b>	SILVA	Inhouse database consisting of: Greengenes, SILVA and 16s core bacterial database	RDP tools version 2.12
<b>Filtering</b>	ASVs present at count < 1 Comparison of multiple cutoffs: - >4% overall - >50% per group - >50% overall	Presence in at least 70% of samples & >100 OTUs	Minimum of 20 sequence reads
<b>Bioinformatic Pipeline</b>	QIIME2	QIIME2	Geneious Prime Softwares (Geneious Prime 2020.1.2)
<b>Taxonomic lineage assignment</b>	ASVs	OTUs	Neither

A step-by-step description of our methodology is depicted in Figure 1, highlighting different methodologies compared to Rajasekaran’s study. Initial taxonomic lineage assignment assigned 2415 ASVs (Figure 1, step 8). Decontam eliminated 120 ASVs (step 9) mainly affecting ASVs belonging to the phylum Proteobacteria, Actinobacteria and Firmicutes and on genus level this mainly affected ASVs belonging to Escheria-Shigella, Staphylococcus and Pelomonas. The second filtration step eliminated ASVs found in fewer than either 4 % or 50 % of samples with counts greater than 1 (step 10). This resulted in the removal of over 2000 ASVs, which leaves a final count of 180 and 26 ASVs, respectively.

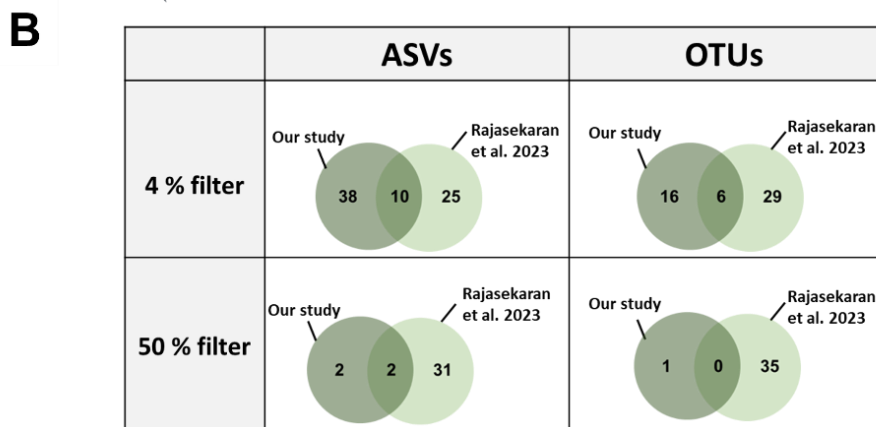
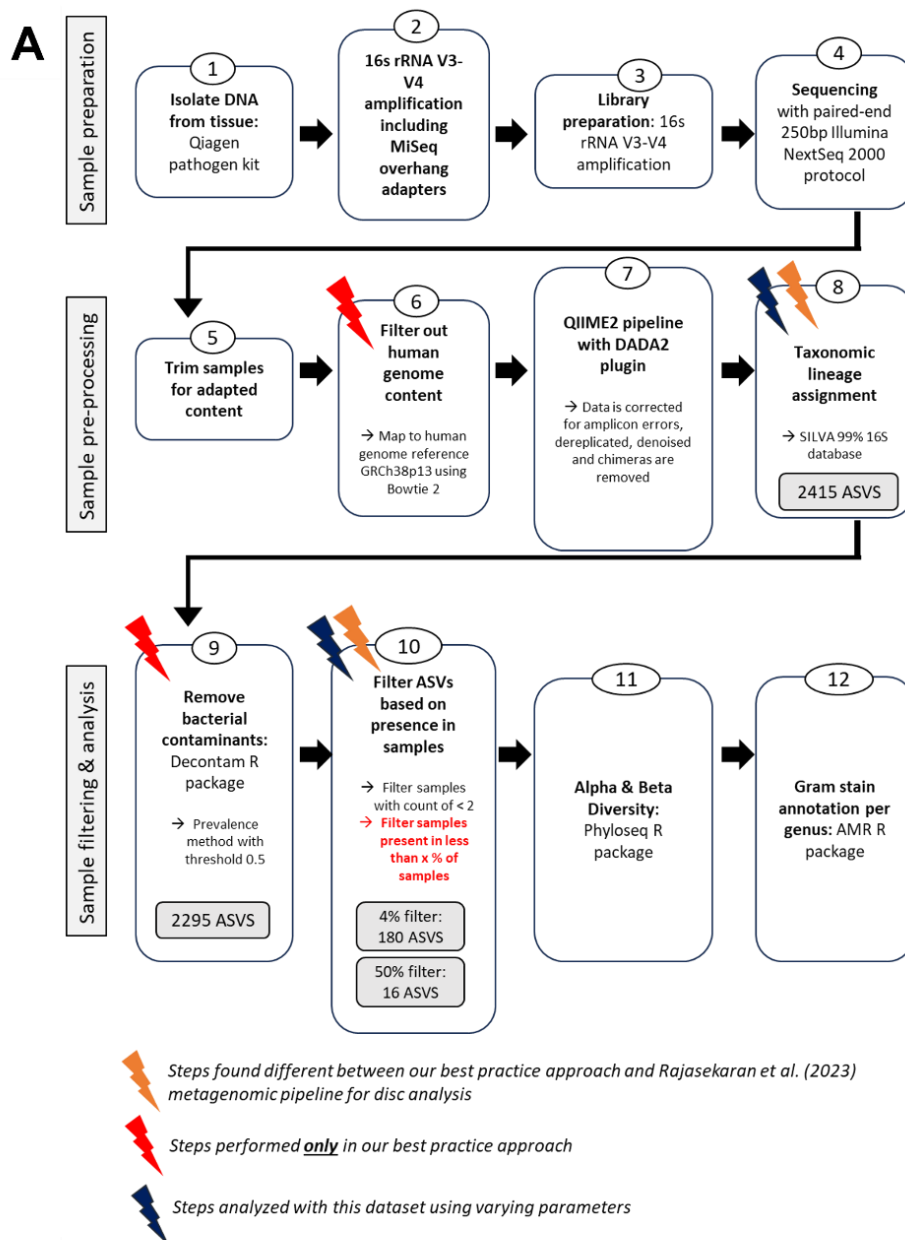


**Figure 1. (A)** The workflow used to perform our study in a best practice approach. Orange lightning bolts indicate steps found to differ from the prior investigation of the MC metagenome by Rajasekaran et al. (2023), while red indicates steps done only in this workflow and not in prior MC microbiome studies. Blue lightning bolts indicate the steps which were further investigated with the use of the dataset from this study. **(B)** Direct comparison of the number of genera detected in our study compared to the number presented by Rajasekaran et al. (2023). Different parameters were used for the analysis of our samples including the use of either ASVs or OTUs as well as the application of two different prevalence cut-off filters for the number of samples indicating the presence of these genera.

Both Rajasekaran et al.'s and our study aimed to identify differences in disc microbiome in MC discs. Therefore, we compared in-depth the two methodologies. The discrepancies consist of two steps that had different parameters (steps 8 & 10), two steps which were only implemented in this microbiome study (steps 6 & 9) (Figure 1). The two steps that differed between our and Rajasekaran's study were selected for further comparison. We found that different filters had a large effect and that ASVs detected more genera than OTU (Figure B). All possible combinations of filters and taxonomic lineage assignment failed to converge our results with Rajasekaran's result. No overlaps in genera were found when using the same parameters as in Rajasekaran's study, indicating that the observed differences are not due to filtering thresholds or taxonomic lineage assignment. Using a setup similar to Rajasekaran's setup (OTU, 50% filtering), *Methylobacterium-Methylorubrum* was the sole remaining genera in our dataset, a bacterium that Rajasekaran did not detect. They reported as the top four bacteria *Psuedomonas*, *Acinetobacter*, *Prevotella*, and *Orchobactrum*. In contrast, under our preferred parameters for exploratory screening (ASVs, 4% filtering) as well as with our most stringent filter (ASVs, 50% filtering), the top four genera were *Pelmonas*, *Sphingomonsa*, *Methylobacterium-Methylorubrum*, and *Cutibacterium*.

### *Effect of ASVs vs OTUs with respect to MC microbiome*

A decrease in bacterial diversity in MC groups was observed, which was not influenced by using ASVs or OTUs. Alpha diversity was similar in all groups (Supplementary Figure 1). Beta diversity was lowest for MC1 compared to all other groups and highest for nonMC compared to all other groups (Figure 2A).

The number of genera detected with ASV and OTU were largely different. OTU annotation identified 22, ASV annotation 48 different genera with use of a 4 % prevalence cut-off. All genera identified by OTUs were also identified with ASVs (Figure 2B), indicating that ASVs provided better resolution. The distribution of genera was also strongly affected by taxonomic lineage assignment. ASVs revealed four prominent genera, namely *Sphingomonas*, *Pelmonas*, *Methylobacterium-Methylorubrum* and *Blastomonas* while OTUs were characterized mainly by *Methylobacterium-Methylorubrum* and *Hathewayia* in nonMC and MC1 and by *Methylobacterium-Methylorurum* together with *Acinetobacter* in MC2 (Figure 2C/D). Interestingly, two out of the four dominant genera that contributed significantly to the microbiome with the use of ASVs were absent in the OTU data, which resulted in the pronounced overrepresentation of the previously named bacteria evident in the pie charts of the OTUs (Figure 2C/D).

The analysis of median abundance for all ASVs across the groups resulted in a significantly lower median ASV abundance in nonMC compared to both MC1 ( $p < 0.001$ ) and MC2 ( $p < 0.001$ ). Additionally, MC1 displayed a higher overall median ASV abundance compared to MC2 ( $p = 0.003$ ) (Figure 2E). Gram-negative bacteria significantly increased in MC1 compared to nonMC for ASVs and OTUs, with an additional increase in MC1 compared to MC2 in ASVs (Figure 2F). For gram-positive bacteria, ASVs but not OTU revealed a significantly greater abundance in MC1 compared to nonMC (Figure 2G).



Consistent findings independent of the use of ASV or OTU were that MC1 had lower beta diversity, yet more bacteria, in particular gram-negative genera (Figure 2A/E/F). In addition, similar patterns can be observed when looking at *Hathewayia* which was found to make up a large part of the microbiome in nonMC and MC1 but not in MC2, while *Acinetobacter* took its place in MC2.

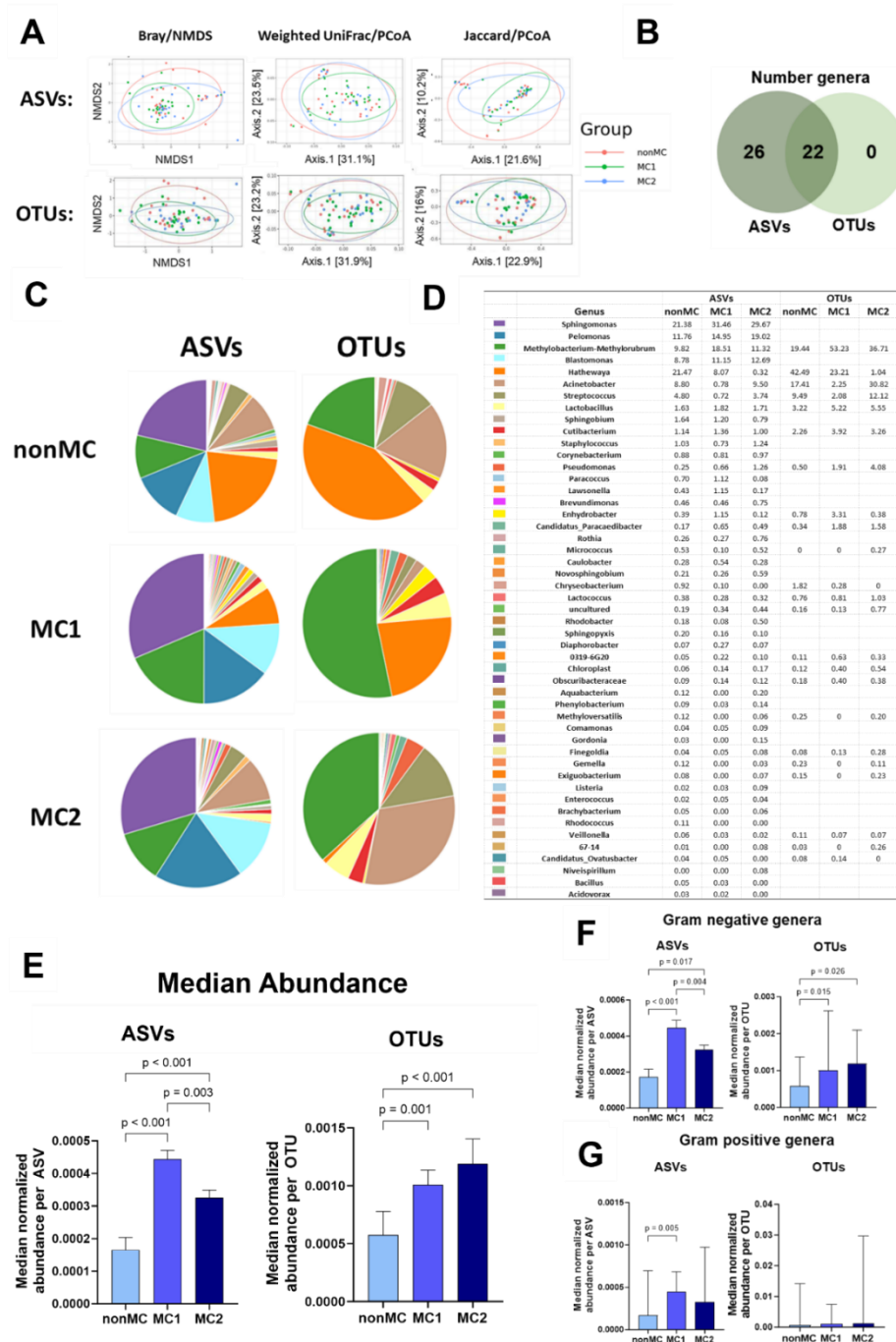


**Figure 2.** ASV compared to OTU annotation of genera found in at least 4 % of all samples. (A) Beta-diversity calculated with Bray/NMDS, Weighted UniFrac/PCoA and Jaccard/PCoA with either ASV annotation or OTU annotation. (B) The overlap of genera detected with ASVs compared to OTUs. (C) The microbial distribution of ASVs compared to OTU on the genera level with a corresponding (D) table indicating the percentage of each genus based on the median normalized abundance. (E) The median abundance of genera extracted with ASVs or OTUs compared between nonMC, MC1 and MC2. (F) Gram-negative or (G) gram – positive extracted ASVs and OTUs compared between nonMC, MC1 and MC2. Significance tested with Friedman’s test and corrected for multiple comparisons with Dunn’s statistical hypothesis testing.

## Comparison of different filter cut-offs

Using different filter cut-offs strongly affected the number and type of detected ASVs and genera (Figure 3). While a 4 % cut-off leaves 180 ASVs and 48 genera, a 50 % prevalence cut-off leaves only the genera Pelmonsa, Methylobacterium-Methylorubrum, Sphingomonas and Cutibacterium (Figure 3B/C). However, when a group specific 50 % prevalence cut-off was applied, four additional genera make the cut, as they are predominantly found in nonMC discs. These include Hathewayia, Lactobacillus, Corynebacterium, and Staphylococcus (Figure 3B/C).

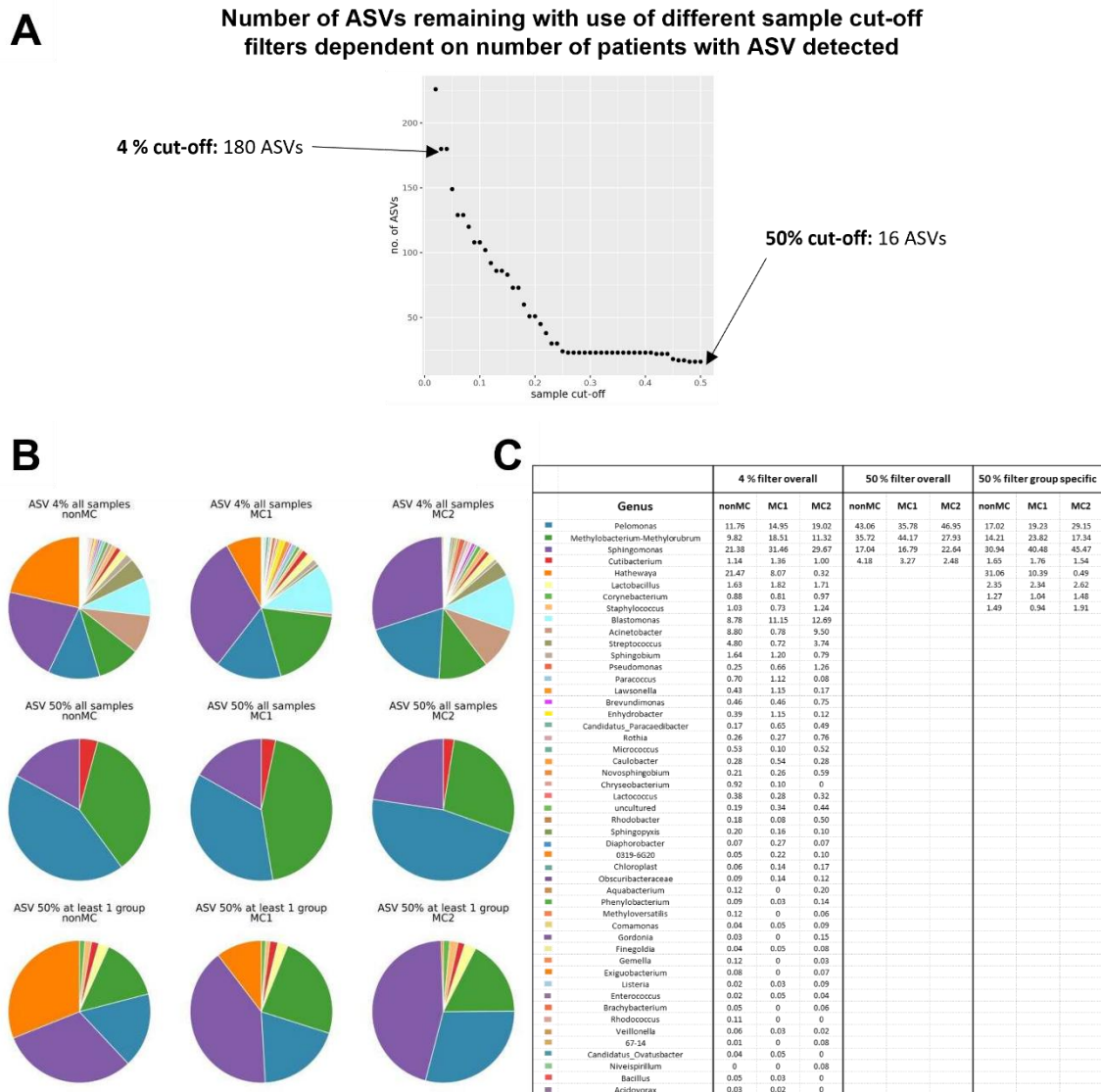


**Figure 3.** Comparison of different filter cut-offs. (A) The graph shows the number of ASVs left when the prevalence filter cut-off is set at different percentages. (B) Genera distribution based on the median abundance per genera with three different filters: genera detected in more than 4 % of patients overall (top row), genera detected in more than 50 % of patients in at least one group (middle row) and genera detected in overall more than 50 % of patients (bottom row). (C) The table depicts the information from the pie charts in percentages based on the median abundance per genus.

## *Cutibacterium in the spotlight*

Two ASVs were extracted which belong to the genus *Cutibacterium*. One was detected in 43 samples, the other in 44 out of the 70 samples, with all of them overlapping and the 44 just having one additional patient. *Cutibacterium* ASVs were present in 71 % of nonMC patients, 56 % of MC1, and 62 % of MC2 discs without statistical difference. This high rate of occurrence led to the genera *Cutibacterium* being one of four bacteria that was retained throughout all bioinformatic approaches tested.

### **3.5 Discussion**

The microbiome of the disc challenges the paradigm of a sterile disc and represents a novel and relatively unexplored domain that is currently receiving careful and critical consideration in the field. Disc dysbiosis has previously been reported for MC discs by Rajasekaran et al and with this study we provide further evidence that the disc harbors its own microbiome. In this study, consistent with Rajasekaran et al., reduced bacterial diversity in MC discs was found, indicating a state of dysbiosis. In addition, absolute number of bacteria was higher in MC1 discs, mainly of gram-negative bacteria. This suggests that they either infiltrated MC1 discs or that the environment of MC1 discs favored their proliferation. However, large differences in the number and speciation of bacteria were found compared to Rajasekaran's study. There are three possible explanations for the observed differences: 1.) true biological differences due to e.g., geographic, and ethnic differences, 2.) differences in sample preparation, e.g. DNA isolation, contaminations in buffers, 3.) differences in bioinformatic analysis. Point 1 is the most clinically relevant, yet it cannot be addressed until the source of data variance originating from points 2 and 3 is understood and minimized using a harmonized protocol. With this goal in mind, we used our dataset to test if the bioinformatic discrepancies between Rajasekaran's and our study could account for the observed differences in results. We compared the results generated by our dataset when using: A) different taxonomic assignments, i.e. ASVs vs. OTUs and B) three different filter cut-offs. We found that changing taxonomic assignment and filter cut-offs largely affects results but cannot explain the discrepancies to Rajasekaran's study. They reported 35 different genera using OTU and a 50 % filter—parameters that, as evidenced by our dataset, lead to a reduction in the number of identified bacteria. In this study, these settings resulted in only one genus. To match the high number of genera detected in their study, a less restrictive 4 % filter had to be used. Yet, the majority of genera detected remained different from the ones reported by Rajasekaran et al. This suggests that either their patients had a much richer and different microbiome (biologic variance), or that more and different bacteria were introduced during their sample preparation (e.g., different buffer solutions).

It is known that different taxonomic assignments affect the results of microbiome analysis<sup>20</sup>. OTU uses a 97 % sequence similarity to assign taxonomy. This causes grouping of similar sequences. In contrast, ASVs capture single nucleotide differences, and hence provide higher resolution and specificity than OTU. It has been suggested to use ASVs as standard due to their comprehensiveness and easier reproducibility<sup>20-22</sup>. In this study, using ASV instead of OTU almost doubled the number of genera found and mainly increased the

abundance of the bacteria found in MC2 discs. Yet, both ASV and OTU consistently showed reduced bacterial diversity in MC discs and more gram-negative bacteria in MC1 discs potentially making these robust results.

Filtering is an important step to reduce noise and errors from sequencing, mitigate sample contamination, to focus on dominant bacteria, to avoid statistical zero-inflation, and enhance statistical power. However, in low microbiome biomass tissue like the disc, stringent filtering can remove potentially important bacteria species that are only present in a subset of samples. In this study we found that a stringent filter, which only retained ASVs present in over 50 % of patients, excluded group specific ASVs. For example, *Hathewayia*, *Lactobacillus*, *Corynebacterium* and *Staphylococcus* were filtered out, because they were predominantly found in nonMC samples. To avoid this risk, the 50 % cut-off filter was applied to each group rather than all samples. This filtering strategy overcomes the mentioned drawbacks by emphasizing the bacteria most relevant for the majority of patients, potentially identifying those crucial for clinical treatments. However, when the aim of the study is to explore the diversity of the microbiome in a low biomass sample, it is not advisable to use such stringent filtering and for this case we propose the use of the 4 % cut-off. To address the risk of contamination reads when using a 4 % cut-off filter, 10 contamination control samples (not tissue) were used along with the decontamination algorithm “Decontam” in R. Decontam leverages the inverse relationship between contaminant-derived sequences and total DNA concentration for effective decontamination without data loss in low-biomass metagenomic data (Davis et al., 2018). It has previously been suggested to use *ligamentum flavum* or surrounding tissues as decontamination controls (Astur et al., 2022). However, considering them as 'negative controls' may be inappropriate because soft tissue may also harbor a microbiome (Cheng et al., 2023). In addition, the exclusion of discs with microbial presence in the surrounding tissues could eliminate critical samples if the assumption is that pathogenic bacteria enter the disc through surrounding tissue. Besides bioinformatic variations, physical sample processing before sequencing is a likely source of variance<sup>23,24</sup>. Therefore, we suggest that a harmonized protocol for disc microbiome analysis should encompass bioinformatic analysis and protocols to isolate bacterial DNA from disc tissue.

Lastly, this dataset adds further evidence for the presence of *Cutibacterium* in the disc. Notably, the genus *Cutibacterium* persisted among the five genera even under stringent filter methods using ASVs, being detected in over 50 % of samples. Our data is in agreement with Rajasekaran et al. (2023) who also found *Cutibacterium* in discs, not as one of the most abundant genera, and also without a clear association with MC discs. However, the complexity of factors that influence bacterial pathogenicity beyond absolute abundance, underscores the need to further investigate the potential pathogenic role of *Cutibacterium* in MC<sup>25,26</sup>.

This study has some limitations. Multiple surgeons and technical operation assistants were involved in collecting the tissue. Different harvesting techniques may have different risks for contamination. There was no assurance that fresh surgical tools were used to collect the disc into sterile containers. While this could have affected the observed microbiome, this random effect does not affect the observed dysbiosis in MC nor does it restrict the notion that bioinformatic processing has a large impact.

In conclusion, changing key bioinformatic parameters, i.e. taxonomic lineage assignment and filtering cut-offs had a large impact on the resulting microbiome. However, using similar parameters as a prior study

investigating the MC microbiome did not converge results. Therefore, the observed discrepancies were either introduced during sample processing or are true biologic differences. Before any clinically relevant conclusions about the role of bacteria in MC and disc degeneration can be drawn, the source of variance needs to be identified and understood, and harmonized protocols for sample processing and bioinformatic analysis are required. Ultimately, the availability of a robust and reproducible methodology will allow the exploration of this untapped metagenomic landscape as a new source of biomarkers and potential treatment targets.

### **3.6 Ethics Statement**

The study was approved by the local Ethics Commission #2018-01486; approved on 24 August 2018. The study was conducted in accordance with the local legislation and institutional requirements. The participants provided their written informed consent to participate in this study.

### **3.7 Author Contributions**

TM: patient recruitment, sample collection, methodology (DNA extraction), data acquisition, writing–original draft, and visualization. NZ: bioinformatic data analysis, writing-original draft, visualization. LB: methodology (DNA extraction), data curation, writing–review. IH: methodology, writing–review and editing. NH: writing–review and editing and methodology. JD: writing–review and editing. RM: data curation and writing–review. FB: writing–review and editing. CL: data curation, writing-review. MF: writing–review and editing. OD: funding acquisition and writing–review and editing. SD: funding acquisition and writing–review and editing.

### **3.8 Funding**

This study was supported by a career research grant from the Foundation for Research in Rheumatology (FOREUM) (SD and OD), by a FOREUM Research Voucher (SD) and by a grant from the Swiss National Fond (SD, Grant No. 207989).

### **3.9 Conflicts of Interest**

none

### **3.10 Acknowledgements**

We would also like to thank the Swiss Center for Musculoskeletal Biobanking (SCMB), which worked together with us to provide the samples in the shortest time possible for further processing. Lastly, we would like to thank the Functional Genomic Center Zurich staff for giving their inputs in the project planning and performing the sequencing.

### 3.11 References chapter 4

1. Perry, A. & Lambert, P. Propionibacterium acnes: Infection beyond the skin. *Expert Review of Anti-Infective Therapy* vol. 9 1149–1156 Preprint at <https://doi.org/10.1586/eri.11.137> (2011). doi:10.1586/eri.11.137.
2. Stirling, A. , Worthington, T. , Rafiq, M. , Lambert, P. A. , & Elliott, T. S. Association between sciatica and Propionibacterium acnes. *The Lancet* **357**, 2024–2025 (2001). doi: 10.1016/S0140-6736(00)05109-6.
3. Dudli, S. *et al.* Propionibacterium acnes infected intervertebral discs cause vertebral bone marrow lesions consistent with Modic changes. *Journal of Orthopaedic Research* **34**, 1447–1455 (2016). doi: 10.1002/jor.23265.
4. Manniche, C. & O’Neill, S. New insights link low-virulent disc infections to the etiology of severe disc degeneration and Modic changes. *Future Science OA* vol. 5 Preprint at <https://doi.org/10.2144/fsoa-2019-0022> (2019). doi: 10.2144/fsoa-2019-0022.
5. Astur, N. *et al.* Next-generation sequencing (NGS) to determine microbiome of herniated intervertebral disc. *Spine Journal* **22**, 389–398 (2022). doi: 10.1016/j.spinee.2021.09.005.
6. Rajasekaran, S. *et al.* Human intervertebral discs harbour a unique microbiome and dysbiosis determines health and disease. *European Spine Journal* **29**, 1621–1640 (2020). doi: 10.1007/s00586-020-06446-z.
7. Chen, P., Sun, W. & He, Y. Comparison of the next-generation sequencing (NGS) technology with culture methods in the diagnosis of bacterial and fungal infections. *J Thorac Dis* **12**, 4924–4929 (2020). doi: 10.21037/jtd-20-930.
8. Rajasekaran, S. *et al.* “Are we barking up the wrong tree? Too much emphasis on Cutibacterium acnes and ignoring other pathogens”— a study based on next-generation sequencing of normal and diseased discs. *Spine Journal* (2023) doi: 10.1016/j.spinee.2023.06.396.
9. Mühl, H., Kochem, A. J., Disqué, C. & Sakka, S. G. Activity and DNA contamination of commercial polymerase chain reaction reagents for the universal 16S rDNA real-time polymerase chain reaction detection of bacterial pathogens in blood. *Diagn Microbiol Infect Dis* **66**, 41–49 (2010). doi: 10.1016/j.diagmicrobio.2008.07.011.
10. Capoor, M. N. *et al.* Prevalence of propionibacterium acnes in intervertebral discs of patients undergoing lumbar microdiscectomy: A prospective cross-sectional study. *PLoS One* **11**, (2016). doi: 10.1371/journal.pone.0161676.
11. Agarwal, V., Golish, S. R. & Alamin, T. F. Bacteriologic Culture of Excised Intervertebral Disc From Immunocompetent Patients Undergoing Single Level Primary Lumbar Microdiscectomy. *Clin Spine Surg* **24**, (2011). doi: 10.1097/BSD.0b013e3182019f3a.
12. Albert, H. B. *et al.* Does nuclear tissue infected with bacteria following disc herniations lead to Modic changes in the adjacent vertebrae? *European Spine Journal* **22**, 690–696 (2013). doi: 10.1007/s00586-013-2674-z.
13. Rajasekaran, S. *et al.* “Are we barking up the wrong tree? Too much emphasis on Cutibacterium acnes and ignoring other pathogens”— a study based on next-generation sequencing of normal and diseased discs. *Spine Journal* (2023) doi:10.1016/j.spinee.2023.06.396. doi: 10.1016/j.spinee.2023.06.396.

14. Pfirrmann, C. W. A., Metzdorf, A., Zanetti, M., Hodler, J. & Boos, N. *Magnetic Resonance Classification of Lumbar Intervertebral Disc Degeneration*. *SPINE* vol. 26 (2001). doi: 10.1097/00007632-200109010-00011.
15. Modic, M. T., Steinberg, P. M., Ross, J. S., Masaryk, T. J. & Carter, J. R. Degenerative disk disease: assessment of changes in vertebral body marrow with MR imaging. *Radiology* **166**, 193–199 (1988). doi: 10.1148/radiology.166.1.3336678.
16. Walker, S. P. *et al.* Non-specific amplification of human DNA is a major challenge for 16S rRNA gene sequence analysis. *Sci Rep* **10**, (2020). doi: 10.1038/s41598-020-73403-7.
17. Prodan, A. *et al.* Comparing bioinformatic pipelines for microbial 16S rRNA amplicon sequencing. *PLoS One* **15**, (2020). doi: 10.1371/journal.pone.0227434.
18. Pruesse, E. *et al.* SILVA: a comprehensive online resource for quality checked and aligned ribosomal RNA sequence data compatible with ARB. *Nucleic Acids Res* **35**, 7188–7196 (2007). doi: 10.1093/nar/gkm864.
19. DeSantis, T. Z. *et al.* Greengenes, a Chimera-Checked 16S rRNA Gene Database and Workbench Compatible with ARB. *Appl Environ Microbiol* **72**, 5069–5072 (2006). doi: 10.1128/AEM.03006-05.
20. Chiarello, M., McCauley, M., Villéger, S. & Jackson, C. R. Ranking the biases: The choice of OTUs vs. ASVs in 16S rRNA amplicon data analysis has stronger effects on diversity measures than rarefaction and OTU identity threshold. *PLoS One* **17**, (2022). doi: 10.1371/journal.pone.0264443.
21. Callahan, B. J., McMurdie, P. J. & Holmes, S. P. Exact sequence variants should replace operational taxonomic units in marker-gene data analysis. *ISME J* **11**, 2639–2643 (2017). doi: 10.1038/ismej.2017.119.
22. Inglis, C., Rahmani, D., Yeung, D. & Mun, D. *A Comparison of Metabarcoding Analysis between ASVs and OTUs-Using Data Regarding the Effects of Chronic Radiation on the Bank Vole Gut Microbiota. Undergraduate Journal of Experimental Microbiology and Immunology (UJEMI)* vol. 27 <https://jemi.microbiology.ubc.ca/> (2022).
23. Hallmaier-Wacker, L. K., Lueert, S., Roos, C. & Knauf, S. The impact of storage buffer, DNA extraction method, and polymerase on microbial analysis. *Sci Rep* **8**, 6292 (2018). doi: 10.1038/s41598-018-24573-y.
24. Brooks, J. P. *et al.* The truth about metagenomics: quantifying and counteracting bias in 16S rRNA studies. *BMC Microbiol* **15**, 66 (2015). doi: 10.1186/s12866-015-0351-6.
25. Dudli, S., Miller, S., Demir-Deviren, S. & Lotz, J. C. Inflammatory response of disc cells against *Propionibacterium acnes* depends on the presence of lumbar Modic changes. *European Spine Journal* **27**, 1013–1020 (2018). doi: 10.1007/s00586-017-5291-4.
26. Capoor, M. N. *et al.* Pro-inflammatory and neurotrophic factor responses of cells derived from degenerative human intervertebral discs to the opportunistic pathogen cutibacterium *acnes*. *Int J Mol Sci* **22**, 1–16 (2021). doi: 10.3390/ijms22052347.
27. Määttä, J. H. *et al.* Refined phenotyping of modic changes. *Medicine (United States)* **95**, (2016). doi: 10.1097/MD.0000000000003495.





# Chapter 5: Pro-inflammatory and catabolic gene expression in cartilage endplate cells after stimulation of toll-like receptor 2

**Tamara Mengis<sup>1,2</sup>, Laura Bernhard<sup>1,2</sup>, Irina Heggli<sup>1,2</sup>, Nick Herger<sup>1,2</sup>, Jan Devan<sup>1,2</sup>, Roy Marcus<sup>3</sup>, Christoph Laux<sup>4</sup>, Florian Brunner<sup>2</sup>, Mazda Farshad<sup>4</sup>, Oliver Distler<sup>1,2</sup>, Stefan Dudli<sup>1,2</sup>**

<sup>1</sup>Center of Experimental Rheumatology, Department of Rheumatology, University Hospital, University of Zurich, Switzerland

<sup>2</sup>Department of Physical Medicine and Rheumatology, Balgrist University Hospital, University of Zurich, Switzerland

<sup>3</sup>Department of Radiology, Balgrist University Hospital, University of Zurich

<sup>4</sup>Department of Orthopedics, Balgrist University Hospital, University of Zurich, CH

**In preparation**

## 5.1 Abstract

**Introduction:** The vertebral cartilage endplate (CEP), vital for intervertebral disc health, can undergo degeneration associated with chronic low back pain, disc degeneration, and Modic changes. While structural and biochemical changes in the CEP are well-established, the biological functions of CEP cells (CEPC), with markedly higher cell density than the adjacent disc, remain overlooked. This study aimed to identify TLRs on CEPC and explore their involvement in activating pro-inflammatory and catabolic gene expression.

**Methods:** Gene expression of TLR1-10 was measured with quantitative real-time polymerase chain reaction in human CEP cells (CEPC). Additionally, CEPC were stimulated with inflammatory cytokines tumor necrosis factor alpha and interleukin 1 beta, specific TLR2/6, TLR2/1 and TLR4 agonist (Pam2csk4, Pam3csk4 and lipopolysaccharide) and a representative damage associated molecular pattern (fibronectin fragment 30 kDa). Finally, flow cytometry was used to measure surface level TLR2 expression.

**Results:** CEPC were found to express TLR1, 2, 3, 4, 5, 6, 7 and 10. TLR2 was the only TLR which significantly increased after the applied stimulations. Stimulation with the TLR2/6 heterodimer agonist Pam2csk4 induced a significant upregulation of TLR2 on protein level as well as strong inflammatory and protease expression increases. After 48 hours of stimulation all applied ligands were able to induce an increase in inflammatory genes and MMP1, 3 and 13. TLR2 inhibition was able to specifically inhibit the upregulated genes.

**Conclusion:** In conclusion, this study reveals the previously unknown expression of TLRs 1-10, except for TLR8 and TLR9, in CEPC. The transcriptional differences between CEPC and other intervertebral disc cells indicate a need for separate investigation. The study highlights the potential significance of TLRs, particularly TLR2, suggesting an important biological role for CEPC in the inflammation and degeneration of the cartilage endplate.

**Keywords:** Toll-like receptors, cartilage endplate cells, cartilage endplate, disc degeneration

## 5.2 Introduction

The vertebral cartilage endplate (CEP) is a thin hyaline cartilage structure separating the intervertebral disc from the vertebra. Its intactness is critical for the health of the disc <sup>1,2</sup>. CEP degeneration has been associated with chronic low back pain (CLBP) <sup>3</sup>, disc degeneration (DD) <sup>4-8</sup>, and Modic changes (MC) <sup>9-11</sup>. Yet, the mechanisms linking CEP degeneration to DD and MC remain unclear. In-vivo and animal disc explant model showed that structural damage of the CEP can cause DD and MC <sup>5,12,13</sup>. Biochemical changes of the CEP, like dehydration, calcification, and fibrosis diminish its nutrient transport properties leading to reduced nutrient availability in the disc, disc cell death, and DD <sup>2,14,15</sup>. While it has become clear that structural and biochemical changes of the CEP are important in DD and MC, the role of biological changes of the CEP have remained largely unexplored. In the intervertebral disc, the degenerative mechanisms are well studied, but in the CEP which has an approximate 4-fold higher cell density than the intervertebral disc <sup>16</sup>, these changes are poorly

understood. Expression of matrix metalloproteinases (MMPs) and interleukins in cartilage endplate cells (CEPC) are suggested to play a role on CEP degradation <sup>17</sup>.

In the intervertebral disc, expression of matrix proteases and of pro-inflammatory cytokines is increased during degeneration <sup>18–20</sup>, and expression of pro-inflammatory cytokines is even higher with adjacent MC <sup>21–23</sup>. Together this leads to the resorption of the disc matrix, dehydration of the disc, and disc collapse. Disc cells also express various toll-like receptors (TLRs), with TLR2 being the only one that is responsive to inflammatory milieu such as interleukin 1 $\beta$  exposure. Additionally, TLR2 possesses the highest number of ligands, attributed to its capability to form diverse heterodimers <sup>24</sup>. The presence of TLRs conveys them the capacity to sense and respond to danger signals from damage-associated molecular pattern (DAMPs) and from pathogen-associated molecular patterns (PAMPs) <sup>25</sup>. For example, the 30 kDa N-terminal fibronectin fragment (FNf30), short hyaluronic acid fragments, and decorin are extracellular-matrix derived DAMPs that cause inflammatory and catabolic changes in disc cells by signaling through TLR2 and TLR4 <sup>26–28</sup>. This is important, because these fragments can be generated during DD and hence trigger a vicious inflammatory-catabolic loop within the disc <sup>29–31</sup>. Growing evidence also attests a role of intradiscal bacteria, mainly *Cutibacterium acnes* (*C. acnes*) in DD and MC <sup>32–37</sup>. Disc cells sense *C. acnes* through TLR2 <sup>38,39</sup>, leading to inflammatory and catabolic changes in the disc <sup>36,40</sup>, which extend to the endplate and eventually cause marrow changes visible as MC <sup>36</sup>. Co-regulation of the expression of the TLR/MyD88/NF $\kappa$ B pathway in the disc and the bone marrow at levels with MC further support a role of TLRs in MC <sup>23</sup>. Taken together, these studies demonstrate a strong involvement of TLRs, and in particular of TLR2, in DD and MC, and hence targeting TLR2 is a discussed treatment for DD<sup>41,42</sup>.

In the CEP, understanding the role of TLRs, in particular of TLR2, is important because the higher cell density could cause strong local pro-inflammatory and catabolic changes. This could have detrimental consequences, because the function and stability of the thin CEP layer could quickly be impaired leading to DD, MC and ultimately LBP. Furthermore, sensing DAMPs and PAMPs from the disc could propel the inflammation from the disc to the bone marrow and assist in triggering MC. However, the expression and regulation of TLRs in CEPC is unknown to date. Therefore, the aims of this study were first to prove the expression of TLRs in CEPC, and second to show that TLR2 signaling causes pro-inflammatory and pro-catabolic changes in CEPC.

## 5.3 Methods

### *CEPC isolation and culture*

CEPC from degenerated discs were isolated from fresh cartilage endplate tissue of spinal fusion surgery patients that signed informed consent for further use of surgically removed biological material. Inclusion criteria for the selection of the patients were the absence of current or chronic systemic inflammatory or infectious diseases, as well as no prior lumbar fusion.

CEPs were minced into small pieces within 2 hours after surgical removal. They were then enzymatically digested overnight with 0.05% collagenase P (Roche, Basel, Switzerland) in Dulbecco's modified eagle's medium (DMEM) (Gibco, Reinach, Switzerland) supplemented with 10 % fetal calf serum (FCS), 50 U/ml penicillin streptomycin, 10 mM HEPES, 2 mM L-Glutamine. After digestion, the solution was passed through a 70  $\mu$ m cell strainer, and the cells were then expanded to passages 1-2.

### *Stimulation of CEPC*

Prior to stimulation all cells were treated with polymyxin B (10 ng/ml) (Invivogen, Toulouse, Switzerland) for 2 hours. To assess the response of CEPC to inflammatory stimuli, CEPC were treated for 24 hours or 48 hours with tumor necrosis factor  $\alpha$  (TNF- $\alpha$ ) (10 ng/ml) or 10 ng/ml interleukin 1 beta (IL-1 $\beta$ ) to simulate the inflammatory milieu provided by the degenerating disc. To selectively activate TLR2/1, TLR2/6, and TLR4, which are recognized to respond to different DAMPs or PAMPs, diverse ligands were administered to the cell cultures for 24 and 48 hours. For TLR2/6 and TLR2/1 specific activation the synthetic ligand Pam2CysSerLys4 (Pam2csk4) (Invivogen) (10 ng/ml and 1000 ng/ml) and Pam3CysSerLys4 (Invivogen) (Pam3csk4) (10 ng/ml and 1000 ng/ml) were used, respectively. TLR4 specific activation was targeted with ultrapure E. coli lipopolysaccharide (LPS) (Invivogen) (10  $\mu$ g/ml and 50  $\mu$ g/ml). In addition, the 30kDa N-terminal fibronectin fragment (FNf30) (Sigma, Buchs, Switzerland) (2.5  $\mu$ g/ml and 5  $\mu$ g/ml) was used to represent potential activation through ECM-derived DAMPs.

To test for the specificity of Pam2csk4 signaling through TLR2, CEPC were pre-treated for 2 hours with three different TLR2 inhibitor TL2-C29 (Invivogen) concentrations (200  $\mu$ M, 100  $\mu$ M and 50  $\mu$ M) before 10 ng/ml Pam2csk4 was added. TL2-C29 is known to block both TLR2/1 and TLR2/6 heterodimer signaling.

#### *5.3.3 RNA isolation and gene expression analysis*

Cell lysis conducted in RLT buffer containing 1 %  $\beta$ -Mercaptoethanol (Gibco, Reinach, Switzerland) and RNA isolation was carried out using the RNeasy Mini Kit (QIAGEN, Hilden, Germany) following manufacturer's instructions, including the optional DNase digestion step.

Subsequently, reverse transcription of 100 ng RNA was performed using the SensiFAST cDNA Synthesis Kit (Meridian Bioscience, United States). Relative mRNA levels were quantified with use of the SensiFAST SYBR No-Rox kit (Labgene, Châtel-Saint-Denis, Switzerland) on a magnetic induction real-time qPCR cycler (Labgene). Cycle conditions after initial denaturation at 95°C for 300s were as follows: 40 cycles of 5 seconds at 95 °C, 20 seconds at 60 °C, 10 seconds at 72 °C, followed by melting curve analysis. Analysis was done with the  $\Delta\Delta$ Cq method and with normalization to the housekeeping genes Glyceraldehyde-3-Phosphate Dehydrogenase (GADPH). All used primer sequences are listed in Table 1.

Gene expression was measured with quantitative real-time polymerase chain reaction (qPCR). The  $2^{-\Delta\Delta$ Ct method was used for analysis with Glyceraldehyde-3-Phosphate Dehydrogenase (GAPDH) as the reference gene. Basal TLR expression was measured on unstimulated CEPC of 23 patients. In stimulation experiments a total of 11 patients were used. TLR1, TLR2, TLR4 and TLR6 as well as of inflammatory genes IL6, IL8 and

CCL2 and matrix metalloproteases MMP1, MMP3, MMP9 and MMP13 were measured for all conditions. For TLR2 inhibition experiments, a total of 6 patients were used and IL6, TLR2, MMP1, MMP3 and MMP13 gene expression was measured.

**Table 1.** Primers used for qPCR.

Primers	Forward	Reverse
<b>CCL2</b>	5'-CAG CCA GAT GCA ATC AAT GCC-3'	5'-TGG AAT CCT GAA CCC ACT TCT-3'
<b>GAPDH</b>	5'-ATTCCACCCATGGCAAATTC-3'	5'-GGGATTTCCATTGATGACAAGC-3'
<b>IL6</b>	5'-AGA CAG CCA CTC ACC TCT TCA G-3'	5'-TTC TGC CAG TGC CTC TTT GCT G-3'
<b>IL8</b>	5'-GAG AGT GAT TGA GAG TGG ACC AC-3'	5'-CAC AAC CCT CTG CAC CCA GTT T-3'
<b>MMP1</b>	5'-ATG AAG CAG CCC AGA TGT GGA G-3'	5'-TGG TCC ACA TCT GCT CTT GGC A-3'
<b>MMP3</b>	5'-CAC TCA CAG ACC TGA CTC GGT T-3'	5'-AAG CAG GAT CAC AGT TGG CTG G-3'
<b>MMP9</b>	5'-GCCACTACTGTGCCTTTGAGTC-3'	5'-CCCTCAGAGAATCGCCAGTACT-3'
<b>MMP13</b>	5'-CCT TGA TGC CAT TAC CAG TCT CC-3'	5'-AAA CAG CTC CGC ATC AAC CTG C-3'
<b>TLR1</b>	5'-CAGTGTCTGGTACACGCATGGT-3'	5'-TTTCAAAAACCGTGTCTGTTAAGAGA-3'
<b>TLR2</b>	5'-GGCCAGCAAATTACCTGTGTG-3'	5'-AGGCGGACATCCTGAACCT-3'
<b>TLR3</b>	5'-CCTGGTTTGTAAATTGGATTAACGA-3'	5'-TGAGGTGGAGTGTTCGAAAGG-3'
<b>TLR4</b>	5'-CAGAGTTTCCTGCAATGGATCA-3'	5'-GCTTATCTGAAGGTGTTGCACAT-3'
<b>TLR5</b>	5'-TGCCTTGAAGCCTTCAGTTATG-3'	5'-CCAACCACCACCATGATGAG-3'
<b>TLR6</b>	5'-GAAGAAGAACAACCTTTAGGATAGC-3'	5'-AGGCAAACAAAATGGAAGCTT-3'
<b>TLR7</b>	5'-TTTACCTGGATGAAAACCAGCTA-3'	5'-TCAAGGCTGAGAAGCTGTAAGCTA-3'
<b>TLR8</b>	5'-TTATGTGTTCCAGGAACTCAGAGAA-3'	5'- TAATACCCAAGTTGATAGTCGATAAGTTTG- 3'
<b>TLR9</b>	5'-GGACCTCTGGTACTGCTTCCA-3'	5'-AAGCTCGTTGTACACCCAGTCT-3'
<b>TLR10</b>	5'-CTGATGACCAACTGCTCCAA-3'	5'-AGTCTGCGGGAACCTTTCTT-3'

### *Flow cytometry*

Flow cytometry was utilized to assess the surface expression levels of TLR2 from (Biolegend) unstimulated CEPC, 72h Pam2csk4-stimulated CEPC, and Pam3csk4-stimulated CEPC, in addition to HEK cells as a negative control and THP1 cells (human leukemia monocytic cell line) (Invivogen) as a positive control for TLR2 expression. CEPC were blocked with according to manufacturer's instructions with 5 ul of True-Stain Monocyte Blocker™ for 10 minutes before the TLR2 antibody (10 ug/ml) was added and cells were stained for 45 minutes. The TLR2 antibody used was a monoclonal PE anti-human CD282 (TLR2) antibody (isotype: Mouse IgG2a, κ) (Biologened). After washing, cells were also stained for 10 minutes with 4',6-Diamidino-2-Phenylindole, Dilactate (DAPI) to differentiate live and dead cells. Finally, cells were washed and analyzed with BD LSRFortessa cell analyser (BD Biosciences, New Jersey, USA). Data was analyzed with FlowJo v10.8 software. Cell doublets and dead cells were excluded from the analysis.

### *Statistical Analysis*

Correlation between each TLR and Pfirrmann Grade was calculated using Spearman correlation. A simple linear regression model was fit to determine correlation of TLR1, TLR4, TLR6 to TLR2. Statistical analysis for both stimulation and inhibition experiments was done by one-way analysis of variance (ANOVA), followed

by conducting multiple comparisons on the log<sub>2</sub> fold change of delta delta C<sub>q</sub> values after testing for normal distribution with use of Kolmogorov-Smirnov test and Shapiro Wilk test. Corrections for multiple comparisons were implemented using Dunnett's multiple comparison testing. For flow cytometry experiments, median fluorescence was used and tested by one-way ANOVA followed by Dunnett's multiple comparison testing.

All statistical analyses were performed using GraphPad Prism V10.2.0. The significance level was  $\alpha = 0.05$ , if not stated otherwise.

## 5.4 Results

### *Patient demographics*

The CEPs originated from the lumbar levels L3/4, L4/5 and L5/S1 and the adjacent discs had an average Pfirrmann grade of 3.8 across all participants. The mean age was 58.9 years and ranged from 28 to 87 years. Both men and women were included (Supplementary Table 1). Different patients were used for each stimulation and inhibition experiments.

### *Basal TLR expression*

Basal expression of TLR genes was assessed with unstimulated CEPC from 10 patients. All cell surface TLRs (TLR1, TLR2, TLR3, TLR4, TLR6 and TLR10) were expressed. TLR3 and TLR5 expression was highest, TLR8 and TLR9 were not detectable (Figure 1A). Pfirrmann grade did not show significant correlation to the individual TLRs (Supplementary Figure 1). Since TLR2 can dimerize with TLR1 and TLR6, correlation of TLR2 with these TLRs was tested (Figure 1B-D). TLR2 expression only correlated with TLR6 expression ( $R = 0.581$ ,  $p = 0.004$ ).

### *TLR2 upregulation*

TLR1 was only increased upon 24 hours ( $p < 0.001$ ) and 48 hours ( $p = 0.030$ ) of IL-1 $\beta$  stimulation as well as 48 hours 10 ng/ml TNF- $\alpha$  stimulation ( $p < 0.001$ ) (Figure 1E). After 24 hours TLR2 was significantly upregulated in response to both high ( $p < 0.001$ ) and low ( $p = 0.007$ ) Pam2csk4 stimulation as well as the higher Pam3csk4 ( $p = 0.030$ ) stimulation. Additionally, the inflammatory cytokine TNF- $\alpha$  induced a significant upregulation of TLR2 after 24 hours ( $p < 0.001$ ) (Figure 1F). After 48 hours all applied stimulations except the lower Pam3csk4 concentration of 10 ng/ml induced a significant increase of TLR2 expression (Figure 1F). In contrast, TLR4 expression cannot be altered through any of the applied stimulations (Figure 1G). For TLR6 expression, a 48-hour exposure to 10 ng/ml LPS ( $p = 0.042$ ) and 10ng/ml TNF- $\alpha$  ( $p = 0.009$ ) induced a significant increase (Figure 1H).

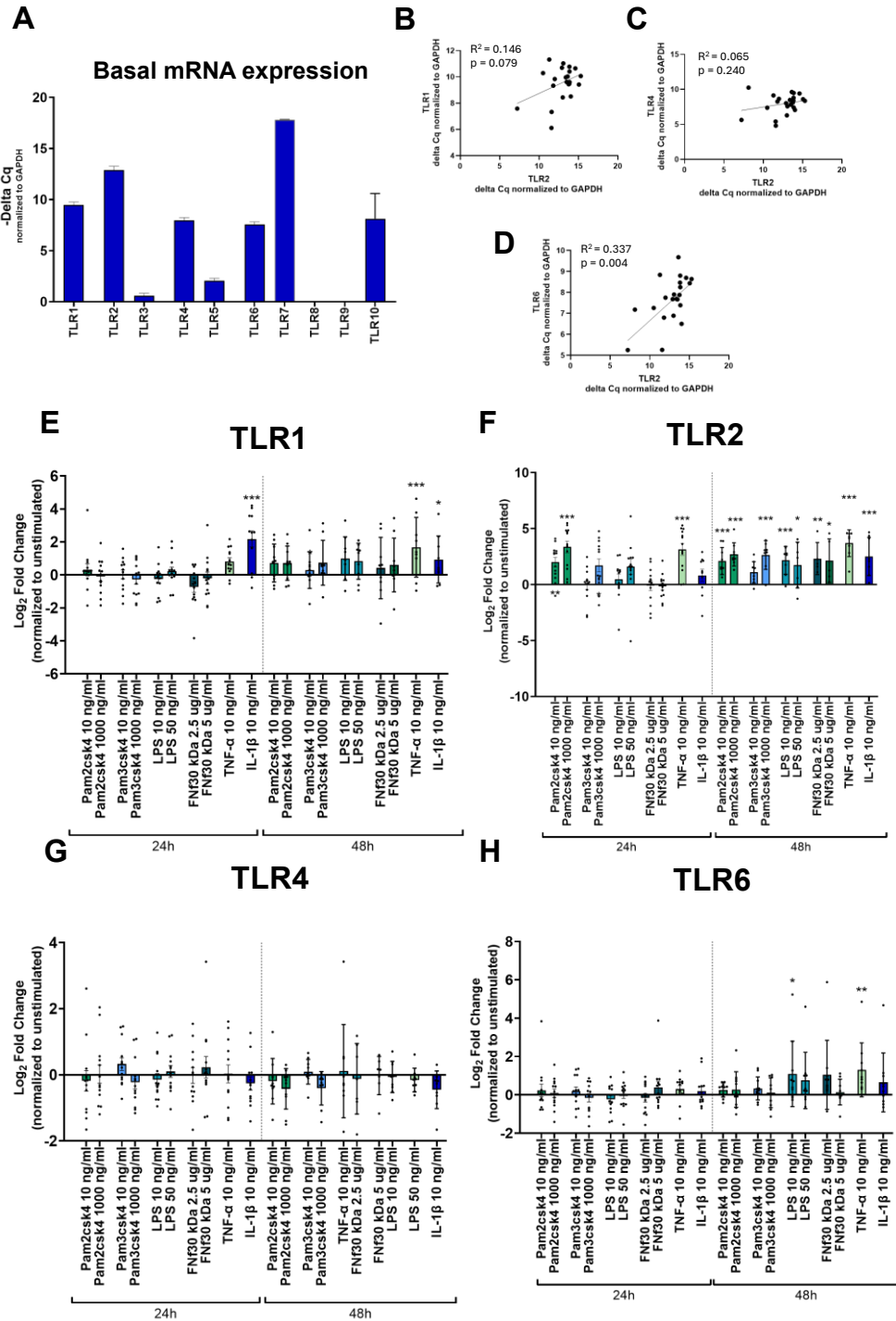


**Figure 1.** (A) Basal TLR gene expression in CEPC presented as negative delta Cq values compared to reference gene GAPDH (mean GAPDH value = 24.91) (B, C, D, E) Gene expression of TLRs in CEPC following 24-hour and 48-hour stimulation with varying concentrations of Pam2csk4, Pam3csk4 (10 ng/ml and 1000 ng/ml), LPS (10 ng/ml and 50 ng/ml), FN fragment 30 kDa (FNf 30kDa) (2.5 ug/ml and 5 ug/ml), TNF- $\alpha$  (10 ng/ml), and IL-1 $\beta$  (10 ng/ml) is depicted. The panels illustrate the expression levels of (B) TLR1, (C) TLR2, (D) TLR4, and (E) TLR6. Significance was tested on log2 fold change of delta delta Cq values by repeated measures one-way ANOVA, followed by multiple comparisons which compared each condition to the unstimulated condition at the respective timepoint. Dunnet statistical hypothesis testing was applied to correct for multiple comparisons. Asterisk signify significance: \*  $p < 0.05$ , \*\*  $p < 0.001$ , \*\*\*  $p < 0.0001$ .



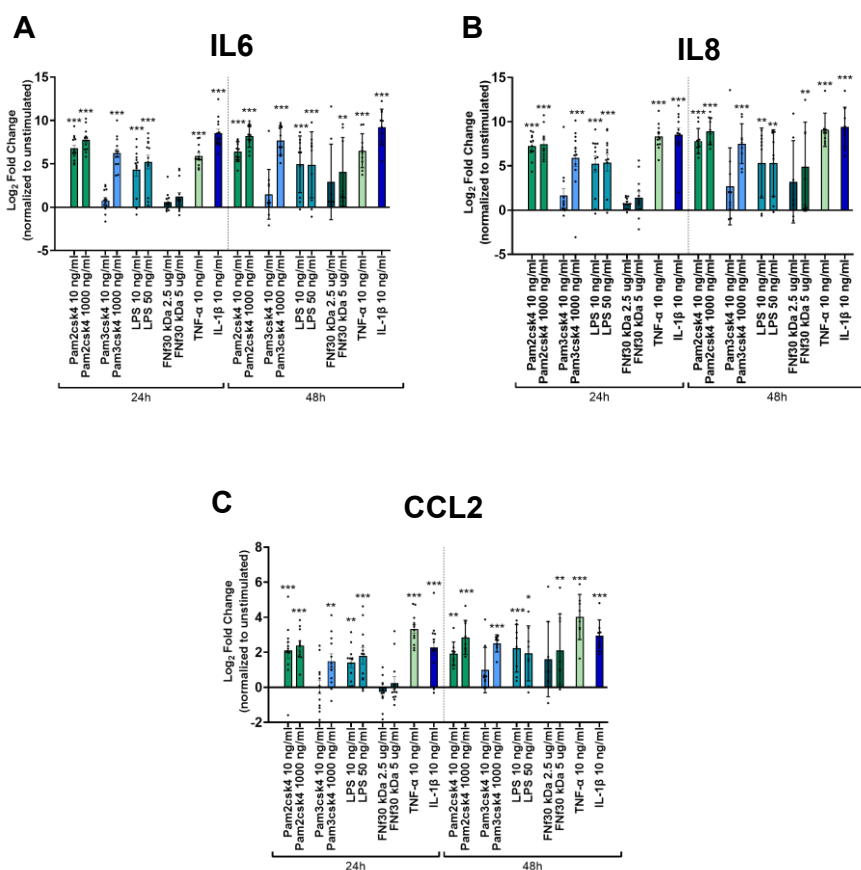


**Figure 2.** Inflammatory gene expression of (A) IL6, (B) IL8 and (C) CCL2 in CEPC following 24-hour and 48-hour stimulation with varying concentrations of Pam2csk4, Pam3csk4 (10 ng/ml and 1000 ng/ml), LPS (10 ng/ml and 50 ng/ml), FN fragment 30 kDa (FNf) (2.5 ug/ml and 5 ug/ml), TNF- $\alpha$  (10 ng/ml), and IL-1 $\beta$  (10 ng/ml) is depicted. Significance was tested on log<sub>2</sub> fold change of delta delta Cq values by repeated measures one-way ANOVA, followed by multiple comparisons which compared each condition to the unstimulated condition at the respective timepoint. Dunnet statistical hypothesis testing was applied to correct for multiple comparisons. Asterisk signify significance: \*  $p < 0.05$ , \*\*  $p < 0.001$ , \*\*\*  $p < 0.0001$ .

### *Inflammatory gene upregulation upon TLR activation*

Exposure to TLR ligands led to an inflammatory response, as indicated by the heightened expression of three key inflammatory genes – IL6, IL8, and CCL2. All three measured genes showed a similar upregulation pattern. After 24 hours, all experimental conditions induced a significant increase in response, except for FNf30 kDa and the lower dosage of 10 ng/ml Pam3csk4 (Figure 2). However, after 48 hours, in addition to the other stimulations, the 5 ug/ml FNf30 kDa also resulted in a significant increase in IL6 expression ( $p = 0.006$ ) (Figure 2).

### *Protease upregulation through TLR2/6 activation*

Stimulation with TLR agonists as well as inflammatory cytokines TNF- $\alpha$  and IL-1 $\beta$  were able to upregulate several different proteases in CEPC. MMP1 and MMP3 were significantly increased through both 10 ng/ml and 1000 ng/ml Pam2csk4 stimulations, the higher concentration of Pam3csk4 of 1000 ng/ml and 50 ng/ml LPS as well TNF- $\alpha$  and IL-1 $\beta$  stimulation after 24 hours (Figure 3A/B). This pattern persisted after 48 hours, with addition of both concentrations of the FNf30 kDa which after this time also increased MMP1 and MMP3



significantly (Figure 3A/B). For MMP9, the 24-hour timepoint was similar to MMP1 and MMP3 however, even after 48 hours of stimulation the FNf30 kDa could not induce a significant upregulation of MMP9 (Figure 3C). After 24 hours, MMP13 exhibited a less pronounced response, with only 10 ng/ml ( $p = 0.037$ ) and 1000 ng/ml ( $p = 0.001$ ) Pam2csk4, 10 ng/ml IL-1 $\beta$  ( $p = 0.002$ ), and 10 ng/ml TNF- $\alpha$  ( $p = 0.011$ ) causing a significant upregulation. However, after 48 hours, MMP13 showed a significant increase in response to all applied stimulations, except for the lower dosage of Pam3csk4 and the lower concentration of FNf30kDa (Figure 3D). Among all measured proteases, MMP3 demonstrated the strongest increase after the applied stimulations with an average fold change of  $856.3 \pm 456.2$  after 48-hour exposure to 1000 ng/ml Pam2csk4.

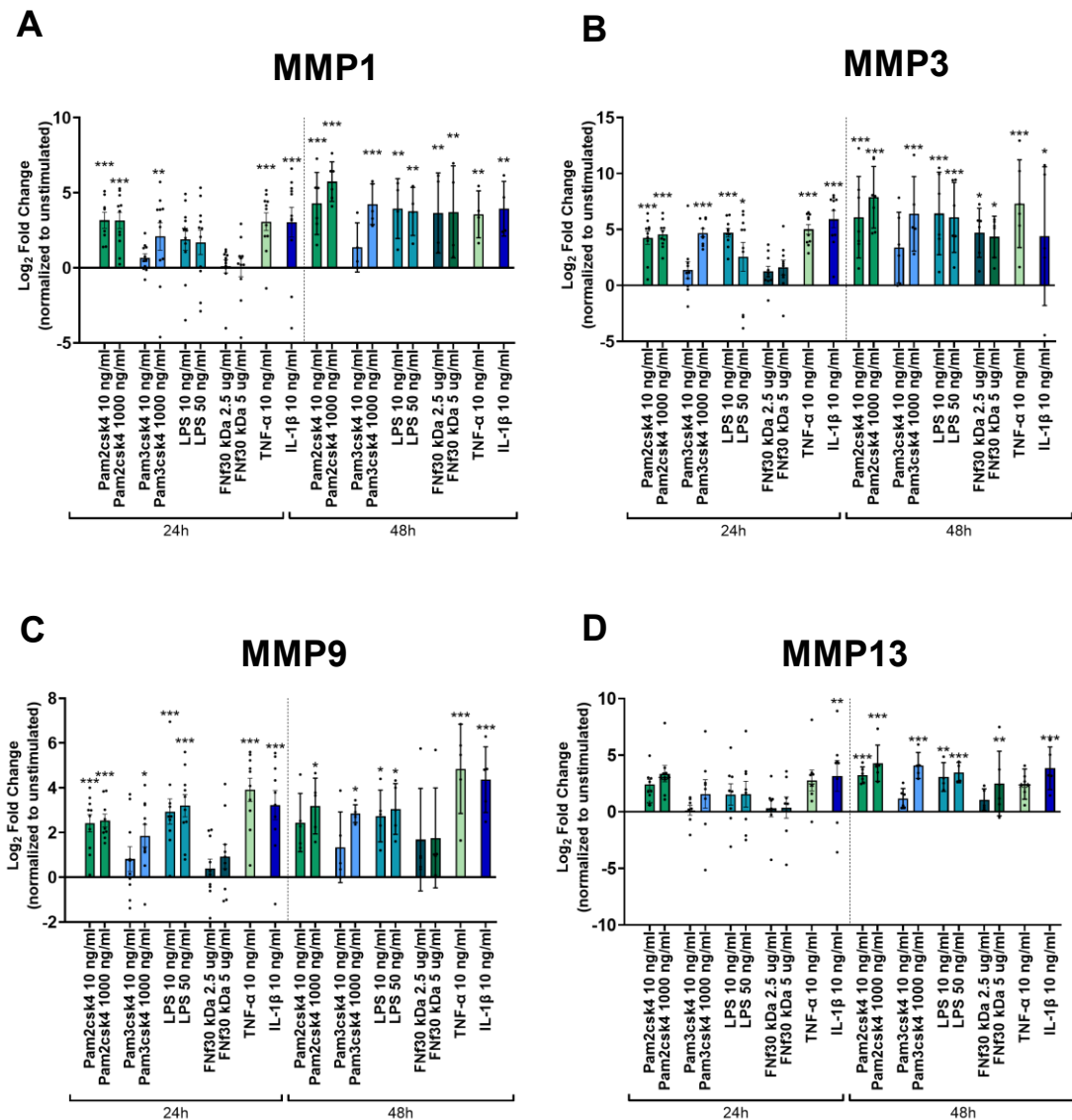


**Figure 3.** Protease gene expression of (A) MMP1, (B) MMP3, (C) MMP9 and (D) MMP13 in CEPC after either 24 or 48 hours of Pam2csk4, Pam3csk4 (10 ng/ml and 1000 ng/ml), LPS (10 ng/ml and 50 ng/ml), FNf fragment 30 kDa (FNf) (2.5 ug/ml and 5 ug/ml), TNF- $\alpha$  (10 ng/ml), and IL-1 $\beta$  (10 ng/ml) stimulation. Significance was tested on log<sub>2</sub> fold change of delta delta Cq values by repeated measures one-way ANOVA, followed by multiple comparisons which compared each condition to the unstimulated condition at the respective timepoint. Dunnett statistical hypothesis testing was applied to correct for multiple comparisons. Asterisk signify significance: \*  $p < 0.05$ , \*\*  $p < 0.001$ , \*\*\*  $p < 0.0001$ .

## Stimulation of TLR2/6 heterodimer increases TLR2 cell surface levels

Flow cytometry showed a more TLR2 on CEPC compared to HEK cells (used as a negative control) and a lower number compared to the monocyte cell line THP1 (Figure 4A). A significant increase in surface TLR2 on CEPC (fold change = 1.4,  $p = 0.005$ ) was observed after a 72-hour stimulation with 1000 ng/ml Pam2csk4 (Figure 4B), but not with Pam3csk4 (Figure 4C).

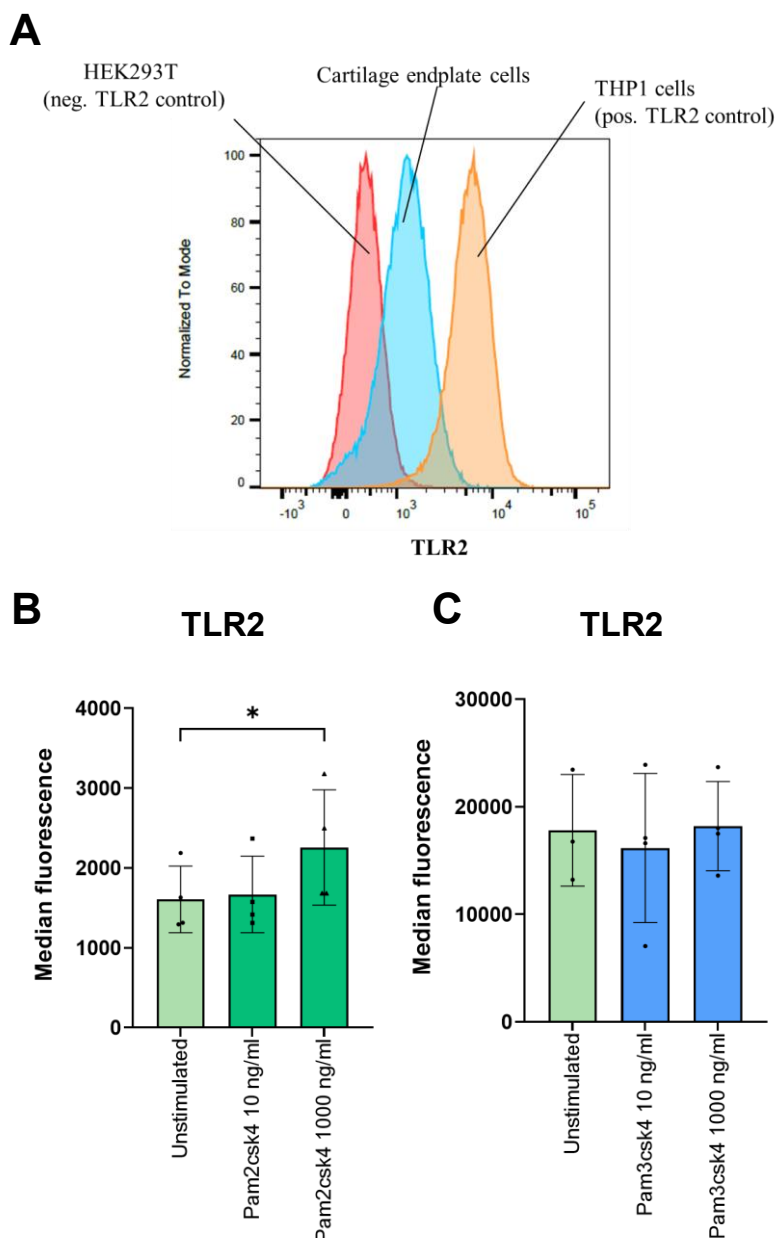


**Figure 4.** Protein expression of TLR2. **(A)** Representative case of TLR2 measured on CEPC (orange), with HEK cells (red) serving as the negative control and THP1 cells (orange) as the positive control. **(B/C)** Effect of 72 hours of stimulation with **(B)** Pam2csk4 and **(C)** Pam3csk4 at concentrations of 10 ng/ml and 1000 ng/ml on TLR2 levels illustrated as percentage normalized to unstimulated CEPC. Significance was tested with one-way ANOVA on median fluorescence corrected for multiple comparisons using Dunnett multiple comparison test.

## TL2-C29 inhibits TLR2 signaling

The addition of TL2-C29 decreased TLR2 signaling in a concentration dependent manner when additionally exposed to 10 ng/ml Pam2csk4 stimulation. The addition of 50  $\mu$ M TL2-C29 was only sufficient to create a significant decrease in IL6 ( $p < 0.001$ ) and MMP3 ( $p = 0.034$ ) expression (Figure 5A/D). However, with the addition of 100  $\mu$ M and 200  $\mu$ M of the TL2-C29 inhibitor the upregulation of IL6, TLR2, MMP1, MMP3, and MMP13 induced by through Pam2csk4 were all significantly reduced (Figure 5A-E).

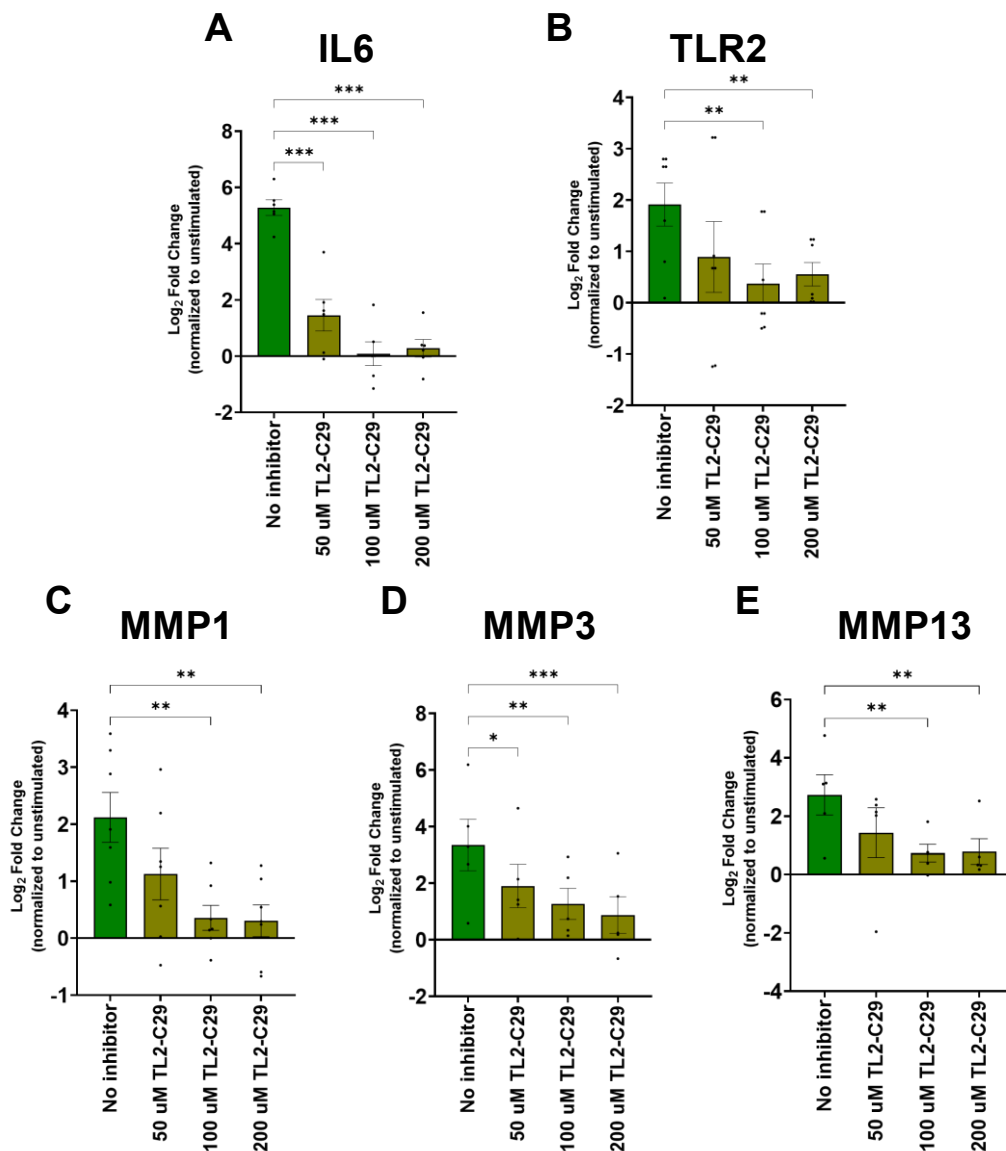


**Figure 5.** Inhibition of TLR2 with three different dosages (50  $\mu$ M, 100  $\mu$ M and 200  $\mu$ M) of TL2-C29. Genes that showed upregulation through Pam2csk4 stimulation were used to see if this upregulation could be inhibited by blocking TLR2. The inflammatory gene (A) IL6, the responding TLR (B) TLR2, as well as the proteases (C) MMP1, (D) MMP3 and (E) MMP13 were measured. Statistical significance was tested on log<sub>2</sub> fold change of delta delta Cq values by repeated measures one-way ANOVA, followed by multiple comparisons which compared each condition to the unstimulated condition at the respective timepoint. Dunnet statistical hypothesis testing was applied to correct for multiple comparisons. Asterisk signify significance: \*  $p < 0.05$ , \*\*  $p < 0.001$ , \*\*\*  $p < 0.0001$ .

## 5.5 Discussion

This is the first systematic study showing that CEPC expresses all TLR1-10, except TLR8 and TLR9. Expression of the TLR2 and TLR7 genes have previously been reported using micro arrays<sup>43</sup>. Single cell RNA sequencing and bulk RNA sequencing showed that CEPC are transcriptionally different from nucleus pulposus and annulus fibrosus cells of the intervertebral disc, and hence CEPC should be investigated separately<sup>43,44</sup>. Disc cells express TLR1-6, 9, and 10<sup>25</sup>. Therefore, the expression of TLR7 seems to be specific to CEPC and TLR9 specific to disc cells. In contrast to disc cells, expression of TLRs is independent of the degree of disc degeneration, indicating that regulation of TLR expression is different than in the disc. This underscores that CEPC should be investigated separately from disc cells.

CEPC expressed all cell surface TLRs, i.e. TLR1, TLR2, TLR4, TLR5, and TLR6. Of those, TLR2 and TLR4 are of particular importance in DD and MC, because they can be activated by extracellular matrix (ECM) fragments generated during DD and by *C. acnes*, a bacterium that has been found at increased concentrations in discs at MC levels, and that can trigger DD and MC in animal model<sup>26,36,37,40,45,46</sup>. TLR2 signaling requires heterodimerization with TLR1 or TLR6<sup>26</sup>. TLR4 homodimerizes for activating downstream signaling. To test the regulation of TLR1, 2, 4, and 6 under inflammatory conditions, CEPC were stimulated with the TLR1/2 and TLR2/6 specific ligands Pam3csk4 and Pam2csk4, with TLR4 specific ultra-pure LPS, and with IL-1 $\beta$  or TNF- $\alpha$  to test TLR-signaling independent regulation<sup>47</sup>. TLR2 expression was found to be upregulated under all these conditions. TLR4 and TLR6 were not affected at all, and TLR1 was only upregulated by IL-1 $\beta$ . On protein level, stimulation with Pam2csk4 but not with Pam3csk4 enhanced TLR2 expression, indicating a positive feedback loop of TLR2/6 stimulation with TLR2 expression. Correlation of TLR2 expression with TLR6 but not with TLR1 further supports the relevance of TLR2/6 signaling in CEPC. In intervertebral disc cells and chondrocytes from osteoarthritic joints, similar to our data, only TLR2 was upregulated after IL-1 $\beta$  stimulation<sup>47,48</sup>. Together, this suggests that TLR2/6 signaling could be of importance in CEPC. Whether this affects sensitivity or intensity of TLR2/6 signaling in-vivo cannot be concluded from these experiments.

Expression of pro-inflammatory cytokines and MMPs is enhanced after TLR2 and TLR4 signaling in the disc and in hyaline cartilage, leading to matrix resorption and impaired function<sup>27,28,47-51</sup>. Here, stimulation of TLR1/2, TLR2/6, and TLR4 enhanced expression of pro-inflammatory cytokines and of MMPs, suggesting a potential detrimental role of TLR2 and TLR4 signaling in endplate degradation<sup>17</sup>. Blocking TLR2 signaling abrogated the TLR2/6 enhanced expression of pro-inflammatory cytokines and MMPs. This proves that signaling indeed occurs through TLR2 and that the observed upregulation of cytokines and MMPs is functionally linked to TLR2 stimulation.

TLR2 signaling could occur in CEPC through DAMPs or PAMPs that have been shown to be present in degenerating intervertebral discs. For examples, FNf30 generated during DD activates TLR2<sup>27,30,31</sup>, and *C. acnes* engage TLR2<sup>38</sup>. Which *C. acnes* factors activate TLR2 is unclear. In keratinocytes during acne vulgaris, Christie-Atkins-Munch-Petersen 1 factor (CAMP1) binds TLR2<sup>52</sup>, and di- and tri-acylated lipoproteins engage TLR1/2 and TLR2/6 heterodimers, respectively<sup>53</sup>. *C. acnes* also secretes hyaluronidase, which can cleave

hyaluronic acid into fragments acting as DAMPs<sup>28,54</sup>, and sialidases, which can disrupt TLR-inhibitory mechanisms<sup>52,55</sup>. While it can be expected that CEPC respond to FNf30 and *C. acnes*, this needs to be proven.

A TLR2 response in the CEP may have other consequences than a TLR2 response in the disc because sensory nerve fibers end in the CEP<sup>56</sup>, and hence pro-inflammatory and neurotrophic factors secreted by CEPC after TLR2 stimulation could directly act in a paracrine manner on these fibers and enhance pain sensitization. Importantly, nerve fiber density in CEPs is even increased in MC and therefore TLR2 signaling in MC endplates could even more strongly affect pain sensitization<sup>57,58</sup>. Overexpression of MMPs could also degrade the matrix of the anyway thin CEP and increase the risk for damaging with detrimental consequences like MC<sup>59</sup>, avulsion-type herniations<sup>60</sup>, Schmorl's nodes<sup>61</sup>, and endplate fractures<sup>62</sup>. Lastly overexpression of pro-inflammatory cytokines and MMPs by CEPC may also affect the adjacent bone marrow and lead to inflammatory changes even before the CEP is damaged.

This study has some limitations. First, TLR expression has been investigated in isolated CEPC after in-vitro expansion and not directly after isolation. Expansion could have influenced the expression levels of TLRs. Second, synthetic ligands were used to measure the response to TLR2 stimulation. It needs to be tested, if clinically more relevant TLR2 stimulants, like FNf30 and *C. acnes* cause a similar response. Third, it cannot be concluded from this study if TLR signaling in CEPC is a relevant pathomechanism in DD and MC.

In conclusion, this study shows that CEPC expresses TLRs, that TLR2 is overexpressed under pathologic relevant inflammatory conditions, and that TLR2 signaling causes overexpression of pro-inflammatory cytokines and MMPs. This is important because the CEP has a critical function in maintaining disc health and compromising this function is associated with DD and MC.

## 5.6 Ethics Statement

The study was approved by the local Ethics Commission #2018-01486; approved on 24 August 2018. The study was conducted in accordance with the local legislation and institutional requirements. The participants provided their written informed consent to participate in this study.

## 5.7 Author Contributions

TM: data acquisition (patient recruiting, cell isolation, stimulation/inhibition experiments, qPCR, flow cytometry) , methodology, writing–original draft, and visualization. LB: data acquisition of stimulation experiments, data curation. IH: methodology, writing–review and editing. NH: writing–review and editing and methodology. JD: writing–review and editing. RM: data curation and writing–review. FB: writing–review and editing. CL: data curation, writing–review. MF: writing–review and editing. OD: funding acquisition and writing–review and editing. SD: funding acquisition and writing–review and editing.

## 5.8 Funding

This study was supported by a career research grant from the Foundation for Research in Rheumatology (FOREUM) (SD and OD) and by a grant from the Swiss National Fond (SD, Grant No. 207989).

## 5.9 Conflicts of Interest

none

## 5.10 Acknowledgements

We would like to thank the Swiss Center for Musculoskeletal Biobanking (SCMB), which worked together with us to provide the samples in the shortest time possible for further processing. Furthermore, we also thank the spine surgery team at the Balgrist University Hospital for providing us with fresh samples. Lastly, we would like to thank Rayana Daudovan for her contribution to the project by doing her high school (Matura) thesis with us.

## 5.11 Supplementary

**Table S1.** Patients used for the isolation of cartilage endplate cells (CEPCs) and subsequent experiments involving diverse stimulations with TLR ligands. Pfirrmann grade of the adjacent disc as well as age, gender and body mass index are listed.

Patient ID	Level	Pfirrmann Grade	Age	Gender	BMI
88	L4/5	5	77	Female	29.7
90	L5/S1	5	52	Female	30.3
92	L4/5	5	58	Male	50
93	L4/5	4	87	Male	25.9
97	L5/S1	3	43	Male	27
98	L3/4	5	84	Female	28.4
99	L3/4	4	60	Male	24.5
100	L4/5	3	64	Female	34.4
105	L4/5	2	49	Female	23.4
106	L4/5	4	39	Male	26.5
109	L4/5	3	36	Male	30.2
111	L5/S1	3	63	Female	21.3
112	L5/S1	4	54	Male	32.6
Average		3.8	58.9	Female: Male (6:7)	29.6

**Table S2.** Demographics of the patients from which the CEPCs derived were used for measuring TLR2 inhibition. The level of the surgery as well as the Pfirrmann grade of the disc adjacent to the harvested cartilage endplate is included. In addition, age, gender and body mass index was assessed.

Patient ID	Level	Pfirrmann Grade	Age	Gender	BMI
44	L3/4	5	79	Female	22
58	L3/4	4	66	Female	30.9
77	L4/5	5	59	Male	32.4
82	L4/5	4	50	Male	28.5
101	L5/S1	2	73	Male	29.1
110	L5/S1	4	28	Female	29.4
112	L5/S1	4	54	Male	32.6
		Median = 4	Mean = 58.4	42.9 % Female	Mean = 29.3

## 5.12 References chapter 5

1. Roberts, S., Urban, J. P., Evans, H. & Eisenstein, S. M. Transport properties of the human cartilage endplate in relation to its composition and calcification. *Spine (Phila Pa 1976)* **21**, 415–20 (1996). doi: 10.1097/00007632-199602150-00003.
2. Wong, J. *et al.* Nutrient supply and nucleus pulposus cell function: effects of the transport properties of the cartilage endplate and potential implications for intradiscal biologic therapy. *Osteoarthritis Cartilage* **27**, 956–964 (2019). doi: 10.1016/j.joca.2019.01.013.
3. Bailey, J. F. *et al.* The Relationship Between Endplate Pathology and Patient-reported Symptoms for Chronic Low Back Pain Depends on Lumbar Paraspinal Muscle Quality. *Spine (Phila Pa 1976)* **44**, 1010–1017 (2019). doi: 10.1097/BRS.0000000000003035.
4. Fields, A. J., Ballatori, A., Liebenberg, E. C. & Lotz, J. C. Contribution of the Endplates to Disc Degeneration. *Curr Mol Biol Rep* **4**, 151–160 (2018). doi: 10.1007/s40610-018-0105-y.
5. Dudli, S., Haschtmann, D. & Ferguson, S. J. Fracture of the vertebral endplates, but not equienergetic impact load, promotes disc degeneration in vitro. *Journal of Orthopaedic Research* **30**, 809–16 (2012). doi: 10.1002/jor.21573.
6. Law, T. *et al.* Ultrashort time-to-echo MRI of the cartilaginous endplate: technique and association with intervertebral disc degeneration. *J Med Imaging Radiat Oncol* **57**, 427–34 (2013). doi: 10.1111/1754-9485.12041.
7. Berg-Johansen, B. *et al.* Cartilage Endplate Thickness Variation Measured by Ultrashort Echo-Time MRI Is Associated With Adjacent Disc Degeneration. *Spine (Phila Pa 1976)* **43**, E592–E600 (2018). doi: 10.1097/BRS.0000000000002432.
8. Finkenstaedt, T. *et al.* Ultrashort time-to-echo MR morphology of cartilaginous endplate correlates with disc degeneration in the lumbar spine. *Eur Spine J* **32**, 2358–2367 (2023). doi: 10.1007/s00586-023-07739-9.
9. Farshad-Amacker, N. A., Hughes, A., Herzog, R. J., Seifert, B. & Farshad, M. The intervertebral disc, the endplates and the vertebral bone marrow as a unit in the process of degeneration. *Eur Radiol* **27**, 2507–2520 (2017). doi:10.1007/s00330-016-4584-z.

10. Crump, K. B. *et al.* Cartilaginous endplates: A comprehensive review on a neglected structure in intervertebral disc research. *JOR Spine* 1–22 (2023) doi: 10.1002/jsp2.1294. doi:10.1002/jsp2.1294.
11. Heggli, I. *et al.* Modic type 2 changes are fibroinflammatory changes with complement system involvement adjacent to degenerated vertebral endplates. *JOR Spine* 1–16 (2022) doi:10.1002/jsp2.1237. doi: 10.1002/jsp2.1237.
12. Dudli, S., Ferguson, S. J. & Haschtmann, D. Severity and pattern of post-traumatic intervertebral disc degeneration depend on the type of injury. *Spine J* **14**, 1256–64 (2014). doi: 10.1016/j.spinee.2013.07.488.
13. Wang, D. *et al.* Lumbar endplate microfracture injury induces Modic-like changes, intervertebral disc degeneration and spinal cord sensitization - an in vivo rat model. *Spine J* **23**, 1375–1388 (2023). doi: 10.1016/j.spinee.2023.04.012.
14. Dolor, A. *et al.* Matrix modification for enhancing the transport properties of the human cartilage endplate to improve disc nutrition. *PLoS One* **14**, e0215218 (2019). doi: 10.1371/journal.pone.0215218.
15. Shirazi-Adl, A., Taheri, M. & Urban, J. P. G. Analysis of cell viability in intervertebral disc: Effect of endplate permeability on cell population. *J Biomech* **43**, 1330–6 (2010). doi: 10.1016/j.jbiomech.2010.01.023.
16. Liebscher, T., Haefeli, M., Wuertz, K., Nerlich, A. G. & Boos, N. Age-related variation in cell density of human lumbar intervertebral disc. *Spine (Phila Pa 1976)* **36**, 153–9 (2011). doi: 10.1097/BRS.0b013e3181cd588c.
17. JF, Z. *et al.* Expression of Matrix Metalloproteinases, Tissue Inhibitors of Metalloproteinases, and Interleukins in Vertebral Cartilage Endplate. *Orthop Surg* **10**, (2018). doi:10.1111/OS.12409.
18. Bachmeier, B. E. *et al.* Matrix metalloproteinase expression levels suggest distinct enzyme roles during lumbar disc herniation and degeneration. *European Spine Journal* **18**, 1573–86 (2009). doi: 10.1007/s00586-009-1031-8.
19. Weiler, C., Nerlich, A. G., Zipperer, J., Bachmeier, B. E. & Boos, N. 2002 SSE Award Competition in Basic Science: expression of major matrix metalloproteinases is associated with intervertebral disc degradation and resorption. *European Spine Journal* **11**, 308–20 (2002). doi: 10.1007/s00586-002-0472-0.
20. Makarand, V. R. & M Shapiro, I. Role of Cytokines in Intervertebral Disc Degeneration: Pain and Disc-content. *Nat Rev Rheumatol.* **10**, 44–56 (2016). doi: 10.1038/nrrheum.2013.160.Role.
21. Schroeder, G. D. *et al.* Are Modic changes associated with intervertebral disc cytokine profiles? *The Spine Journal* **17**, 129–134 (2017). doi: 10.1016/j.spinee.2016.08.006.
22. Burke, J. *et al.* Modic changes are associated with increased disc inflammatory mediator production. *The Spine Journal* **2**, 3–4 (2002). doi:10.1016/S1529-9430(01)00210-8.
23. Dudli, S. *et al.* ISSLS PRIZE IN BASIC SCIENCE 2017: Intervertebral disc/bone marrow cross-talk with Modic changes. *Eur Spine J* **26**, 1362–1373 (2017). doi: 10.1007/s00586-017-4955-4.
24. Janeway, C. A. & Medzhitov, R. Innate Immune Recognition. *Annu Rev Immunol* **20**, 197–216 (2002). doi: 10.1146/annurev.immunol.20.083001.084359.
25. Klawitter, M. *et al.* Expression and regulation of toll-like receptors (TLRs) in human intervertebral disc cells. *Eur Spine J* **23**, 1878–91 (2014). doi: 10.1007/s00586-014-3442-4.



26. Bisson, D. G., Mannarino, M., Racine, R. & Haglund, L. For whom the disc tolls: intervertebral disc degeneration, back pain and toll-like receptors. *Eur Cell Mater* **41**, 355–369 (2021). doi: 10.22203/eCM.v041a23.
27. Krock, E. *et al.* Toll-like Receptor Activation Induces Degeneration of Human Intervertebral Discs. *Sci Rep* **7**, 17184 (2017). doi: 10.1038/s41598-017-17472-1.
28. Quero, L. *et al.* Hyaluronic acid fragments enhance the inflammatory and catabolic response in human intervertebral disc cells through modulation of toll-like receptor 2 signaling pathways. *Arthritis Res Ther* **15**, R94 (2013). doi:10.1186/ar4274.
29. Greg Anderson, D., Li, X., Tannoury, T., Beck, G. & Balian, G. A fibronectin fragment stimulates intervertebral disc degeneration in vivo. *Spine (Phila Pa 1976)* **28**, 2338–45 (2003). doi: 10.1097/01.BRS.0000096943.27853.BC.
30. Oegema, T. R., Johnson, S. L., Aguiar, D. J. & Ogilvie, J. W. Fibronectin and its fragments increase with degeneration in the human intervertebral disc. *Spine (Phila Pa 1976)* **25**, 2742–7 (2000). doi: 10.1097/00007632-200011010-00005.
31. Ruel, N. *et al.* Fibronectin fragments and the cleaving enzyme ADAM-8 in the degenerative human intervertebral disc. *Spine (Phila Pa 1976)* **39**, 1274–9 (2014). doi: 10.1097/BRS.0000000000000397.
32. Urquhart, D. M. *et al.* Could low grade bacterial infection contribute to low back pain? A systematic review. *BMC Med* **13**, 13 (2015). doi: 10.1186/s12916-015-0267-x.
33. Chen, Z. *et al.* Modic Changes and Disc Degeneration Caused by Inoculation of Propionibacterium acnes inside Intervertebral Discs of Rabbits: A Pilot Study. *Biomed Res Int* **2016**, 9612437 (2016). doi: 10.1155/2016/9612437.
34. Rajasekaran, S. *et al.* “Modic changes are associated with activation of intense inflammatory and host defense response pathways - molecular insights from proteomic analysis of human intervertebral discs” *Spine J* (2021) doi: 10.1016/j.spinee.2021.07.003.
35. Rajasekaran, S. *et al.* ISSLS PRIZE IN CLINICAL SCIENCE 2017: Is infection the possible initiator of disc disease? An insight from proteomic analysis. *Eur Spine J* **26**, 1384–1400 (2017). doi: 10.1007/s00586-017-4972-3.
36. Dudli, S. *et al.* Propionibacterium acnes infected intervertebral discs cause vertebral bone marrow lesions consistent with Modic changes. *J Orthop Res* **34**, 1447–55 (2016). doi: 10.1002/jor.23265.
37. Heggli, I. *et al.* Low back pain patients with Modic type 1 changes exhibit distinct bacterial and non-bacterial subtypes. *Osteoarthr Cartil Open* 100434 (2024) doi: 10.1016/J.OCARTO.2024.100434.
38. Jiao, Y. *et al.* Propionibacterium acnes induces discogenic low back pain via stimulating nucleus pulposus cells to secrete pro-algesic factor of IL-8/CINC-1 through TLR2–NF-κB p65 pathway. *J Mol Med* **97**, 25–35 (2019). doi: 10.1007/s00109-018-1712-z.
39. Schmid, B., Hausmann, O., Hitzl, W., Achermann, Y. & Wuertz-Kozak, K. The Role of Cutibacterium acnes in Intervertebral Disc Inflammation. *Biomedicines* **8**, 186 (2020). doi: 10.3390/biomedicines8070186.
40. Shan, Z. *et al.* The Influence of Direct Inoculation of Propionibacterium acnes on Modic Changes in the Spine: Evidence from a Rabbit Model. *J Bone Joint Surg Am* **99**, 472–481 (2017). doi: 10.2106/JBJS.16.00146.

41. Qin, C. *et al.* MyD88-dependent Toll-like receptor 4 signal pathway in intervertebral disc degeneration. *Exp Ther Med* 611–618 (2016) doi: 10.3892/etm.2016.3425.
42. Mannarino, M. *et al.* Toll-like receptor 2 induced senescence in intervertebral disc cells of patients with back pain can be attenuated by o-vanillin. *Arthritis Res Ther* **23**, 117 (2021). doi: 10.1186/s13075-021-02504-z.
43. De Luca, P. *et al.* Intervertebral disc and endplate cells response to IL-1 $\beta$  inflammatory cell priming and identification of molecular targets of tissue degeneration. *Eur Cell Mater* **39**, 227–248 (2020). doi: 10.22203/eCM.v039a15.
44. Kuchynsky, K. *et al.* Transcriptional profiling of human cartilage endplate cells identifies novel genes and cell clusters underlying degenerated and non-degenerated phenotypes. *Arthritis Res Ther* **26**, 12 (2024). doi: 10.1186/s13075-023-03220-6.
45. Piccinini, A. M. & Midwood, K. S. DAMPening Inflammation by Modulating TLR Signalling. *Mediators Inflamm* **2010**, 1–21 (2010). doi: 10.1155/2010/672395.
46. da Rocha, V. M. *et al.* Would Cutibacterium acnes Be the Villain for the Chronicity of Low Back Pain in Degenerative Disc Disease? Preliminary Results of an Analytical Cohort. *J Pers Med* **13**, 598 (2023). doi: 10.3390/jpm13040598.
47. Klawitter, M., Hakozaki, M. & Kobayashi, H. Expression and regulation of toll-like receptors (TLRs) in human intervertebral disc cells. *Eur Spine J* **23**, (2014). doi: 10.1007/s00586-014-3442-4.
48. Su, S.-L., Tsai, C.-D., Lee, C.-H., Salter, D. M. & Lee, H.-S. Expression and regulation of Toll-like receptor 2 by IL-1 $\beta$  and fibronectin fragments in human articular chondrocytes. *Osteoarthritis Cartilage* **13**, 879–86 (2005). doi: 10.1016/j.joca.2005.04.017.
49. Mannarino, M. *et al.* Toll-like receptor 2 induced senescence in intervertebral disc cells of patients with back pain can be attenuated by o-vanillin. *Arthritis Res Ther* **23**, 117 (2021). doi: 10.1186/s13075-021-02504-z.
50. Sillat, T. *et al.* Toll-like receptors in human chondrocytes and osteoarthritic cartilage. *Acta Orthop* **84**, 585–92 (2013). doi: 10.3109/17453674.2013.854666.
51. Huang, Q.-Q. & Pope, R. M. The role of toll-like receptors in rheumatoid arthritis. *Curr Rheumatol Rep* **11**, 357–64 (2009). doi: 10.1007/s11926-009-0051-z.
52. Brüggemann, H. Skin: Cutibacterium (formerly Propionibacterium) acnes and Acne Vulgaris. in *Health Consequences of Microbial Interactions with Hydrocarbons, Oils, and Lipids* 1–20 (Springer International Publishing, Cham, 2019). doi:10.1007/978-3-319-72473-7\_20-1. doi: 10.1007/978-3-319-72473-7\_20-1.
53. Zhang, B. *et al.* Toll-like receptor 2 plays a critical role in pathogenesis of acne vulgaris. *Biomedical Dermatology* **3**, 4 (2019). doi: 10.1186/s41702-019-0042-2.
54. Scheibner, K. A. *et al.* Hyaluronan Fragments Act as an Endogenous Danger Signal by Engaging TLR2. *The Journal of Immunology* **177**, 1272–1281 (2006). doi: 10.4049/jimmunol.177.2.1272.
55. Paulson, J. C. & Kawasaki, N. Sialidase inhibitors DAMPen sepsis. *Nat Biotechnol* **29**, 406–7 (2011). doi: 10.1038/nbt.1859.
56. Brown, M. F. *et al.* Sensory and sympathetic innervation of the vertebral endplate in patients with degenerative disc disease. *J Bone Joint Surg Br* **79**, 147–53 (1997). doi: 10.1302/0301-620x.79b1.6814.

57. Ohtori, S. *et al.* Tumor necrosis factor-immunoreactive cells and PGP 9.5-immunoreactive nerve fibers in vertebral endplates of patients with discogenic low back Pain and Modic Type 1 or Type 2 changes on MRI. *Spine (Phila Pa 1976)* **31**, 1026–31 (2006). doi: 10.1097/01.brs.0000215027.87102.7c.
58. Fields, A. J., Liebenberg, E. C. & Lotz, J. C. Innervation of pathologies in the lumbar vertebral end plate and intervertebral disc. *Spine Journal* **14**, 513–521 (2014). doi: 10.1016/j.spinee.2013.06.075.
59. Määttä, J. H. *et al.* Strong association between vertebral endplate defect and Modic change in the general population. *Sci Rep* **8**, 16630 (2018). doi: 10.1038/s41598-018-34933-3.
60. Djuric, N. *et al.* Influence of endplate avulsion and Modic changes on the inflammation profile of herniated discs: a proteomic and bioinformatic approach. *Eur Spine J* (2021) doi: 10.1007/s00586-021-06989-9.
61. Takatalo, J. *et al.* Association of modic changes, Schmorl’s nodes, spondylolytic defects, high-intensity zone lesions, disc herniations, and radial tears with low back symptom severity among young Finnish adults. *Spine (Phila Pa 1976)* **37**, 1231–9 (2012). doi: 10.1097/BRS.0b013e3182443855.
62. Hulme, P. A., Boyd, S. K. & Ferguson, S. J. Regional variation in vertebral bone morphology and its contribution to vertebral fracture strength. *Bone* **41**, 946–57 (2007). doi: 10.1016/j.bone.2007.08.019.

# Chapter 6: Elevated Abundance of HTRA1-Generated Fragments in MC1 Discs Induces Cartilage Endplate Degeneration

**Tamara Mengis<sup>1,2</sup>, Jan Devan<sup>1,2</sup>, Bernd Roschitzki<sup>3</sup>, Irina Heggli<sup>1,2</sup>, Nick Herger<sup>1,2</sup>, Roy Marcus<sup>4</sup>, Florian Brunner<sup>2</sup>, Christoph Laux<sup>5</sup>, Mazda Farshad<sup>5</sup>, Oliver Distler<sup>1,2</sup>, Stefan Dudli<sup>1,2</sup>**

<sup>1</sup>Center of Experimental Rheumatology, Department of Rheumatology, University Hospital, University of Zurich, Switzerland

<sup>2</sup>Department of Physical Medicine and Rheumatology, Balgrist University Hospital, University of Zurich, Switzerland

<sup>3</sup>Functional Genomics Center Zurich, University and ETH Zurich, Zurich, Switzerland

<sup>4</sup>Department of Radiology, Balgrist University Hospital, University of Zurich

<sup>5</sup>Department of Orthopedics, Balgrist University Hospital, University of Zurich, CH

**Ongoing research**

## 6.1 Abstract

**Background:** Vertebral bone marrow lesions, known as Modic type 1 (MC1) changes are linked to accelerated disc degeneration and endplate damage. Although degenerated discs are a prerequisite for MC1 development, not all degenerated discs have adjacent MC1. This observation suggests that MC1 discs possess unique characteristics compared to non-MC discs. However, the specific way these discs contribute to MC development remains unclear. We propose that MC1 discs undergo a distinct degenerative pathway, resulting in heightened production of extracellular matrix (ECM) fragments. These fragments may serve as Damage-Associated Molecular Patterns (DAMPs), initiating degenerative alterations not only within the disc but also affecting adjacent endplates. Consequently, vertebral endplate damage occurs, compromising its barrier function and enabling inflammation to spread to the bone marrow and induce MC1.

**Methods:** Degenerated MC1 discs (n = 30) and degenerated non-Modic (nonMC) discs (n = 25) underwent N-terminal amine isotopic labeling of substrates (TAILS) followed by mass spectrometry, to identify ECM-derived fragments and their abundance. The protease high temperature requirement serine protease 1 (HTRA1) was examined for its potential of cleaving these fragments. Assays using reporter cell lines for nuclear factor kappa-light-chain-enhancer of activated B cells (NFκB) as well as flow cytometry of phosphorylated NFκB were used to investigate the ability of the found fragments to act pro-inflammatory. Further, gene expression of the DAMP receptive Toll-like receptors (TLR) was evaluated in MC1 compared to nonMC cartilage endplate (CEP) cells. Finally, CEP destruction was measured after TLR2 activation through sulfated glycosaminoglycan (sGAG) release.

**Results:** The proteome analysis revealed an increased abundance of ECM-derived fragments in MC1 discs, particularly those related to fibronectin (FN), cartilage intermediate layer protein 1 (CILP1), and collagen alpha 1 chain (COL1A1). HTRA1 was identified as increased in the MC1 disc and with the potential to cleave FN, CILP1, and COL1A1. The N-terminal fragments of CILP1 produced by HTRA1 were found to induce NFκB activation through TLR4, indicating their role as DAMPs. Furthermore, MC1 CEP cells exhibited higher expression of TLR2 suggesting prior exposure to DAMPs. Activation of TLR2 in CEP tissue led to the upregulation of inflammatory genes and matrix breakdown enzymes as well as tissue destruction as measured by sulfated glycosaminoglycan release into the media.

**Conclusion:** The study found that the degradome of the MC1 disc is made up of a greater abundance of fragments compared to nonMC discs, underscoring its distinct degenerative pathway. Notably, fragments of CILP1 generated through HTRA1 cleavage, along with full-length COMP, were identified as pro-inflammatory and prominently elevated in the MC1 disc. This implies a cascade of events initiated by the unique degeneration of the MC1 disc, as these fragments have the capability to activate TLRs within the disc, ultimately resulting in endplate damage through biologically triggered mechanisms. These findings enhance our understanding of MC1 development and offer therapeutic targets to impede its progression. Targeting ECM-derived DAMPs, HTRA1, or TLR-mediated pathways could effectively hinder MC1 advancement.

**Keywords:** Degradome, Modic changes, DAMPs, Toll-like receptors, HTRA1

## 6.2 Introduction

Modic type 1 changes (MC1) are vertebral bone marrow signal intensity changes that are predominantly observed in patients with degenerated intervertebral discs and damaged cartilage endplates. MC1 is observed in approximately 40 % of all chronic low back patients <sup>1</sup>. Discs adjacent to MC1 undergo an accelerated degenerative process and release more pro-inflammatory and pro-fibrotic factors, accompanied by inflammation and destruction of the adjacent endplates <sup>2,3</sup>. Yet, it remains unknown if the degenerative process of MC1 discs differs from non-MC discs and what the mechanistic link is which connects disc degeneration and endplate damage in MC1. This knowledge gap is crucial, as endplate damage is strongly linked to MC1 development. Damage to the endplate results in the loss of its barrier function between the bone marrow and the disc, thereby facilitating the initiation of MC. Therefore, MC1 is described as a pathology involving the entire disc-endplate-bone marrow complex, with significant crosstalk between these compartments <sup>3-5</sup>. Hence, the prevention of endplate damage could potentially disrupt the destructive pathomechanisms associated with MC1. Therefore, the overall aim of this study was to demonstrate a causal mechanism of disc degeneration with endplate damage in MC1.

Disc degeneration leads to rapid breakdown of the extracellular matrix (ECM), yielding numerous ECM fragments some of which act as damage-associated molecular patterns (DAMPs), potentially triggering inflammation by binding to toll-like receptor 2 (TLR2) or TLR4 <sup>3,6</sup>. These ECM-derived DAMPs can induce inflammatory pathway activation in surrounding cells and tissue <sup>7</sup>. Past studies have found that the chronic administration of TLR4 inhibitor showed positive results in diminishment of low back pain and disc degeneration in a mouse model <sup>8</sup>. Interestingly, chemonucleolysis, an outdated proteolytic therapy for spinal stenosis, has been linked to the rapid development of MC1 in adjacent bone marrow, suggesting a causal relationship between ECM disc fragmentation and MC1 occurrence <sup>9</sup>.

The role of the cartilage endplate (CEP), separating the disc from the vertebra and tightly controlling nutrient flow to the disc, is critical in MC1 <sup>10-12</sup>. MC1 initiates in the endplates before extending into the bone marrow, and endplate damage is considered a prerequisite for MC1 development <sup>13</sup>. Recent transcriptional analysis of CEP cells supports an active biological role in disc degeneration <sup>14</sup>. This, coupled with the observation that the cell density in the CEP is notably higher than in the adjacent discs <sup>15</sup>, underscores the potential of CEP cells to play a crucial role in the pathomechanisms of MC1.

In summary, the disc degenerates faster in MC1, endplates are inflamed and damaged and a mechanistic link between disc and endplate degeneration is missing. We hypothesize i.) that the MC1 discs contain more ECM-derived fragments which are generated through a MC1-specific mechanism and ii.) that these fragments act as pro-inflammatory DAMPs, activating not only TLRs in the disc but also in the adjacent CEP and inducing tissue destruction.

## 6.3 Methods

### *Patient recruitment*

Discs derived from patients that gave informed consent and underwent spinal lumbar fusion surgery. Inclusion criteria for the selection of the patients were the absence of current or chronic systemic inflammatory or infectious diseases, as well as no prior open back surgery. Each patient's MRI was evaluated by a board-certified radiologist and scored for Pfirrmann grade and presence of MC1<sup>16</sup>.

### *MC1 disc degradome analysis*

The samples were analyzed using N-terminal amine labeling of substrate (TAILS) mass spectrometry allowing identification of cleaved proteins as well as the respective cleavage site. The tissue was frozen and pulverized by cryomilling before undergoing protein extraction with 4 % sodium dodecyl sulfate and high intensity focused sonication. Each sample was reduced in 10 mM tris (2-carboxyethyl)phosphine hydrochloride (TCEP), alkylated through addition of 500 mM chloroacetamide (CIAA) to a final concentration of 25 mM, and specifically labeled using 16 plex tandem mass tag (TMT) labeling allowing pooling of samples into 5 batches of 13 samples each. Single-pot, solid phase-enhanced sample preparation (Sp3) digest with carbamidomethylation was followed by cleavage to peptides using trypsin (1:50, peptide: enzyme ratio). For pre-TAILS analysis 5 % of the solution was removed and stored up until the desalting step. A hyperbranched polyaldehyde polymer (HPG-ALDII) (Flintbox) was used to bind and remove internal trypsin-generated peptides (5:1 polymer:peptide ratio), with the immediate addition of NABH<sub>3</sub>CN to a final concentration of 20 mM and incubated overnight. The reaction was terminated with the addition of 1 M ammonium bicarbonate to 100 mM concentration. The polymer was removed with 30 kDa MWCO centrifugal filters. Both the TAILS and preTAILS samples were desalted with Sep-Pak® C18 Cartridges (Waters, USA) according to manufacturer's protocol and lyophilized. For analysis with liquid chromatography tandem mass spectrometry (LC-MS/MS) the sample was reconstituted in 3 % acetonitrile in formic acid was used for analysis. Q Exactive HF 2 with online high-performance liquid chromatography was used for analysis.

Peptide-spectrum matching was performed using Proteome Discoverer 2.5 searching against the human UniProt protein database. Static modifications included carbamidomethyl (C) and TMTpro (K), while dynamic modifications at protein termini included Methionine-loss (M) and Acetyl (N-Term). Additional dynamic modifications encompassed Met-loss + Acetyl, and the overall dynamic modification was oxidation (M). Furthermore, TMTpro labeling was added as a static peptide terminus modification for the TAILS fraction, but not the pre-TAILS fraction. Subsequent statistical analysis and normalization to standard sample was performed using R Studio 4.2.0. Statistical analysis for group comparison involved the use of Mann-Whitney U tests on the median-normalized abundance.

### *HTRA1 cleavage potential of candidate proteins*

To determine cleavage potential of HTRA1 on various proteins the recombinant proteins (CILP1 (R&D Systems), COL1A1 (LSBio, USA), COMP (Abcam, United Kingdom), Fibronectin (R&D Systems)) were

incubated in 50 mM tris-hydrochloric acid (HCl), 150 mM NaCl (pH 8.0) buffer for 18 h at a 1:10 ratio either with active HTRA1 or mutant HTRA1 S328A (courtesy of Professor Michael Ehrmann, University Duisburg). HTRA1 S328 is an inactive mutant form of HTRA1 with a serine to alanine mutation at amino acid 328. Furthermore, the HTRA1 inhibitor Galegenimab (Genentech, California, USA) was tested at various concentrations using a well-established HTRA1 substrate, beta-casein.

Whether cleavage took place or not was visualized through sodium dodecyl sulfate–polyacrylamide gel electrophoresis (SDS-PAGE) followed by Coomassie blue staining. Specifically, the samples were mixed in a 1:1 ratio with Lämmli Buffer (Biorad, CH) followed by denaturation through boiling for 3 minutes at 95°C. Subsequently, the treated samples were loaded onto 4–15 % Mini-PROTEAN® TGX™ precast protein gels, running initially for 15 minutes at 60 Volts, followed by 1 hour at 100 Volts. Protein bands were made visible with use of 1h PageBlue™ Protein Staining Solution (Thermo Fisher Scientific). Further experiments were continued only with the proteins that were cleaved by HTRA1.

Additionally, to determine the N-terminal cleavage site the enzyme protein mix was analyzed with TAILS mass spectrometry. The proteins were digested individually as described above, with either active or mutant HTRA1. After overnight digestion, the mix was snap frozen, lyophilized and reconstituted in 50 mM triethylammonium bicarbonate (TEAB) buffer. The remaining steps of the protocol adhered to the established TAILS protocol employed for measuring the disc degradome, as described previously with the difference of using a 6-plex TMT label. Specifically, TMT labels 126, 127 and 128 were assigned for proteins digested with active HTRA1, and TMT labels 129, 130 and 131 were assigned to the proteins digested with mutant HTRA1. The spectrum-to-peptide matching procedure adhered to the protocol described above. Found peptide sequences were compared to the fragments found in the MC1 disc degradome to determine potential overlaps. The normalized abundances of the peptides found also in the nonMC and MC1 disc degradomes were compared by unpaired t-test on abundances normalized to batch standards.

### *Degradomics of HTRA1 digested disc*

A disc obtained from the L3/4 level, graded Pfirrmann 2, was collected during spinal fusion surgery of a 13-year-old patient with scoliosis, which served as a model for a less degenerated discs. Following collection, the disc was washed with phosphate-buffered saline (PBS). Subsequently, 100 mg of the tissue was cryomilled, and 400 µl of a buffer solution consisting of 50 mM Tris-HCl and 150 mM NaCl (pH 8.0) was added. The protein quantity was determined using the Bicinchoninic Acid (BCA) assay. For each experimental condition, 60 µg of protein was utilized, with the enzyme HTRA1 added at a ratio of 1:10 relative to the protein amount. Four different conditions were tested: i) tissue alone (2 technical replicates), ii) tissue with active HTRA1 (4 technical replicates), iii) tissue with mutant HTRA1 (4 technical replicates), iv) tissue with HTRA1 and Galegenimab (3 technical replicates), and v) tissue with Galegenimab (3 technical replicates). Each digest was performed overnight at 37 ° C. To remove the salt a TCA precipitation was performed before the previously described TMT 16-plex TAILS protocol was performed to analyze the degradome induced through HTRA1



exposure. Before conducting TMT 16-plex TAILS according to the protocol used for the disc degradome analysis, a TCA precipitation was carried out to eliminate the salt from the digestion buffer.

N-terminal fragment abundance was compared between the different conditions using one-way ANOVA followed by Dunn's multiple comparison testing.

### *Pro-inflammatory potential of fragments using THP1 NFkB reporter cells*

The NFkB activation was tested using THP1-Blue™ NFkB Cells, a NFkB-SEAP reporter monocyte cell line (Invivogen). Cells were cultured in RPMI 1640, 2 mM L-glutamine, 25 mM HEPES, 10 % FCS, Pen-Strep (100 U/ml-100 µg/ml) with the addition of the selective antibiotics Zeocin and Normocin at concentrations of 100 µg/ml. A total of 30 µl of a 1 mio cells/ ml cells suspension was seeded in a 384 well plate. The cells were treated for 2 hours with Polymyxin B (Invivogen) at a concentration of 100 µg/ml. Following incubation, CILP1, COMP, and FN were added either as whole proteins, pre-incubated with HTRA1, or pre-incubated with mutant HTRA1. The incubation of the proteins was conducted as described previously, with the addition of an extra step involving desalting using Pierce™ Protein Concentrators PES, 3K, followed by lyophilization with a freeze dryer before resuspending in THP1 growth media.

After 24 hours, NFkB activity was indirectly measured through the production of Secreted Embryonic Alkaline Phosphatase (SEAP) by the reporter cell line upon NFkB activation. For this, a total of 30 µl of Quanti Blue along with 15 µl of the supernatant from each individual well was used and incubated for 6 hours at 37° C. Absorbance was then measured at 620 nm.

Statistical analysis was conducted on the absorbance measurement values using one-way ANOVA, followed by Dunnett's multiple comparisons test to assess statistical significance between all conditions used.

### *Assessment of NFkB phosphorylation following fragment stimulation*

Cells were seeded into 52 wells of 96-well U-bottom plates at a concentration of  $1 \times 10^6$  cells/ml in 22.5 µl of complete RPMI media per well. Candidate NFkB phosphorylating agonists (HTRA1-derived COMP, CILP1 and FN fragments) were prepared as previously described. The fragments together with well-known TLR agonists (Pam2csk4, LPS and FNf30 kDa) were prepared at a concentration of 1 mg/ml. Subsequently, 2.5 µl of the agonist solution was added to each well inside the incubator, with additional doses added after 30, 50, and 55 minutes. Five minutes after the final agonist addition, the plate was removed from the incubator, placed on ice, and treated with 200 µl/well of cold PBS. Cells were fixed with pre-warmed fixation buffer for 10 minutes at 37°C. After washing in permeabilization wash buffer at 4°C cells were permeabilized in permeabilization buffer for 30 minutes on ice. Subsequently, phosphorylated NFkB was stained using anti-pNFkB antibody diluted in permeabilization buffer at room temperature for one hour. Finally, cells were washed with staining buffer and immediately analyzed using Cytex Aurora. Data was analyzed with FlowJo v10.8 software. Cell doublets and dead cells were excluded from the analysis.

The same procedure was repeated for experiments which also included TLR2 inhibitor TL2-C29 (200 uM) (Invivogen) and TLR4 inhibitor CLI-095 (5 uM) (Invivogen) as well as Polymixin B (50 ug/ml) (Invivogen). The inhibitors were added to the cells 2 hours prior to the addition of the stimulating agonists.

### *Culture of CEP cells*

CEP cells were isolated from fresh CEP tissue of spinal fusion surgery patients that signed informed consent for further use of surgically removed biological material. CEPs were enzymatically digested overnight with 0.05% collagenase P (Roche, Basel, Switzerland) in Dulbecco's modified eagle's medium (DMEM) (Gibco, Reinach, Switzerland) supplemented with 10 % fetal calf serum (FCS), 50 U/ml penicillin streptomycin, 10 mM HEPES, 2 mM L-Glutamine and expanded to passage 1-2. The media used for expansion consisted of 10 % FCS, 50 U/ml penicillin streptomycin, 10 mM HEPES, 2 mM L-Glutamine in DMEM.

### *RNA isolation and qPCR*

RNA isolation was performed according to the RNeasy Mini Kit (Qiagen, Hilden, Germany) manufacturer protocol with cell lysis performed in RLT buffer containing 1 %  $\beta$ -mercaptoethanol (Gibco) including the optional DNase digestion step. Reverse transcription of 100 ng RNA was performed according to the SensiFast cDNA synthesis kit (Meridian Bioscience, USA).

Relative mRNA levels were quantified with use of the SensiFAST SYBR No-Rox kit (Labgene, Châtel-Saint-Denis, Switzerland) on a magnetic induction real-time qPCR cycler (Labgene). Cycle conditions after initial denaturation at 95°C for 300s were as follows: 40 cycles of 5 seconds at 95 °C, 20 seconds at 60 °C, 10 seconds at 72 °C, followed by melting curve analysis. Analysis was done with the  $\Delta\Delta Cq$  method and with normalization to the housekeeping genes Glyceraldehyde-3-Phosphate Dehydrogenase (GADPH). All used primer sequences are listed in Table 1. MC1 was normalized to the average of all nonMC delta Cq values. Unpaired Friedman's tests with Dunn's multiple comparison correction were employed for statistical analysis on fold change values. Correlation between HTRA1 and TLRs was tested with Spearman correlation analysis.

**Table 1.** qPCR Primers

<b>Primers</b>	<b>Forward</b>	<b>Reverse</b>
<b>ADAMTS 5</b>	5'-CCT GGT CCA AAT GCA CTT CAG C-3'	5'-TCG TAG GTC TGT CCT GGG AGT T-3'
<b>GAPDH</b>	5'-ATTCCACCCATGGCAAATTC-3'	5'-GGGATTTCCATTGATGACAAGC-3'
<b>IL6</b>	5'-AGA CAG CCA CTC ACC TCT TCA G-3'	5'-TTC TGC CAG TGC CTC TTT GCT G-3'
<b>MMP1</b>	5'-ATG AAG CAG CCC AGA TGT GGA G-3'	5'-TGG TCC ACA TCT GCT CTT GGC A-3'
<b>MMP3</b>	5'-CAC TCA CAG ACC TGA CTC GGT T-3'	5'-AAG CAG GAT CAC AGT TGG CTG G-3'
<b>MMP9</b>	5'-GCCACTACTGTGCCTTTGAGTC-3'	5'-CCCTCAGAGAATCGCCAGTACT-3'
<b>MMP13</b>	5'-CCT TGA TGC CAT TAC CAG TCT CC-3'	5'-AAA CAG CTC CGC ATC AAC CTG C-3'
<b>TLR2</b>	5'-GGCCAGCAAATTACCTGTGTG-3'	5'-AGGCGGACATCCTGAACCT-3'
<b>TLR4</b>	5'-CAGAGTTTCTGCAATGGATCA-3'	5'-GCTTATCTGAAGGTGTTGCACAT-3'
<b>TLR6</b>	5'-GAAGAAGAACAACCCTTTAGGATAGC-3'	5'-AGGCAAACAAAATGGAAGCTT-3'

## *CEP Explant Model*

To test if TLR2 stimulation in CEP explants causes CEP degeneration, CEP explants were stimulated with Pam2csk4. In a first step, it was tested if Pam2csk4 can diffuse into CEP tissue and affect CEP cells gene expression. For this, CEPs were collected during surgery, washed and a punch biopsy of 4 mm was taken and cut in half. Both were incubated in CEP cells growth media with one half additionally exposed to 10 ug/ml Pam2csk4. After 24 h the tissue was collected and pulverized by a cryomill. The powder was immediately dissolved in RLT lysis buffer. Subsequently, RNA extraction was carried out using a previously described protocol.

The capacity of Pam2csk4 to induce CEP degeneration was assessed by an extended incubation period of the tissue with Pam2csk4, as described earlier, to 14 days. Degeneration was then assessed by quantifying release of GAGs to the media using 1,9-dimethylmethylene blue (DMMB) assay. Briefly, both the tissue and the supernatant were gathered, and the tissue was lyophilized. Subsequently, the tissue was digested overnight in 1 ml solution of 1 mg/ml papain from papaya latex (Sigma). To eliminate debris, a centrifugation step of 10 minutes at 10'000 x g was done before carrying out the DMMB assay, which enables the detection of sulfated glycosaminoglycans (sGAGs), on both the supernatant and the digested tissue mixture. The combination of the supernatant and the tissue mixture accounted for 100 % of the sGAGs in the tissue. This allowed the calculation of the proportion released into the supernatant during the 14-day incubation period. Chondroitin sulfate sodium salt from shark cartilage (Sigma-Aldrich, Darmstadt, Germany) was used to create the standard curve.

## *Statistical Analysis*

All statistical analyses were performed using GraphPad Prism V10.2.0, unless stated otherwise. The significance level was  $\alpha = 0.05$ .

## **6.4 Results**

### *Patient demographics*

Two different patient cohorts were used for proteomic analysis (n = 54) (Table 2) and cell culture experiments with CEP cells (n = 17) (Table 3). Importantly, no difference could be noted between the degree of degeneration in nonMC and MC1 discs as shown by the Pfirrmann grade. Additionally, no difference could be found in either cohort in the pain level as assessed by the VAS and ODI. Only the body mass index (BMI) and weight showed a significant difference between the groups in the cohort used for TAILS analysis.

**Table 2.** Patient demographics of patient cohort used for analysis of the proteome and degradome of the disc through TAILS. Groups were divided into nonMC and MC1. Statistical differences in Pfirrmann grade, age, height, weight and body mass index (BMI) were assessed through unpaired t-tests. Visual analog scale (VAS) scores for leg and back pain, as well as Oswestry Disability Index (ODI), were analyzed using Mann-Whitney comparisons. The ratio of males to females and smokers to non-smokers was included and compared through contingency analysis.

		<b>nonMC</b>	<b>MC1</b>	<b>P-value</b>
<b>Number of patients</b>		22	32	
<b>Pfarrmann</b>		4.2 ± 0.9	4.4 ± 0.6	0.495
<b>Age</b>		59.5 ± 19.8	62.9 ± 14.5	0.473
<b>Weight (kilograms)</b>		90.7 ± 25.4	77 ± 14.7	0.020
<b>Height (cm)</b>		168.9 ± 10.4	169.1 ± 9.8	0.956
<b>BMI</b>		31.3 ± 6.1	26.9 ± 4.7	0.005
<b>VAS Back Pain</b>		6.8 ± 1.7	6.7 ± 2.3	0.817
<b>VAS Leg Pain</b>		6.6 ± 2.1	5.7 ± 3.3	0.496
<b>Oswestry Disability Score (ODI)</b>		42.9 ± 16.9	43.5 ± 20.5	0.920
<b>Females:Males</b>		10:12	17:14	0.583
<b>Smoker (Yes : Ex : No)</b>				>0.999
	<b>Yes</b>	5.0	7	
	<b>No</b>	17.0	24	
<b>Level</b>				
	<b>L1/2</b>	1	0	
	<b>L2/3</b>	1	1	
	<b>L3/4</b>	2	13	
	<b>L4/5</b>	9	14	
	<b>L5/S1</b>	9	3	

**Table 3.** Patient demographics of patient cohort used for CEP cell culture experiments. Groups were divided into nonMC and MC1. Statistical differences in Pfarrmann grade, age, height and body mass index (BMI) were assessed through unpaired t-tests. Visual analog scale (VAS) scores for leg and back pain, as well as Oswestry Disability Index (ODI), were analyzed using Mann-Whitney comparisons. The ratio of males to females and smokers to non-smokers was included and compared through contingency analysis.

		<b>nonMC</b>	<b>MC1</b>	<b>P-value</b>
<b>Number of patients</b>		10	7	
<b>Pfarrmann</b>		4.3 ± 0.8	4.0 ± 1.2	0.675
<b>Age</b>		57.4 ± 13.8	57.0 ± 18.1	0.959
<b>Height (cm)</b>		165.4 ± 12.2	173.9 ± 13.6	0.200
<b>BMI</b>		32.0 ± 8.0	26.7 ± 3.4	0.126
<b>VAS Back Pain</b>		6.1 ± 2.0	4.4 ± 3.7	0.454
<b>VAS Leg Pain</b>		5.6 ± 1.8	6.1 ± 2.3	0.541
<b>Oswestry Disability Score (ODI)</b>		30.5 ± 15.6	35.4 ± 24.8	0.617
<b>Females : Males</b>		5:5	3:4	>0.999
<b>Smoker (Yes : No)</b>		4: 6	3:4	>0.999
<b>Level</b>				
	<b>L3/4</b>	2	1	
	<b>L4/5</b>	5	4	
	<b>L5/S1</b>	3	2	

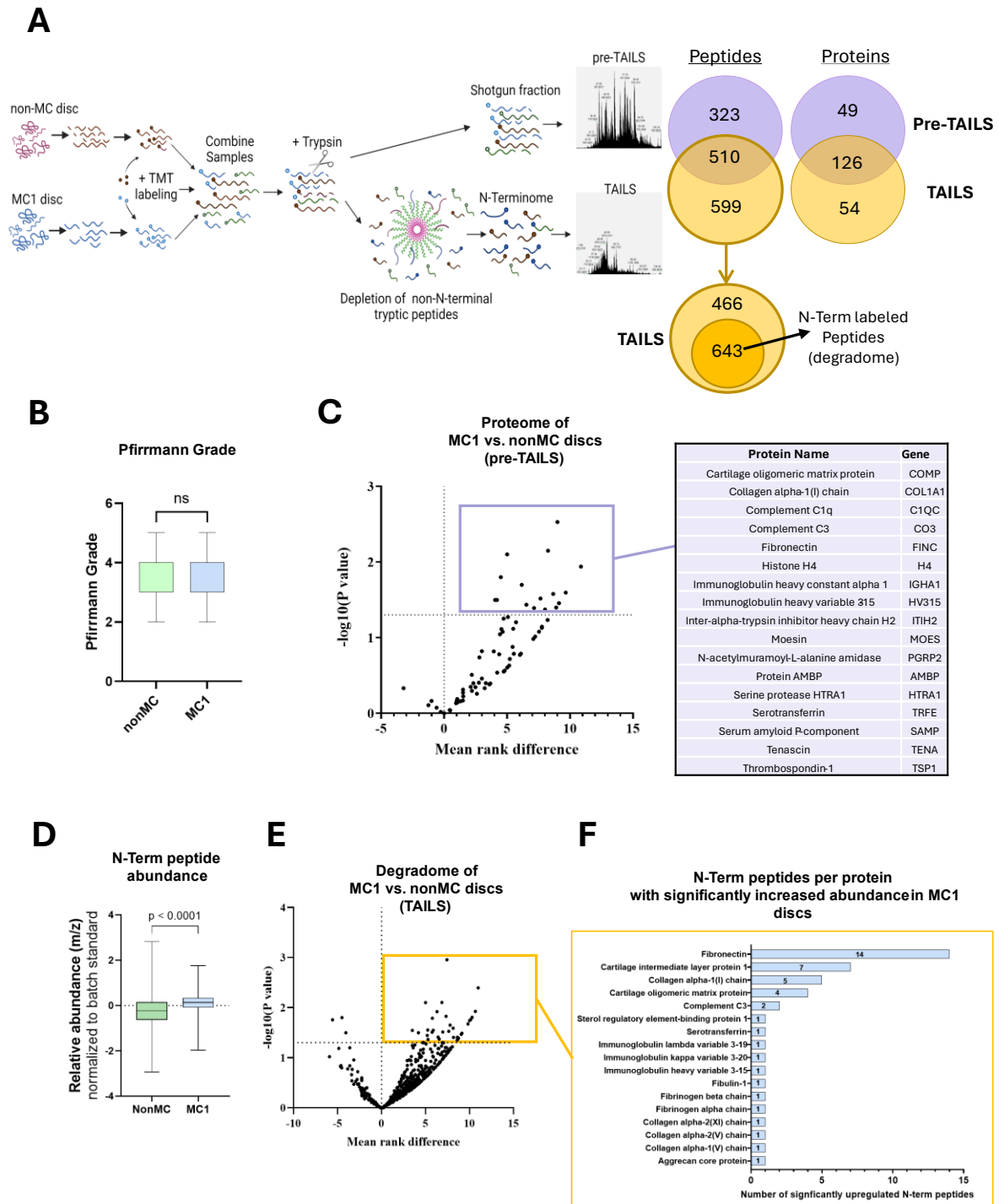


**Figure 1.** Proteome and degradome of the MC1 disc. **(A)** Experimental outline of N-TAILS analysis with the main steps illustrated followed Venn diagrams which indicate the number of detected proteins and peptides in both pre-TAILS and TAILS analysis as well as their overlap. Additionally, TAILS peptides are categorized into N-terminally labeled peptides, which constitutes the degradome. **(B)** Degree of degeneration as Pfirrmann grades in analyzed nonMC and MC1 discs assessed for significance with unpaired t-tests. **(C)** Volcano plot of proteins identified with pre-TAILS mass spectrometry comparing MC1 to nonMC discs using Mann Whitney U tests on protein abundances normalized to batch standards prior to correction for multiple comparisons. **(D)** Difference in N-terminal peptide abundance between nonMC and MC1 discs measured by TAILS. **(E)** Volcano plot of N-terminal peptides identified with TAILS mass spectrometry comparing MC1 to nonMC discs using Mann Whitney U tests on protein abundances normalized to batch standards prior to correction for multiple comparisons. **(F)** Peptides with increased abundance in MC1 discs grouped by the corresponding proteins which they derive from.

### *MC1 discs have a greater abundance of fragments*

The proteome analysis of all examined discs revealed 833 peptides corresponding to 175 proteins. The N-TAILS fraction, designed to enrich N-terminal fragments, identified a higher number of peptides compared to the pre-TAILS fraction, totaling 1,109 peptides, with 510 overlapping with the pre-TAILS. Among these, 643 had an N-terminal label attached, which made up the so called degradome (Figure 1A).

When dividing the discs into the groups nonMC and MC1, no difference between the disc degeneration level could be found (Figure 1B). Sixteen proteins were differentially abundant in MC1 and nonMC1 in the pre-TAILS fraction ( $p < 0.05$  before correction for multiple comparisons) and no proteins were more present in nonMC discs (Figure 1C). The only protease identified within this group of proteins is the serine protease High Temperature Requirement A serine peptidase 1 (HTRA1). It will be employed in subsequent experiments.

The TAILS analysis focused on the 643 different N-terminally labelled peptides which constitute the degradome of the discs upon analysis of all discs. On average, the number of these N-terminal peptides found per disc was 335 in MC1 discs and 332 in non-MC discs. This suggests that approximately half of the N-terminal peptides are consistent among the patients, while the remaining part of the degradome is patient-specific. Although none of the fragments were unique to MC1 patients, the MC1 discs contained had a higher abundance of the protein fragments than nonMC discs ( $p < 0.001$ ) (Figure 1D), of which 44 showed an increased abundance in MC1 discs (Figure 1E). The majority of the fragments, specifically 14 of them, belonged to the protein fibronectin (FN), followed by seven fragments associated with cartilage intermediate layer protein 1 (CILP1), five with collagen alpha 1 chain (COL1A1), and four fragments linked to cartilage oligomeric matrix protein (COMP) (Figure 1E).

### *HTRA1 produces CILP1, COMP and FN fragments*

The link between the increased HTRA1 presence and the fragments found in greater number in MC1 discs was investigated and found that CILP1, COMP and FN were all cleaved by HTRA1 while COL1A1 was not (Figure 2A). When examining the number of N-terminal fragments of CILP1, COMP, and FN in degenerated discs, they constitute more than a third of the degradome (Figure 2B). Through TAILS analysis, the precise cleavage sites of COMP, CILP1, and FN by HTRA1 were determined. Notably, 9 out of the 19 cleavage sites identified from the in-vitro digest of these three recombinant proteins overlapped with those detected in the degradome of the discs (Figure 2B). The number of patients in which these 9 fragments were detected was not significantly different between the group (Figure 2C). Nevertheless, upon consideration of the normalized abundance of these fragments, a statistically significant increased ( $p < 0.001$ ) abundance was observed in MC1 (Figure 2D). This shows the degeneration process of COMP, CILP, FN is a process that also takes place in non-MC discs but this degradation mechanism is stronger in MC1.

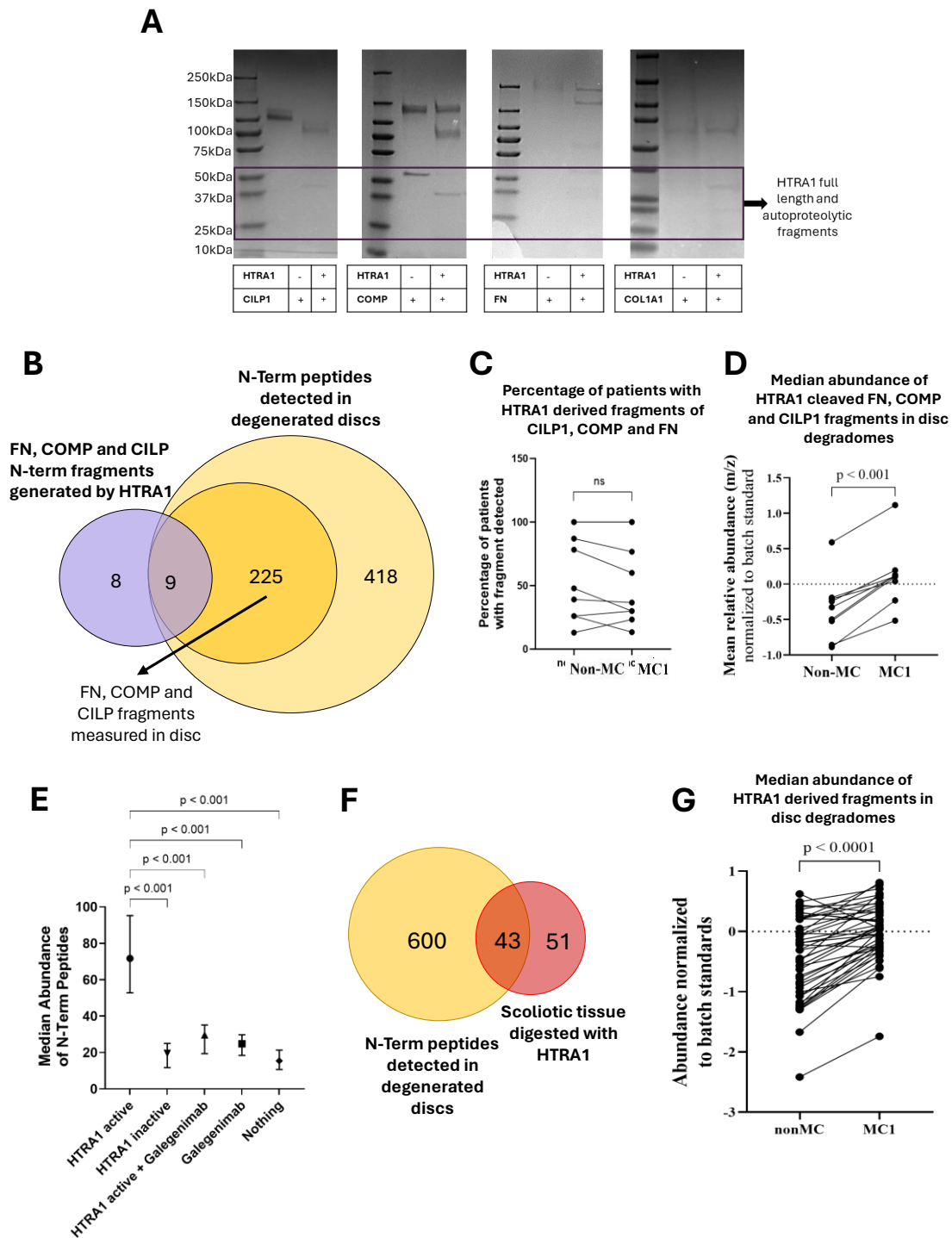


**Figure 2.** Role of HTRA1 in fragment production and MC1 disc degeneration. **(A)** Potential of HTRA1 to cleave cartilage intermediate layer protein (CILP1), cartilage oligomeric matrix protein (COMP), collagen alpha 1 chain (COL1A1) and fibronectin (FN) as well as **(B)** effect of Galegenimab to inhibit HTRA1 shown by PageBlue™ Protein Staining of SDS-PAGE gel staining. **(C)** Overlap of fragments detected by N-TAILS after digestion of recombinant CILP1, COMP and FN by HTRA1 with the previously identified MC1 disc degradome. **(D)** Percentage of patients and **(E)** normalized abundance of the 11 HTRA1-derived COMP, CILP1 or FN peptides cleaved by HTRA1 overlapping with the original TAILS analysis. **(F)** Median abundance of peptides detected in the HTRA1 digested scoliotic disc compared to scoliotic disc exposed to inactive HTRA1, HTRA1 together with its inhibitor Galegenimab as well as only Galegenimab and no additional compound. **(G)** Overlap of the peptides found in the scoliotic disc after digestion with active HTRA1 with the N-terminal peptides detected in the MC1 disc.



Subsequently, the impact of HTRA1 on the entire disc was investigated to determine the proportion of the degradome for which HTRA1 is responsible. Tissue treated with active HTRA1 had a significantly higher abundance of N-terminally labelled fragments compared to tissue digested with mutant HTRA1 or HTRA1 with the inhibitor Galegenimab (Figure 2E). Additionally, negative controls containing only Galegenimab or no additional additives also showed a significantly lower abundance similar to the inhibited and mutant HTRA1. The total number of N-terminally labelled peptides detected in the scoliotic disc digested with HTRA1 was 94, considerably lower than the initial detection in degenerated disc tissue. However, nearly half (46 %) of the degradome from the HTRA1-digested disc exhibited overlap with the degradome of degenerated discs (Figure 2F). This indicates that HTRA1 is responsible for the direct production of approximately 7 % of the degradome of the discs. Upon comparison of the abundance of these 43 fragments measured within the nonMC and MC1 disc it shows that these are significantly more abundant in the MC1 disc (Figure 2G) which further highlights the presence of this degeneration mechanism in both discs but a higher cleavage rate in the MC1 disc.

### *NFκB activation upon CILP1 fragments and COMP stimulation*

The activation of the THP1 NFκB reporter cell line with fragments derived from the digestion of CILP1, COMP, and FN by HTRA1 allowed to investigate whether these fragments can induce inflammation through NFκB activation. When the digestion was carried out prior to addition to the cells (Figure 3A-C), it was found that CILP1 with active HTRA1 induced a significantly higher NFκB activation compared to negative controls, which included CILP1 alone and CILP1 with the mutant HTRA1 enzyme (Figure 3A). COMP elicited the strongest NFκB response in THP1 cells, however, this was the same under all three conditions, with HTRA1 not playing a significant role (Figure 3B). For FN no difference could be detected between the different conditions (Figure 3C).

Using flow cytometry NFκB phosphorylation could be measured after very short incubation times which allowed to understand more closely whether the fragments directly activate the inflammatory pathway or if this is a secondary mechanism. In addition, PBMCs were utilized due to their differences in expression levels of TLRs compared to THP1 cells and accessory molecules as well as the presence of accessory molecules for certain TLR activation processes such as CD14. PBMCs were subdivided into monocytes and lymphocytes during the analysis process. Timepoints ranging from 5 minutes to 60 minutes were tested after addition of Pam2csk4 (positive control for TLR2/6), LPS (positive control for TLR4), FNf30 kDa (representative ECM-derived DAMP) or the three HTRA1 digested proteins of interest CILP1, COMP and FN. Of the three HTRA1 digested proteins, COMP induced the strongest response while FN did not seem to affect NFκB phosphorylation in THP1 cells. Of the positive controls Pam2csk4 induced the fastest phosphorylation in THP1 cells with its peak found after 5 minutes (Figure 3D). After stimulation of THP1 with LPS and FNf30 kDa the strongest phosphorylation signal was measured after 60 minutes.

Stimulation of monocytes with the HTRA1 digested proteins found that COMP and CILP1 both affected NFκB phosphorylation with the strongest effect measured after 60 minutes (Figure 3E). The positive controls showed



a similar trend as within the THP1, however the timepoint was shifted a bit earlier with 30 minutes of incubation being sufficient for NFkB phosphorylation through LPS or FNf30 kDa stimulation.

In lymphocytes, only the HTRA1-digested COMP induced substantial NFkB phosphorylation after just 10 minutes. CILP1 exhibited a minor shift after 60 minutes, while other stimulations did not appear to impact NFkB phosphorylation in lymphocytes (Figure 3F).

To reproduce what was seen in the reporter cell lines after CILP1 stimulation, additional tests were performed for CILP1 to investigate if NFkB phosphorylation occurred upon stimulation with the full-length protein and it was found that this was not the case. Furthermore, to determine whether the HTRA1-cleaved CILP1 signals through either TLR2 or TLR4, well-known DAMP receptors, additional experiments with TLR2 and TLR4 inhibitors were conducted. It was observed that while the TLR2 inhibitor failed to inhibit the NFkB phosphorylation, the TLR4 inhibitor did.

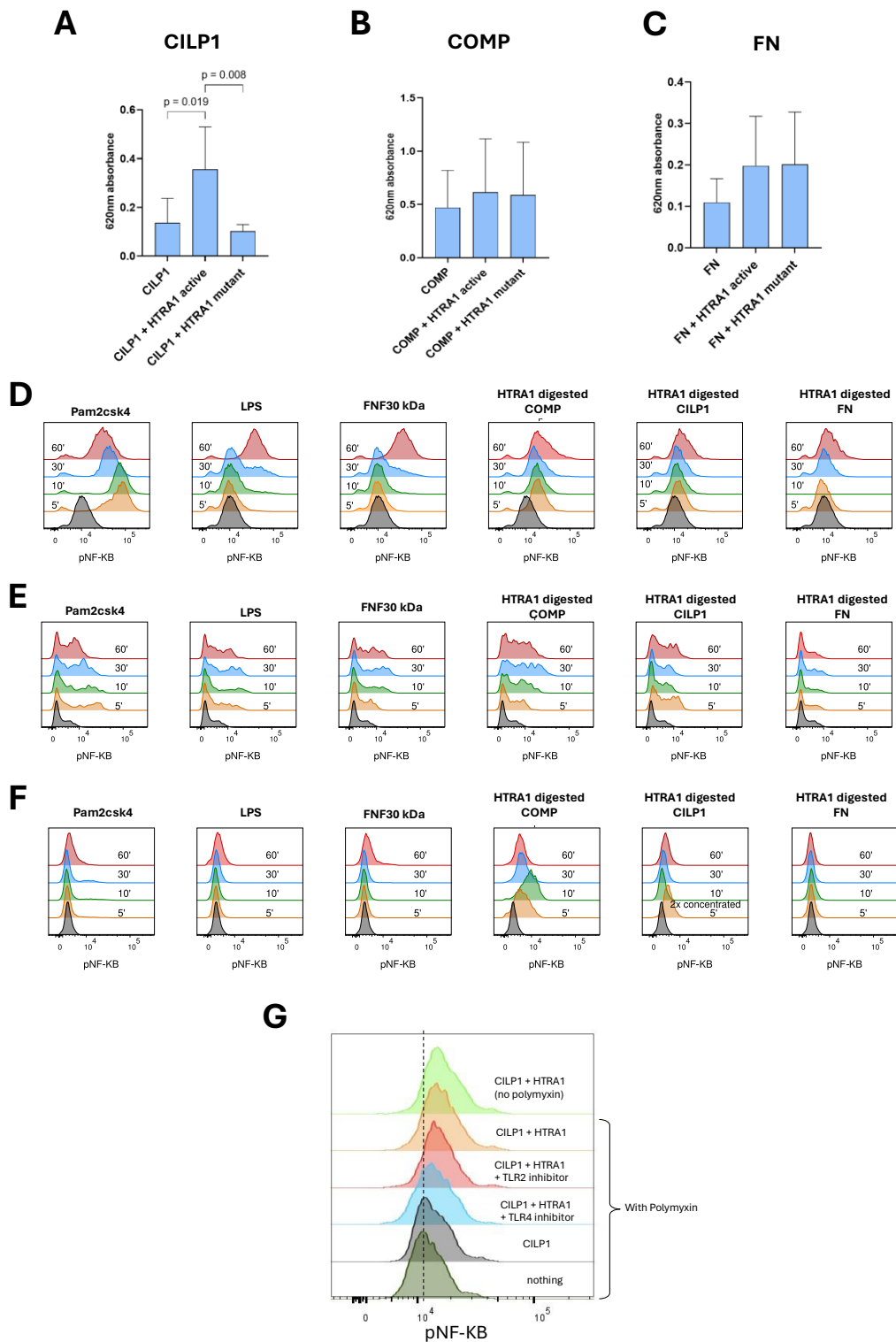


**Figure 3.** HTRA1-derived fragments activate NFκB. THP1 NFκB reporter cells were stimulated for 24 hours with either full-length, HTRA1-pre-fragmented, or mutant HTRA1-pre-fragmented forms of (A) CILP1, (B) COMP, and (C) FN. Graphs illustrate NFκB activation measured by SEAP quantity in the media. Statistical analysis performed on absorbance measured at 620 nm by one-way ANOVA. (D/E/F) NFκB phosphorylation after exposure to HTRA1-derived CILP1, COMP and FN fragments were measured in stimulated (D) wildtype THP1 cells, as well as PBMCs split into (E) monocytes and (F) lymphocytes gated by size, at four different timepoints. Pam2csk4, LPS and commercially acquired FNF30 kDa were used as positive controls. (G) NFκB phosphorylation was additionally tested using full-length CILP1 or fragmented CILP1 with the prior addition of TLR2 or TLR4 inhibitors.

## MC1 CEP cells express higher amounts of TLR2

Gene expression analysis of TLRs in CEP cells revealed significantly greater ( $p = 0.029$ ) TLR2 expression in MC1 CEP cells (Figure 4A). Additionally, gene expression levels of HTRA1 and other proteases were measured, and only MMP13 exhibited significantly greater expression in MC1 CEP cells ( $p = 0.006$ ) (Figure 4B). TLR2 functions as a heterodimer with TLR1 or TLR6. In MC1, TLR2 demonstrates a higher and significant correlation coefficient for the relationship between TLR2 and TLR6 ( $R = 0.897$ ,  $p = 0.010$ ), which is not found in nonMC CEP cells ( $R = 0.328$ ,  $p = 0.354$ ) (data not shown).

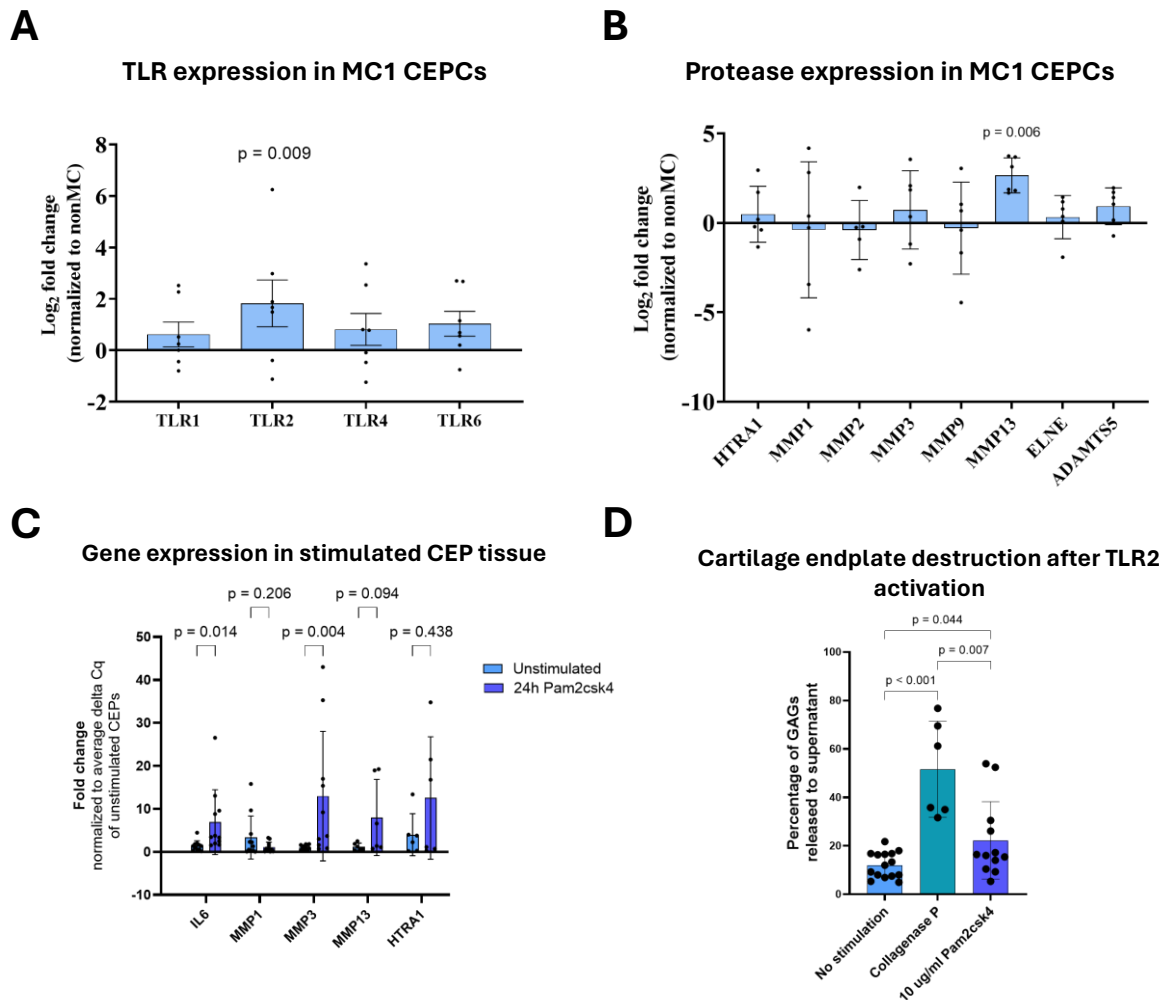


**Figure 4.** Toll-like receptor (TLR) activation creates inflammation and tissue destruction in the cartilage endplate (CEP). **(A)** Expression of TLR1, 2, 4 and 6 in MC1 CEP cells compared to nonMC CEP cells. **(B)** Protease expression level in unstimulated MC1 compared to nonMC CEP cells. **(C)** Gene expression in CEP tissue after 48-hour exposure to Pam2csk4, a TLR2/6 agonist. **(D)** Sulfated glycosaminoglycan (GAG) release by CEP tissue after 14-day exposure to Pam2csk4.

## TLR2 agonist induces CEP destruction

The importance of TLR activation in CEP cells was determined in whole tissue biopsies by treatment of the tissue with TLR2 agonist Pam2csk4 followed by gene expression analysis ( $n = 4$ ). A significant increase is observed in IL6 expression ( $p = 0.014$ ), as well as in MMP3 expression ( $p = 0.004$ ) after 24 hours of treatment

with 10 ug/ml Pam2csk4. MMP13 also showed an increase in the Pam2csk4 treated group, however the observed increase did not reach statistical significance ( $p = 0.094$ ) (Figure 4C).

In addition to gene expression, the GAG release was analyzed after a 14-day incubation period of the CEP tissue with 10 ug/ml Pam2csk4 (Figure 4D). The tissue treated with 10 ug/ml Pam2csk4 exhibited a significantly greater ( $p = 0.044$ ) release of GAGs compared to the tissue incubated solely in media (Figure 4I). Collagenase P, utilized as the positive control for tissue digestion, demonstrated significantly higher release than both the negative control ( $p < 0.001$ ) and the CEP tissue treated with 10 ug/ml Pam2csk4 ( $p = 0.007$ ) (Figure 4D).

## 6.5 Discussion

We identified HTRA1 cleavage of the disc ECM as a MC1-specific degeneration mechanism, discovered a novel ECM-derived DAMP arising from HTRA1 cleavage of CILP1 as well as the strong pro-inflammatory potential of COMP, and observed upregulation of TLR2, an important DAMP receptor, in MC1 CEP cells. Importantly, TLR2 stimulation in CEP explants-initiated CEP degenerative mechanisms. Taken together, these findings suggest a mechanism initiated within the MC1 disc, driven by heightened degeneration through HTRA1. This results in the generation of fragments capable of activating TLRs on adjacent CEP cells, leading to an amplification of inflammation and activation of catabolic mechanisms at the endplate. Consequently, this cascade contributes to endplate destruction ultimately allowing spillover of disc components and inflammatory cytokines to the adjacent bone marrow and potentially triggering MC1.

MC1 are often observed cranial and caudal to a degenerated disc, yet not all degenerated discs have adjacent MC1. In this study, HTRA1 emerged as the sole protease identified through mass spectrometry analysis, displaying higher abundance in the MC1 disc compared to the non-MC disc. This heightened presence of HTRA1 could be shown to substantially contribute to the composition of the degradome in MC1 discs, indicating its potential role in initiating a disc degeneration mechanism that is particularly pronounced in MC1 discs. This aligns with the findings of Rajasekaran et al. in 2020, who exclusively detected HTRA1 in the MC disc proteome and not in the degenerated discs without MCs<sup>17</sup>. The importance of HTRA1 in osteoarthritis is well-established<sup>18-20</sup>, and its role in disc degeneration has gained increasing attention<sup>21,22</sup>. However, until now, its specific association with MCs and the influence on the composition of the MC1 discs' degradome had not been investigated. It is important to highlight that studies which linked HTRA1 to disc degeneration did not categorize the patient cohort based on factors like adjacent MC1, which could potentially influence the findings. The disc adjacent to MC1 should be considered as a separate group or excluded from studies investigating disc degeneration induced through normal aging to gain deeper insights into the different pathologies. Hence, HTRA1 could potentially represent a specific observation for MC1 disc degeneration within the disc, rather than being as pertinent in other disc degeneration pathologies.

A broad spectrum of substrates for HTRA1 has been identified in different contexts such as the cleavage of aggrecan, thrombospondin-1, biglycan, chondroadherin<sup>21</sup> as well as transforming growth factor beta, implicating HTRA1 in a range of developmental processes and varied diseases ranging from arthritis to

Alzheimer's disease <sup>19,23-26</sup>. Previous studies have established a correlation between HTRA1 levels and the degree of disc degeneration, emphasizing its significance in the pathophysiology of this condition <sup>22</sup>. Additionally, it has been shown that the stimulation of disc cells with HTRA1 can induce the upregulation of MMP1, MMP3, and MMP13 expression <sup>22</sup>. Interestingly, our data showed that MC1 CEP cells, which may have been exposed to the increased HTRA1 levels of the adjacent MC1 disc, have a significantly elevated MMP13 expression compared to nonMC CEP cells. According to our findings, nearly 10 % of the N-terminal fragments identified in the degradome of the MC1 disc can be generated through the direct impact of HTRA1 exposure. This number could increase if the secondary mechanism of HTRA1 upregulating additional proteolytic enzymes were included with fresh tissue harboring still live cells. Moreover, since the disc utilized for this analysis was not degenerated and proteins such as FN and COMP increase in frequency with the degree of degeneration, this factor could influence the substrates that were available for HTRA1 cleavage. Consequently, it is possible that this resulted in a reduction in the observed number of fragments for these specific proteins. Nonetheless, selecting a less degenerated disc was unavoidable, as a more degenerated disc would have contained a substantial number of pre-existing fragments prior to incubation with HTRA1, which would also have skewed the impact of HTRA1.

Due to HTRA1 being present more in MC1 discs, it was tested whether HTRA1 was also responsible for the fragments of CILP1, COMP, COL1A1 and FN, which were the proteins with the greatest number of peptides found significantly increased in the MC1 disc. The significance of investigating these fragments lies within the potential of ECM-derived fragments to function as DAMPs, which not only trigger inflammation in the immediate surrounding disc tissue, but also affect the adjacent CEP where cell density is notably higher <sup>15</sup>. Furthermore, due to their small size, these DAMPs may pass through the progressively damaged adjacent endplate, extending the inflammatory process to the bone marrow and potentially inducing MC1.

COMP is important for maintenance of ECM stability and assembly and promotes the secretion of collagens <sup>27,28</sup>. An increase of COMP production by chondrocytes was found in osteoarthritis and rheumatoid arthritis where it has been well established as a biochemical marker for cartilage turnover associated with destruction. Recently, it has also been suggested as a serum biomarker for disc degeneration <sup>29</sup>. The ability of COMP to induce MEK/ERK signaling and PI3K/Akt signaling <sup>30</sup> was found through CD36 <sup>31</sup>, however, no prior studies have yet investigated its ability to induce NFkB activation through TLRs. Our study found that COMP induced an NFkB response, showing no difference in the degree of NFkB activation between COMP fragmented by HTRA1 and COMP itself. The higher abundance of the COMP in MC1 discs and its potential to induce a pro-inflammatory response via NFkB may contribute an additional factor to the heightened inflammatory and degenerative effects observed in MC1 discs.

FN is a key ECM protein involved in maintaining the structural integrity of the disc and regulating cell behavior within the disc tissue. As degeneration progresses, both fibronectin as well as FN fragments increase <sup>6,32</sup>. The 29 kDa FN fragment, a well-described ECM-derived DAMP, has attracted considerable attention in disc degeneration. The 29 kDa fragment DAMP can induce the upregulation of the pro-inflammatory cytokines IL6, IL8, as well as MMP1 and MMP3 in disc cells, which demonstrates its role in inflammation and matrix

breakdown<sup>33,34</sup>. While full-length FN has been shown to induce ERK1/2 signaling, the 29 kDa proteolytic FN fragment was much more potent in cartilage damage induction through ERK1/2, but also p38 and JNK1/2 phosphorylation<sup>35</sup>. Our study additionally found a role for full-length FN activation of an NFkB signaling and identified that HTRA1-derived fragments of FN do not significantly increase this effect.

CILP1 has been investigated in the context of disc degeneration and was found not only to increase in degenerated discs, but also lead to a loss of MRI signal intensity of the discs when overexpressed in transgenic mice<sup>36</sup>. An important role has been attributed to the ability of CILP1 to regulate the TGF-β/SMAD pathway which can lead to disruption of the ECM metabolism<sup>37</sup>. The CILP1 fragments produced through incubation with HTRA1 were found to activate NFkB to a significantly greater extent than CILP1 full-length protein and CILP1 digested with the inactive HTRA1 mutant. This implies that not CILP1 itself, but the fragments derived from the HTRA1 exposure are pro-inflammatory. The effectiveness of the TLR4 inhibitor in blocking the phosphorylation induced by these HTRA1-derived CILP1 fragments suggests that they signal through TLR4, a PRR. Hence, these fragments can be categorized as DAMPs signaling via TLR4, a phenomenon not previously described. Interestingly, the in MC1 discs increased CILP1 fragment DEGDTFPLR was previously found increased in the degradome of osteoarthritic articular knee cartilage compared to normal tissue<sup>38</sup>. Additionally, the N-terminal fragment DWTPAGSTGQVVHGSPR could be re-identified when analyzing the product of CILP1 with HTRA1 incubation, which reveals information to the cleavage preference of HTRA1.

For fragments to exert an impact on the disc and adjacent endplates, it is necessary for these cells to express receptors capable of detecting the fragments. Previous studies have described TLRs on disc cells, with TLR2 found to be most responsive to inflammatory cytokine exposure (Klawitter et al., 2014). In addition, it has been shown that TLR2 activation by Pam2csk4, a TLR2/6 agonist, in disc cells increased COMP and CILP1 expression. Given the found pro-inflammatory properties of COMP and CILP1 fragments, there may be a positive feedback loop in the MC1 disc.

Due to the proximity of the CEP and the importance of the CEP for disc health, it is important to assess whether the inflammation known to be present in degenerated discs, especially MC1 discs, can spread and be amplified by the CEP, specifically the CEP cells. Recent data reported TLR expression by CEP cells, emphasizing TLR2/6 heterodimer signaling which led to an upregulation of inflammatory genes as well as matrix breakdown enzymes such as MMP1, MMP3 and MMP13<sup>39</sup>. Additionally, it was shown that TLR2 activation induced positive feedback on TLR2 expression in CEP cells (chapter 5). Our data demonstrate increased TLR2 expression in MC1 CEP cells, suggesting prior exposure to TLR2 activating ligands and an already increased receptiveness to DAMPs.

Ultimately, the impact of TLR activation by the DAMPs found in MC1 discs on the adjacent CEP lies in its potential to induce endplate destruction. Exposure of CEP tissue to TLR2 agonist Pam2csk4 not only led to an upregulation of MMPs within the CEP cells, consistent with previous observations found in cell culture, but notably, it also triggered GAG release into the media. This suggests that TLR2 activation induces a destructive process in the endplate. While the main substrate for MMPs are not GAGs, GAG release can indicate ongoing tissue turnover, which potentially results in reduced GAG stability. Additionally, due to MMPs not having a

consensus cleavage site it has been shown that they are also able to interact and degrade them<sup>40</sup>. Moreover, although this experiment assessed only the expression of MMPs, serving as an indication of effective TLR2 activation in CEP cells, it is plausible that additional proteases known to cleave GAGs, like chondroitinases, could be impacted by TLR2 activation and potentially play a role in the observed release of sGAG.

## *Outlook*

This project is currently still ongoing, and several planned experiments are expected to enhance the overall comprehensiveness and robustness of the current findings. The follow-up experiments include i.) Western blots of HTRA1 in MC1 compared to nonMC discs, aiming to further increase the evidence for the significance of HTRA1 overrepresentation in MC1 discs. ii.) Stimulation of CEP cells with HTRA1 to comprehend the enzymes effects also on the cells of the adjacent tissue and investigate potential positive feedback loops. iii.) Reproduce the inhibition of TLR2 and TLR4 on THP1 cells before the addition of CILP1 and determine the receptor responsible for COMP recognition by inhibiting various PRRs. iv.) Measure the release of collagen alongside GAG release in the described CEP destruction model, to provide a more direct readout for the effect of MMPs on the tissue destruction as well as determine cell viability after the prolonged incubation time with Pam2csk4. v.) Use the CILP1 fragments to for the CEP explant model and determine whether these are sufficient to induce degenerative effects of the CEP. vi.) Investigate the impact of the identified DAMPs on adjacent bone marrow cells and assess whether they can induce activation of neutrophils or the complement system, both known to be pivotal in inflammation generation within the MC1 bone marrow.

## *Limitations*

The substantial standard deviations observed in the data from the disc proteome and degradome measurements of the MC1 and nonMC groups can be attributed to various factors. Firstly, the MC1 group encompasses all sizes of MC1 lesions, potentially altering the proteomic signature. Moreover, despite applying specific criteria for patient selection, the samples included are limited to patients undergoing surgery, thereby not fully representing a significant portion of MC1 patients who do not undergo surgery. Additionally, the diverse disease histories, medications, and lifestyle factors among the cohort contribute to its heterogeneity, potentially influencing the characteristics of the discs. Third, due to the way the tissue is excised during lumbar spinal fusion and the strong degree of degeneration, it cannot be differentiated between annulus fibrosus and nucleus pulposus. Despite their similarities, these tissues have unique proteomic structures. The variation in the excised part for our study may result in sample differences within one group.

A further limitation of this project, which stems from the methodology of mass spectrometry, is the inability to precisely identify the exact length of protein fragments and their corresponding amino acid sequences. Mass spectrometry primarily measures small peptides, usually trypsinated, which results in cleavage at the C-terminal end whenever a lysine or an arginine amino acid is encountered. Therefore, only the N-terminal cleavage site of the fragments can be reliably determined.

Although pre-TAILS analysis revealed increased levels of HTRA1 in MC1 discs and demonstrated fragmentation of the intact disc ECM, it remains uncertain whether HTRA1 is the primary protease responsible

for all observed cleavage events in vivo. Other proteases might have an equally significant impact but have remained undetected due to not enough sensitivity in the proteomics screening.

Finally, if all steps can be verified in vitro, it is still unclear whether the proposed mechanism is enough to induce MC1 in the bone marrow. Hence, it will be necessary to consider either an animal model or an ex-vivo model using, for example, bovine tails, to investigate whether the degenerative mechanism can induce MC1 changes through the proposed mechanism starting with the increased abundance of HTRA1 which creates the TLR triggering DAMPs.

## *Conclusion*

In summary, HTRA1 was found to be increased in MC1 discs compared to degenerated nonMC discs. COMP, CILP1 and FN were proteins which had the highest number of fragments with increased abundance in MC1 discs and were susceptible to cleavage by HTRA1. While COMP and FN were also found to be increased on a protein level, COMP induced an inflammatory reaction through NFkB signaling as a full-length protein. For CILP1, the pre-fragmentation by HTRA1 was necessary for it to act as a DAMP mainly through TLR4, making HTRA1 a relevant protease for DAMP production. The cells of the CEP were found to play a crucial role in this process, demonstrating their ability to initiate tissue degeneration through TLR activation. The destruction of the CEP tissue ultimately results in removal of the barrier between the disc and the bone marrow, facilitating spillover of inflammatory cytokines as well as DAMPs into the adjacent bone marrow. This cascade of events holds the potential to induce MC1. Taken together, these findings unveil a novel disease mechanism for the development of MC1, based on a biological rather than mechanical process and originating within the disc, extending to the endplate, and ultimately affecting the bone marrow.

## **6.6 Ethics Statement**

The study was approved by the local Ethics Commission #2018-01486; approved on 24 August 2018. The study was conducted in accordance with the local legislation and institutional requirements. The participants provided their written informed consent to participate in this study.

## **6.7 Author Contributions**

TM: involved in all method establishment sample collection, patient recruitment, all data acquisition, writing–original draft, and visualization. JD: method establishment (flow cytometry). BR: method establishment (N-TAILS). IH: methodology (CEP model), writing–review and editing. NH: writing–review and editing and methodology (flow cytometry). RM: data curation (MRI grading) and writing–review. FB: writing–review and editing. CL: data curation (surgeon), writing–review. MF: writing–review and editing. OD: funding acquisition and writing–review and editing. SD: funding acquisition and writing–review and editing.



## 6.8 Funding

This study was supported by a career research grant from the Foundation for Research in Rheumatology (FOREUM) (SD and OD) and by a grant from the Swiss National Fond (SD, Grant No. 207989).

## 6.9 Conflicts of Interest

none

## 6.10 Acknowledgements

We would like to thank the Swiss Center for Musculoskeletal Biobanking (SCMB), which worked together with us to provide the samples in the shortest time possible for further processing. Lastly, we would like to thank the Functional Genomic Center Zurich staff for giving their inputs in the project planning and performing the sequencing.

## 6.11 Supplementary

**Table S1.** Amino acid sequences of upregulated fragments in MC1 discs.

Fragment Sequence	Protein Name	Gene name	UniProt ID
AVTVETSDHDNSLSVSIPQPSPLR	Aggrecan core protein	ACAN	P16112
DWTPAGSTGQVVHGSPR	Cartilage intermediate layer protein 1	CILP-1	O75339
TQTSDSDGR	Cartilage intermediate layer protein 1	CILP-1	O75339
GQVVHGSPR	Cartilage intermediate layer protein 1	CILP-1	O75339
GYKGTFTLHVPQDTER	Cartilage intermediate layer protein 1	CILP-1	O75339
GISKTEER	Cartilage intermediate layer protein 1	CILP-1	O75339
DEGDTFPLR	Cartilage intermediate layer protein 1	CILP-1	O75339
GTFTLHVPQDTER	Cartilage intermediate layer protein 1	CILP-1	O75339
STGPGEQLR	Cartilage oligomeric matrix protein	COMP	P49747
PNWVVLNQGR	Cartilage oligomeric matrix protein	COMP	P49747
KIDVCPENAEVTLTDFR	Cartilage oligomeric matrix protein	COMP	P49747
AVKSSTGPGEQLR	Cartilage oligomeric matrix protein	COMP	P49747
ISVPGPMGSPGPR	Collagen alpha-1(I) chain	COL1A1	P02452
GISVPGPMGSPGPR	Collagen alpha-1(I) chain	COL1A1	P02452
ISVPGPMGSPGPR	Collagen alpha-1(I) chain	COL1A1	P02452
SVPGPMGSPGPR	Collagen alpha-1(I) chain	COL1A1	P02452
GGISVPGPMGSPGPR	Collagen alpha-1(I) chain	COL1A1	P02452
VSAQESQAQAILQQAR	Collagen alpha-1(V) chain	COL5A1	P20908
SVGPVGPR	Collagen alpha-2(V) chain	COL5A2	P05997
GAPPVDVLR	Collagen alpha-2(XI) chain	COL11A2	P13942
DQVPDTESETR	Complement C3	C3	P01024
VGKYPKELR	Complement C4	C3	P01024
CQLQEALLQQERPIR	Fibrinogen alpha chain	FGB	P02675
DWGTFFEEVSGNVSPGTR	Fibrinogen alpha chain	FGA	P02671
VSVSSVYEQHESTPLR	Fibronectin	FN	P02751

GFNCESKPEAEETCFDKYTGNTYR	Fibronectin	FN	P02751
GIGEWHCQLQTYPS	Fibronectin	FN	P02751
TPVVIQQUETTGTTPR	Fibronectin	FN	P02751
SWDAPAVTVR	Fibronectin	FN	P02751
VKDDKESVPISDTIIPAVPPPTDLR	Fibronectin	FN	P02751
CHPVGTDDEEPLQFR	Fibronectin	FN	P02751
CFDKYTGNTYR	Fibronectin	FN	P02751
IYAVEENQESTPVVIQQUETTGTTPR	Fibronectin	FN	P02751
GKHYQINQWER	Fibronectin	FN	P02751
SHYAVGDEWER	Fibronectin	FN	P02751
STATSVNIPDLLPGR	Fibronectin	FN	P02751
CTCIGAGR	Fibronectin	FN	P02751
SEYIISCHPVGTDDEEPLQFR	Fibronectin	FN	P02751
DVLEACCADGHR	Fibulin-1	FBLN1	P23142
EVQLVESGGGLVKPGGSLR	Immunoglobulin heavy variable 3-15	IGHV3-15	A0A0B4J1V0
EIVLTQSPGTLSPGER	Immunoglobulin kappa variable 3-20	IGKV3-20	P01619
SELTQDPAVSVALGQTVR	Immunoglobulin lambda variable 3-19	IGLV3-19	P01714
VPDKTVR	Serotransferrin	TF	P02787
GFLSAPGQR	Sterol regulatory element-binding protein 1	SREBF1	P36956

## 6.12 References chapter 6

1. Saukkonen, J. *et al.* Association Between Modic Changes and Low Back Pain in Middle Age: A Northern Finland Birth Cohort Study. *Spine (Phila Pa 1976)* **45**, (2020). doi: 10.1097/BRS.0000000000003529.
2. Kerttula, L., Luoma, K., Vehmas, T., Grönblad, M. & Käätä, E. Modic type I change may predict rapid progressive, deforming disc degeneration: a prospective 1-year follow-up study. *European Spine Journal* **21**, 1135–1142 (2012). doi: 10.1007/s00586-012-2147-9.
3. Dudli, S. *et al.* ISSLS PRIZE IN BASIC SCIENCE 2017: Intervertebral disc/bone marrow cross-talk with Modic changes. *European Spine Journal* **26**, 1362–1373 (2017). doi: 10.1007/s00586-017-4955-4.
4. Farshad-Amacker, N. A., Hughes, A., Herzog, R. J., Seifert, B. & Farshad, M. The intervertebral disc, the endplates and the vertebral bone marrow as a unit in the process of degeneration. *Eur Radiol* **27**, 2507–2520 (2017). doi: 10.1007/s00330-016-4584-z.
5. Rajasekaran, S. *et al.* The disc-endplate-bone-marrow complex classification: progress in our understanding of Modic vertebral endplate changes and their clinical relevance. *The Spine Journal* **24**, 34–45 (2024). doi: 10.1016/j.spinee.2023.09.002.
6. Oegema, T. R. J., Johnson, S. L., Aguiar, D. J. & Ogilvie, J. W. Fibronectin and Its Fragments Increase With Degeneration in the Human Intervertebral Disc. *Spine (Phila Pa 1976)* **25**, (2000). doi: 10.1097/00007632-200011010-00005.
7. Piccinini, A. M. & Midwood, K. S. DAMPening Inflammation by Modulating TLR Signalling. *Mediators Inflamm* **2010**, 672395 (2010). doi: 10.1155/2010/672395.

8. Krock, E., Millemcamps, M., Currie, J. B., Stone, L. S. & Haglund, L. Low back pain and disc degeneration are decreased following chronic toll-like receptor 4 inhibition in a mouse model. *Osteoarthritis Cartilage* **26**, 1236–1246 (2018). doi: 10.1016/j.joca.2018.06.002.
9. Ishibashi, K., Iwai, H. & Koga, H. Chemonucleolysis with chondroitin sulfate ABC endolyase as a novel minimally invasive treatment for patients with lumbar intervertebral disc herniation. *Journal of Spine Surgery* vol. 5 S115–S121 Preprint at <https://doi.org/10.21037/jss.2019.04.24> (2019). doi:10.21037/jss.2019.04.24.
10. Lotz, J. C., Fields, A. J. & Liebenberg, E. C. The Role of the Vertebral End Plate in Low Back Pain. *Global Spine J* **3**, 153–163 (2013). doi:10.1055/s-0033-1347298.
11. Kerttula, L. I., Serlo, W. S., Tervonen, O. A., Pääkkö, E. L. & Vanharanta, H. V. Post-Traumatic Findings of the Spine After Earlier Vertebral Fracture in Young Patients: Clinical and MRI Study. *Spine (Phila Pa 1976)* **25**, (2000). doi: 10.1097/00007632-200005010-00011.
12. Määttä, J. H. *et al.* Strong association between vertebral endplate defect and Modic change in the general population. *Sci Rep* **8**, 16630 (2018). doi: 10.1038/s41598-018-34933-3.
13. Jensen, T. S. *et al.* Characteristics and natural course of vertebral endplate signal (Modic) changes in the Danish general population. *BMC Musculoskelet Disord* **10**, 81 (2009). doi: 10.1186/1471-2474-10-81.
14. Kuchynsky, K. *et al.* Transcriptional profiling of human cartilage endplate cells identifies novel genes and cell clusters underlying degenerated and non-degenerated phenotypes. *Arthritis Res Ther* **26**, 12 (2024). doi: 10.1186/s13075-023-03220-6.
15. Liebscher, T., Haefeli, M., Wuertz, K., Nerlich, A. G. & Boos, N. Age-Related Variation in Cell Density of Human Lumbar Intervertebral Disc. *Spine (Phila Pa 1976)* **36**, (2011). doi: 10.1097/BRS.0b013e3181cd588c.
16. Pfirrmann, C. W. A., Metzdorf, A., Zanetti, M., Hodler, J. & Boos, N. *Magnetic Resonance Classification of Lumbar Intervertebral Disc Degeneration*. *SPINE* vol. 26 (2001). doi: 10.1097/00007632-200109010-00011.
17. Rajasekaran, S. *et al.* Modic changes are associated with activation of intense inflammatory and host defense response pathways – molecular insights from proteomic analysis of human intervertebral discs. *Spine Journal* **22**, 19–38 (2022). doi: 10.1016/j.spinee.2021.07.003.
18. Wilkinson, D. J. The serine proteinase HtrA1 is ubiquitous and abundant in osteoarthritic joints, but what is it doing? *Osteoarthritis Cartilage* **30**, 1015–1018 (2022). doi: 10.1016/j.joca.2022.03.010.
19. Bhutada, S. *et al.* Forward and reverse degradomics defines the proteolytic landscape of human knee osteoarthritic cartilage and the role of the serine protease HtrA1. *Osteoarthritis Cartilage* **30**, 1091–1102 (2022). doi: 10.1016/j.joca.2022.02.622.
20. Tiaden, A. N. & Richards, P. J. The Emerging Roles of HTRA1 in Musculoskeletal Disease. *Am J Pathol* **182**, 1482–1488 (2013). doi: 10.1016/J.AJP.2013.02.003.
21. Akhatib, B. *et al.* Chondroadherin fragmentation mediated by the protease HTRA1 distinguishes human intervertebral disc degeneration from normal aging. *Journal of Biological Chemistry* **288**, 19280–19287 (2013). doi: 10.1074/jbc.M112.443010.
22. Tiaden, A. N. *et al.* Detrimental role for human high temperature requirement serine protease A1 (HTRA1) in the pathogenesis of intervertebral disc (IVD) degeneration. *Journal of Biological Chemistry* **287**, 21335–21345 (2012). doi: 10.1074/jbc.M112.341032.

23. Chen, C. *et al.* N-Terminomics identifies HtrA1 cleavage of thrombospondin-1 with generation of a proangiogenic fragment in the polarized retinal pigment epithelial cell model of age-related macular degeneration. *Matrix Biology* **70**, 84–101 (2018). doi: 10.1016/j.matbio.2018.03.013.
24. Shiga, A. *et al.* Cerebral small-vessel disease protein HTRA1 controls the amount of TGF- $\beta$ 1 via cleavage of proTGF- $\beta$ 1. *Hum Mol Genet* **20**, 1800–1810 (2011). doi: 10.1093/hmg/ddr063.
25. Chamberland, A. *et al.* Identification of a Novel HtrA1-susceptible Cleavage Site in Human Aggrecan: EVIDENCE FOR THE INVOLVEMENT OF HtrA1 IN AGGREGAN PROTEOLYSIS IN VIVO . *Journal of Biological Chemistry* **284**, 27352–27359 (2009). doi: 10.1074/jbc.M109.037051.
26. Launay, S. *et al.* HtrA1-dependent proteolysis of TGF- $\beta$  controls both neuronal maturation and developmental survival. *Cell Death Differ* **15**, 1408–1416 (2008). doi: 10.1038/cdd.2008.82.
27. Koelling, S., Clauditz, T. S., Kaste, M. & Miosge, N. Cartilage oligomeric matrix protein is involved in human limb development and in the pathogenesis of osteoarthritis. *Arthritis Res Ther* **8**, R56 (2006). doi: 10.1186/ar1922.
28. Schulz, J.-N. *et al.* COMP-assisted collagen secretion – a novel intracellular function required for fibrosis. *J Cell Sci* **129**, 706–716 (2016). doi: 10.1242/jcs.180216.
29. Qi, D.-D., Liu, Z.-H., Wu, D.-S. & Huang, Y.-F. A Study on COMP and CTX-II as Molecular Markers for the Diagnosis of Intervertebral Disc Degeneration. *Biomed Res Int* **2021**, 3371091 (2021). doi: 10.1155/2021/3371091.
30. Liu, T. *et al.* Cartilage oligomeric matrix protein is a prognostic factor and biomarker of colon cancer and promotes cell proliferation by activating the Akt pathway. *J Cancer Res Clin Oncol* **144**, 1049–1063 (2018). doi: 10.1007/s00432-018-2626-4.
31. Li, Q. *et al.* HSCs-derived COMP drives hepatocellular carcinoma progression by activating MEK/ERK and PI3K/AKT signaling pathways. *Journal of Experimental & Clinical Cancer Research* **37**, 1–15 (2018). doi: 10.1186/s13046-018-0908-y.
32. Tam, V. *et al.* Dipper, a spatiotemporal proteomics atlas of human intervertebral discs for exploring ageing and degeneration dynamics. *Elife* **9**, 1–60 (2020). doi: 10.7554/ELIFE.64940.
33. Schmidli, M. R. *et al.* Fibronectin Fragments and Inflammation During Canine Intervertebral Disc Disease. *Front Vet Sci* **7**, (2020). doi: 10.3389/fvets.2020.547644.
34. Greg Anderson, D., Li, X., Tannoury, T., Beck, G. & Balian, G. A Fibronectin Fragment Stimulates Intervertebral Disc Degeneration In Vivo. *Spine (Phila Pa 1976)* **28**, (2003). doi: 10.1097/01.BRS.0000096943.27853.BC.
35. Ding, L., Guo, D. & Homandberg, G. A. The cartilage chondrolytic mechanism of fibronectin fragments involves MAP kinases: comparison of three fragments and native fibronectin. *Osteoarthritis Cartilage* **16**, 1253–1262 (2008). doi: 10.1016/j.joca.2008.02.015.
36. Seki, S. *et al.* Cartilage intermediate layer protein promotes lumbar disc degeneration. *Biochem Biophys Res Commun* **446**, 876–881 (2014). doi: 10.1016/j.bbrc.2014.03.025.
37. Seki, S. *et al.* A functional SNP in CILP, encoding cartilage intermediate layer protein, is associated with susceptibility to lumbar disc disease. *Nat Genet* **37**, 607–612 (2005). doi: 10.1038/ng1557.
38. Fernández-Puente, P. *et al.* Analysis of Endogenous Peptides Released from Osteoarthritic Cartilage Unravels Novel Pathogenic Markers\*, [S]. *Molecular & Cellular Proteomics* **18**, 2018–2028 (2019). doi: 10.1074/mcp.RA119.001554.

39. Mengis, T. *et al.* *Toll-like Receptor 2 Signaling of Cartilage Endplate Cells Amplifies Inflammation in Modic Type 1 Changes.* (2024).
40. Tocchi, A. & Parks, W. C. Functional interactions between matrix metalloproteinases and glycosaminoglycans. *FEBS J* **280**, 2332–2341 (2013). doi: 10.1111/febs.12198.

## Chapter 7: General Discussion

The pathobiology of Modic changes (MC) is highly intricate, and there is limited understanding of it. The complexity arises from the involvement of not only the bone marrow but also the disc and adjacent endplate in the development of MC<sup>1</sup>. This already implies that the mechanism will be a complex interplay among these structures. A particular important question is, which structure triggers MC and by which mechanisms. Furthermore, the existence of three subtypes of MCs, as well as the possibility of the subtypes to occur in mixed form and a lack of comprehensive knowledge regarding the transitions between these subtypes over time, adds another layer of complexity<sup>2-4</sup>. Lastly, the current reliance on magnetic resonance imaging (MRI) for the characterization and grouping of MCs poses a challenge in conducting research on these patients, as patients typically undergo MRI only after experiencing years of back pain<sup>5</sup>. Moreover, the patient samples can only be derived from patients undergoing spinal fusion surgery, which typically occurs as a last treatment resort for the patients back pain, further complicating the identification and study of patients in the early stages of MC development. Therefore, each puzzle piece that can be added to this complex disease advances the progress toward the development of targeted treatments. Within the scope of this thesis different aspects of the disease were investigated, contributing some missing pieces to the puzzle. The main findings included i) that bone marrow stromal cells (BMSCs) play a role in driving neurite growth in the bone marrow, ii) that there is a microbiome which is altered in MC1 and MC2, but that more detailed results can only be considered once a consensus on the methodology for low-biomass metagenomics is found, iii) that cartilage endplate (CEP) cells express toll-like receptors (TLRs) and iv) that the MC1 disc degradome has more fragments including some that act pro-inflammatory on their surroundings. Overall, important steps were made in gaining a clearer understanding of the pathobiology of MC.

## 7.1 Complexity of neurite growth

In chapter 3, the impact of MC1 BMSCs on neurite outgrowth was analyzed. In the co-culture setting with the neuroblastoma cell-line SH-SY5Y it could be clearly observed that MC1 BMSCs had a stronger neurotrophic effect than the control BMSCs. This observation aligned with previous histological findings, indicating increased innervation in MC1 bone marrow and endplates<sup>6,7</sup>. To comprehend the underlying reasons for this phenomenon and explore what distinguishes MC1 BMSCs, which is essential for potential treatment approaches, the investigation continued in the direction of identifying specific pathways or cytokines responsible for the observed effect. However, the inability to pinpoint a particular pathway or cytokine suggested a comprehensive dysregulation of MC1 BMSCs. Earlier studies have demonstrated a pro-fibrotic phenotype in MC1 BMSCs, involving dysregulation of various genes that could collectively impact neurite outgrowth<sup>8</sup>. To consider is also that the co-culture system utilized does not provide clarity on whether BMSCs directly induce neurotrophic activity by producing more neurotrophins or if their pro-fibrotic phenotype triggers a positive feedback loop within the neuroblastoma cells, consequently promoting neurite outgrowth. The latter option seems very plausible as the inhibition of brain-derived neurotrophic factor (BDNF), which was the most likely candidate according to transcriptomic data of the BMSCs, did not result in a decrease of neurite outgrowth. Therefore, the neuroblastoma cells can readily produce neurite outgrowths even without the help of BDNF. This brings forth a new hypothesis which suggests that MC1 BMSCs do not act pro-

neurotrophic through increased production of a single cytokine but rather due to the phenotype brought forth through MCs<sup>8</sup>. This poses a challenge in finding effective ways to counteract this effect and implies that the solution likely will involve addressing BMSCs as an entity.

## 7.2. Role of the disc's microbiome

While the first chapter focused on the bone marrow, the subsequent sections of the thesis shift their focus onto the disc. The exact role of the disc in the development of MCs has not been identified, however, it has been established that although MCs are associated with disc degeneration, not all degenerating discs are found with adjacent MCs<sup>2</sup>. Studies have found that the 'Modic disc' differs from a disc without MCs, even when both are in a degenerated state, in respect to e.g. cytokine production<sup>9,10</sup>. The large number of studies on degenerated discs unfortunately, do not discriminate between MC degenerated discs and nonMC degenerated discs. Therefore, the rest of the thesis aimed towards understanding more closely what makes the MC disc different and how it contributes to MC development.

### *The challenges associated with understanding the disc microbiome.*

An essential feature of the intervertebral disc is its avascularity<sup>11</sup>. This together with the CEP as a barrier tissue helps to keep the disc immune privileged and therewith also a sterile tissue. The invasion of bacteria was considered pathologic, and the focus has been put on *Cutibacterium acnes*<sup>12-16</sup>. Nevertheless, our research, along with two previous studies, utilized a metagenomic approach on disc tissue, successfully identifying a complete microbiome within the disc.<sup>17-19</sup> Remarkably, this microbiome is not exclusive to herniated or damaged discs but is also present in healthy discs without signs of degeneration<sup>18</sup>. Additionally, the composition of the microbiome varies depending on the disc's condition. This shift in paradigm has brought forth an entirely new perspective on how the disc is perceived, as it is now recognized as a potential habitat for bacteria. Moreover, these bacteria seem capable of experiencing dysbiosis. The relationship between disc degeneration and the onset of dysbiosis, or whether dysbiosis serves as a catalyst for disc pathology, remains unclear at this point and warrants further investigation.

Within the scope of this thesis, we were able to reproduce that MC discs have an altered microbiome compared to nonMC discs and that the microbiome has a decreased diversity to the nonMC microbiome. Additionally, for the first time, we also differentiated between MC1 and MC2 discs. Upon comparison of our study to the previous investigation by Rajasekaran et al. on the MC disc microbiome, we unexpectedly found a completely different set of bacteria within the disc<sup>17</sup>. This led us to investigate the differences introduced through the application of different settings for analysis, such as the use of operation taxonomic units (OTUs) or amplicon sequencing variants (ASVs) for annotation as well as employing different cut-offs for the minimum number of patients with a particular bacterial genus. The results yielded surprising outcomes, with OTUs matching different and fewer bacterial genera than ASVs. A less strict prevalence filter cut-off, such as 4 %, was found to be useful for a screening approach or for a broader description of the data focusing, for example only on gram positive or negative bacteria. However, to identify specific genera relevant across a wide range of patients, a stricter cut-off is necessary. To avoid filtering out a genus present in only one group, failing to

surpass the cut-off, each group should be individually examined for genera present in more than half of the patients in that group. This filter method, combined with the use of ASVs, was in our opinion determined to be the most precise and clinically relevant approach for identifying bacterial composition.

After experimenting with different parameters, we revisited the comparison of our data with Rajasekaran et al.'s data, with the use of closely similar parameters. Nevertheless, we were unable to identify all of the same bacterial genera, with almost no overlap. While variations in tissue and sequencing preparation techniques, or potential contaminants in the buffer, could contribute to these discrepancies, it also prompts the hypothesis that the microbiome is notably influenced by the patient's geographical region and possibly lifestyle factors. Much like the well-documented variability in the gut microbiome among individuals and regions, these external factors play an important role in shaping the microbial composition within the disc. Given that the microbiome in the disc is a relatively recent discovery, the exact mechanisms by which these bacteria infiltrate the disc remain speculative. While Rajasekaran et al. suggested the existence of a disc-gut-skin axis, this was not directly measured within the same patients but based on comparison to gut and skin databases<sup>18</sup>. To gain a deeper understanding of this phenomenon, new studies would need to be designed to investigate the three microbiomes within the same patients to determine a possible connection. Furthermore, the inclusion of individuals from various geographical regions is crucial for such studies to exclude biases stemming from the culture and geographical variations. Only through this approach can we draw an overarching conclusion regarding the composition of the microbiome.

With these new insights on the disc the proposed etiologies of MCs may also be influenced, as *Cutibacterium acnes* was long thought to be the most relevant for this process, invading the disc and causing an inflammatory reaction through tissue damage. With the concept of the disc microbiome already being present, this hypothesis may still be true, however, this may not be the only factor to consider. Both, our study and the previous MC microbiome study identified a decreased diversity in MC discs, which can also be seen as a dysbiosis of the microbiome. Hence, it may also be crucial to contemplate the cause of dysbiosis and its impact not only on the disc tissue itself, but also on the adjacent endplate.

This recent discovery brings in a further complexity which needs to be considered in the investigation of the MC pathology. It raises numerous new questions, including whether dysbiosis plays a role in the development of MCs or conversely, whether the adjacent MCs cause alterations in the disc microbiome. Addressing such questions is challenging in the absence of suitable animal models for the disease.

## Outlook

Prior to advancing into mechanistic or therapeutic investigations involving the disc microbiome, it is imperative to first reach a consensus on the methodological approach. This is important to allow proper comparison of studies within the field. Further studies in this direction need to extensively lay out the bioinformatic pipelines used and appropriately set the parameters, as previously discussed, depending on the research questions.



Next, it needs to be established whether geographical and even lifestyle differences could be the reasons for the large discrepancies found between the studies so far conducted. This will give us information on whether it will ever be possible to generalize the findings or if each patient needs to be addressed individually. To do this, samples from different geographical regions need to be analyzed in the same experiment and with the same reagents. This will exclude any bias through contamination from buffers used.

Once these critical questions are addressed, the role of the microbiome in MC pathogenesis as well as potential clinical implications can be further explored.

### **7.3 Cartilage endplate cells – important players in inflammation and degeneration**

MCs are sometimes also referred to as vertebral endplate signal changes (VESC), underlining the pivotal role of the endplate in MCs. The endplate is found damaged in the context of MCs<sup>20–24</sup>. The endplate is frequently discussed in terms of its structural and mechanical characteristics, often neglecting the biological significance of the endplate tissue and its constituent cells. Meanwhile, it could be shown that the CEP cells have a much higher density than the cells in the adjacent disc tissue, amplifying their potential impact when activated. Despite the increasing recognition of the CEP cells their characterization and their impact are still very unexplored<sup>25,26</sup>.

Therefore, with the importance of the CEP cells for MCs becoming clearer, we aimed to further characterize the CEP tissue by identifying its ability to react to stimulants from the disc in the form of either bacteria in the form of pathogen associated molecular patterns (PAMPs) or also to damage associated molecular patterns (DAMPs), from the degenerating disc. The main receptors for the recognition of both PAMPs and DAMPs are the TLRs which have previously been shown to be present and of importance in disc cells<sup>27–29</sup>. With our study we were able to show that CEP cells do express TLR1, 2, 3, 4, 5, 6, 7 and 10. Due to the positive feedback loop of TLR2 activation also inducing increased TLR2 expression.

This finding carries significance for future investigations, particularly in the context of MCs, given the potential of TLR activation to elevate pro-inflammatory and pro-catabolic enzymes. As the disc undergoes degeneration, either bacteria or degenerating disc fragments can activate TLRs on the adjacent endplates, leading to the expansion and potent amplification of inflammation and catabolic enzyme production in the neighboring tissue. If it can be shown that TLR activation alone can induce tissue degeneration, that would make the CEP cells key contributors to the development of MCs. Since key contributors often present promising therapeutic targets, the inhibition of TLRs in the CEP emerges as a plausible approach to consider.

### **7.4 The role of the MC1 disc degradome**

#### *Potential mechanism*

Although disc degeneration is a common phenomenon observed in the aging population, not all degenerating discs progress to adjacent MCs, despite being a prerequisite for MC development<sup>1,30,31</sup>. With the knowledge

that the CEP cells have the potential to recognize DAMPs through TLRs (chapter 5), the focus was set on comprehending the degenerative process within the MC disc itself. Our hypothesis was that the degenerative process in a MC1 disc differs from that in a nonMC disc, leading to increased fragment production. These fragments may subsequently stimulate adjacent CEP cells through TLRs, amplifying the degenerative state within the CEP. This cascade is hypothesized to initiate endplate damage, ultimately facilitating the spillover of disc contents, including pro-inflammatory DAMP fragments, into the bone marrow and triggering the development of MCs.

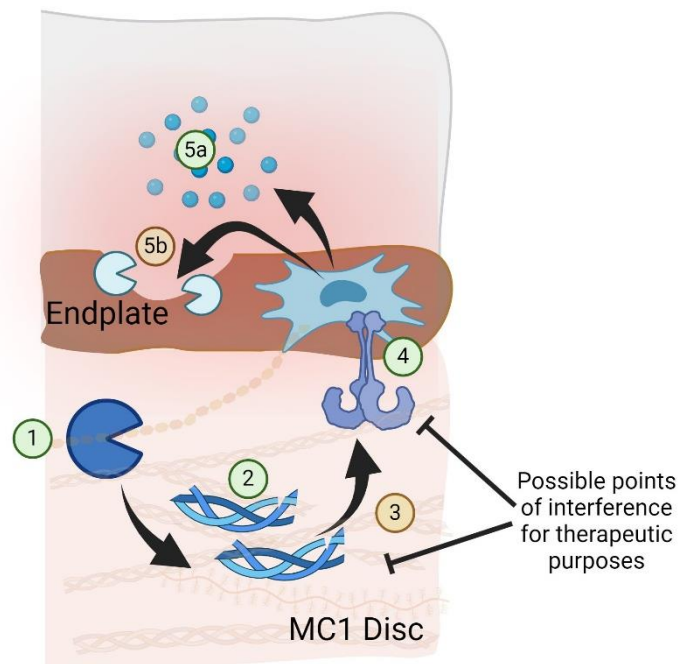


**Figure 1.** Schematic depiction of the proposed mechanism of how the MC1 disc plays a role in initiation of MCs. Points highlighted in orange indicate aspects that have been partially addressed but require additional evidence through further experimentation. Points highlighted in green signify that all necessary experiments have been conducted to validate the step. The hypothesis is based on proteases in the disc (point 1) cleaving the disc-ECM to fragments (point 2) which can act pro-inflammatory on the adjacent CEP cells (point 3) through TLR recognition (point 4). This leads to pro-inflammatory cytokine upregulation and protease production (point 5a) increase by the CEP cells which induces endplate damage (point 5b).

Within the scope of this thesis, various aspects of this cascade of events were addressed and substantiated. Figure 1 illustrates how this mechanism is hypothesized to take place if all components can be linked through appropriate experiments. As this study is currently ongoing, the figure distinguishes between points that have been fully addressed, shown in green, and those still requiring additional evidence, indicated in orange.

Point 1 highlights the identified protease found upregulated through proteomic analysis in the MC1 disc, namely high temperature serine protease 1 (HTRA1). HTRA1 may be a key enzyme contributing to MC1 development due to its potential not only to cleave the disc ECM into potential DAMPs but also due to its ability to induce upregulation of MMP expression in disc cells, further contributing to catabolic processes. Point 2 indicates the fragments generated in the disc, with some of them proven through our experiments to be generated directly through HTRA1 cleavage. Overall, the degradome analysis revealed several fragments,

especially ones originating from fibronectin (FN), cartilage oligomeric matrix protein (COMP), and cartilage intermediate layer protein 1 (CILP1), which were more abundant in the MC1 degradome and could be cleaved by HTRA1. It is however important to note that this does not suggest the absence of these fragments from the nonMC disc, as it is also undergoing catabolic processes, however, these fragments are present in lower abundances compared to MC1 discs.

Step 3 of the hypothesis involves demonstrating the role of the HTRA1-derived CILP1, COMP, and FN fragments identified in previous experiments in their potential to function as DAMPs through for TLRs on CEP cells. The current standing of experiments allows to make the conclusion that HTRA1-derived CILP1 fragments act pro-inflammatory through the NFkB pathway, and this effect can be inhibited through TLR4 inhibition. Moreover, both full-length COMP and HTRA1-derived fragments of COMP have been observed to trigger NFkB pathway activation. However, the experiments conducted thus far have not enabled the identification of the particular receptor accountable for instigating this pathway, underscoring the need for further investigation.

Point number 4 was to provide evidence that CEP cells express TLRs, and this was thoroughly highlighted in chapter 5 of this thesis. This was important, as these receptors would be responsible for recognition of the DAMPs produced within the disc. Additionally, in chapter 6, it was demonstrated that MC1 CEP cells show a significantly higher TLR2 expression compared to nonMC CEP cells. This observation suggests that these cells may have encountered TLR2 agonists previously, as TLR2 activation in CEP cells was shown to induce self-upregulation.

Point 5 is divided into two segments, describing the increase of inflammatory cytokine release by CEP cells after TLR activation (point 5a). Additionally, catabolic enzymes (point 5b) which ultimately lead to endplate destruction are also found to increase upon TLR activation. The upregulation of the expression of inflammatory cytokines and various MMPs was thoroughly examined in chapter 5. It was found that TLR activation induced significant upregulation of MMP1, MMP3 and MMP13 as well as various pro-inflammatory genes, especially through TLR2/6 heterodimer activation. However, to provide evidence that the activation of TLRs, especially TLR2/6 in CEP cells is sufficient to induce tissue destruction the actual proteolytic tissue breakdown needs to be shown. This was briefly addressed with preliminary data in chapter 6 and suggested that fresh CEP tissue releases sulfated glycosaminoglycans (sGAGs) into the media, indicating potential ECM breakdown.

## *Outlook*

This mechanism will continue to be investigated within the framework of my post-doctoral project. While a brief outlook overview was provided in Chapter 6, the comprehensive nature of this project necessitates the addition of further details to each aspect.

Points 1 through 4 of the mechanisms have been partially addressed, additional evidence is required at each stage before progressing to the final phase of inhibiting the entire mechanism and testing it in a model system.

Point 1 identified an increase in HTRA1 identified through a proteomic investigation, representing robust data. However, its significance may be further elucidated through Western blotting of HTRA1 in both nonMC and

MC1 tissue samples to clarify the results of the proteomic analysis. The extensive variability introduced by using numerous patients and the methodological challenge of splitting samples into multiple batches for proteomic measurement added a lot of variation to the proteomic analysis. This will further solidify the increased abundance in MC1 discs of this specific enzyme. Additionally, to determine whether the pro-inflammatory CILP1 fragments can only be produced by HTRA1, the incubation needs to be repeated with other proteases known to play a role in disc degeneration such as MMP1, 3 or 13. Only then, can the importance of HTRA1 in production of these pro-inflammatory fragments be solidified.

Point 3, hypothesizes that the identified fragments are recognized by CEP cells through TLRs. However, to this point this link could not yet be made. Currently the individual parts could be shown namely that TLRs were found on CEP cells and that pro-inflammatory NFkB phosphorylation could be induced through the fragments. However, to understand if these fragments are recognized by TLRs, inhibition of the receptors needs to be performed before stimulation with the fragments. This will initially be done with TLR2 and TLR4 inhibitors as these are the two main PRRs known to recognize DAMPs. If both fail to inhibit NFkB activation, consideration of additional PRRs will be necessary. In a second step, once the receptor is identified, the fragments will be added to CEP cells instead of THP1 cells. The effect will be shown again by use of flow cytometry to measure phosphorylation of NFkB. This last step is important to be able to transfer the findings to the cells relevant for the proposed hypothesis.

Finally, destructive properties resulting from TLR activation on CEP tissue (point 3) need further investigation. Several subprojects are planned to optimize the CEP model system described in chapter 6. First, the viability of the cells within the CEP needs to be tested after exposure to the currently high concentration (10 ug/ml) of Pam2CysSerLys4 (Pam2csk4) used. This is important, as if the cells are dying this will also lead to catabolic processes within the tissue, however this would provide us with false positive results. To examine this, various dosages of Pam2csk4 will be tested on CEP cells in culture to define the highest non-lethal concentration for longer periods of time. Second, gene expression, which was tested only after 48 hours of exposure, needs to be examined at later times to determine relevant proteases and whether Pam2csk4 needs re-application. Third, the CEP model will be repeated, adjusting the concentration and media changes based on the results of prior experiments. In a final step, the test needs to be done with the exposure of the CEP tissue to the fragments instead of the synthetic Pam2csk4 ligand. Only through this approach can the connection between CEP destruction and the fragments be thoroughly substantiated with evidence.

Once each individual point is fully addressed, the relevance of this mechanism based on the presence of DAMPs needs to be further demonstrated in a model system, such as a bovine tail model or rat tail model. A potential study design could involve injecting HTRA1, triggering the cascade of events from the first step. However, this might not conclusively show that fragments are the most crucial aspect for CEP destruction initiation, as HTRA1 itself could also affect the CEP directly. A control that this is not the case would need to be included. Another option would be to inject the fragments themselves, skipping the first step in the series of events but linking potential destruction only and specifically to the fragments.

The proposed mechanism and the experiments conducted so far will have elucidated all the stages, starting from the MC1-specific disc degeneration that creates the high abundance of DAMPs capable of initiating endplate damage. Nonetheless, the final phase investigating the steps following endplate destruction will need to be addressed, as MC1 is a disease of the bone marrow. Hence, around the impact of DAMPs on bone marrow cells, examining whether this induces the changes that have been observed within the MC1 bone marrow, such as neutrophil degranulation or complement activation. In the absence of a suitable animal model which could be used to monitor the entire process starting by inducing MC1 specific disc degeneration, the best way to approach this would be to show the effects step by step. Experiments involving the exposure of various cells that have been shown to be either dysregulated within the MC1 bone marrow or known to play important roles in the MC1 pathobiology would be necessary. This will include investigating whether DAMPs can induce neutrophil activation, through measurement of neutrophil activation surface markers (CD66b, CD11b, CXCR1, CXCR2, CXCR4), reactive oxygen species (ROS) production using flow cytometry. But also, neutrophil extracellular traps (NETs) formation, and the release of neutrophil granules can be measured in the culture supernatant through Sytox Green and colorimetric assays, respectively.

### *Relevance of the mechanism*

If the additionally planned experiments are successful in solidifying the evidence for the proposed mechanism this would provide new targets for therapeutic interventions (Figure 1, point 6). If it shows through further experiments that HTRA1 is solely accountable for the generation of the high quantities of pro-inflammatory DAMPs, then the inhibition of HTRA1 could not only reduce DAMP production but also decelerate disc degeneration. However, this approach will only be sufficient if other proteases like matrix metalloproteinase (MMP) 1, 3, or 13 lack similar capabilities. Alternatively, another approach could involve therapeutically impeding the action of DAMPs, such as using antibodies. This strategy has demonstrated efficacy in various animal models, employing polyclonal antibodies or siRNA to diminish the functioning of the two DAMPs HSP90 or HMGB1 in rheumatoid arthritis, lung inflammation, hepatic ischemia to name only a few<sup>32-35</sup>. Another prospective therapeutic strategy to intervene in the proposed mechanism involves inhibiting Toll-like receptors (TLRs). Current experiments suggest that TLR2 is the most implicated, but it must first be demonstrated that the DAMPs also signal through TLR2.

## **7.5 Conclusion**

In summary, the investigation of various aspects within this thesis highlights the complexity of the pathobiology of MCs involving three different tissues. Some aspects of these tissues are still very unexplored to this point, such as the microbiome of the disc and the biological significance of CEP cells. This thesis aimed to uncover various unknown aspects, progressively enhancing our understanding of the disease.

The complexity of the disease and the current knowledge also allow for multiple different approaches for treatment approaches. The thesis explored multiple facets of the disease, each offering opportunities for the development of new therapeutic interventions. The nerve growth is currently only managed through basivertebral nerve ablation which does provide relief; however, it is unclear for how long as the BMSCs may

trigger further outgrowth<sup>36</sup>. Alternatively, ongoing research could potentially enable the modulation of dysregulated MC1 BMSCs to reduce neurite outgrowth over the long term<sup>37</sup>. Considering the insights from the microbiome study, antibiotic or pro-biotic treatment may become a viable option if further research establishes that dysbiosis of the disc plays a causative role in MCs. Finally, with the knowledge of the MC1 disc degradome, targeted interventions may be developed, involving specific protease inhibitors or inhibitors of the receptors which are activated in a pro-inflammatory manner by the fragments.

In conclusion, advancing research on the pathobiology, as undertaken in this thesis, is crucial for developing effective treatments. Further progress in understanding the complexities of this painful and prevalent condition is essential for addressing it properly.

## 7.6 References chapter 7

1. Dudli, S., Fields, A. J., Samartzis, D., Karppinen, J. & Lotz, J. C. Pathobiology of Modic changes. *European Spine Journal* vol. 25 3723–3734 Preprint at <https://doi.org/10.1007/s00586-016-4459-7> (2016). doi: 10.1007/s00586-016-4459-7.
2. Modic, M. T., Steinberg, P. M., Ross, J. S., Masaryk, T. J. & Carter, J. R. Degenerative disk disease: assessment of changes in vertebral body marrow with MR imaging. *Radiology* **166**, 193–199 (1988). doi: 10.1148/radiology.166.1.3336678.
3. Jensen, T. S. *et al.* Characteristics and natural course of vertebral endplate signal (Modic) changes in the Danish general population. *BMC Musculoskelet Disord* **10**, 81 (2009). doi: 10.1186/1471-2474-10-81.
4. Albert, H. B. *et al.* Modic changes, possible causes and relation to low back pain. *Med Hypotheses* **70**, 361–368 (2008). doi: 10.1016/j.mehy.2007.05.014.
5. Hall, A. M., Aubrey-Bassler, K., Thorne, B. & Maher, C. G. Do not routinely offer imaging for uncomplicated low back pain. *BMJ* **372**, n291 (2021). doi: 10.1136/bmj.n291.
6. Ohtori, S. *et al.* Tumor Necrosis Factor-Immunoreactive Cells and PGP 9.5-Immunoreactive Nerve Fibers in Vertebral Endplates of Patients With Discogenic Low Back Pain and Modic Type 1 or Type 2 Changes on MRI. *Spine (Phila Pa 1976)* **31**, (2006). doi: 10.1097/01.brs.0000215027.87102.7c.
7. Fields, A. J., Liebenberg, E. C. & Lotz, J. C. Innervation of pathologies in the lumbar vertebral end plate and intervertebral disc. *Spine Journal* **14**, 513–521 (2014). doi: 10.1016/j.spinee.2013.06.075.
8. Heggli, I. *et al.* Pro-fibrotic phenotype of bone marrow stromal cells in modic type 1 changes. *Eur Cell Mater* **41**, 648–667 (2021). doi: 10.22203/eCM.v041a42.
9. Schroeder, G. D. *et al.* Are Modic changes associated with intervertebral disc cytokine profiles? *Spine Journal* **17**, 129–134 (2017). doi: 10.1016/j.spinee.2016.08.006.
10. Dudli, S. *et al.* ISSLS PRIZE IN BASIC SCIENCE 2017: Intervertebral disc/bone marrow cross-talk with Modic changes. *European Spine Journal* **26**, 1362–1373 (2017). doi: 10.1007/s00586-017-4955-4.
11. Grunhagen, T., Wilde, G., Soukane, D. M., Shirazi-Adl, S. A. & Urban, J. P. G. Nutrient Supply and Intervertebral Disc Metabolism. *JBJS* **88**, (2006). doi: 10.2106/JBJS.E.01290.

12. Capoor, M. N. *et al.* Propionibacterium acnes biofilm is present in intervertebral discs of patients undergoing microdiscectomy. *PLoS One* **12**, e0174518 (2017). doi: 10.1371/journal.pone.0174518.
13. Dudli, S., Miller, S., Demir-Deviren, S. & Lotz, J. C. Inflammatory response of disc cells against Propionibacterium acnes depends on the presence of lumbar Modic changes. *European spine journal* **27**, 1013–1020 (2018). doi: 10.1007/s00586-017-5291-4.
14. Lin, Y. *et al.* Propionibacterium acnes induces intervertebral disc degeneration by promoting nucleus pulposus cell apoptosis via the TLR2/JNK/mitochondrial-mediated pathway. *Emerg Microbes Infect* **7**, 1–8 (2018). doi: 10.1038/s41426-017-0002-0.
15. Dudli, S. *et al.* Propionibacterium acnes infected intervertebral discs cause vertebral bone marrow lesions consistent with Modic changes. *Journal of Orthopaedic Research* **34**, 1447–1455 (2016). doi: 10.1002/jor.23265.
16. Heggli, I. *et al.* Low back pain patients with Modic type 1 changes exhibit distinct bacterial and non-bacterial subtypes. *Osteoarthr Cartil Open* **6**, (2024). doi: 10.1016/j.ocarto.2024.100434.
17. Rajasekaran, S. *et al.* “Are we barking up the wrong tree? Too much emphasis on Cutibacterium acnes and ignoring other pathogens”— a study based on next-generation sequencing of normal and diseased discs. *Spine Journal* (2023) doi: 10.1016/j.spinee.2023.06.396.
18. Rajasekaran, S. *et al.* Human intervertebral discs harbour a unique microbiome and dysbiosis determines health and disease. *European Spine Journal* **29**, 1621–1640 (2020). doi: 10.1007/s00586-020-06446-z.
19. Astur, N. *et al.* Next-generation sequencing (NGS) to determine microbiome of herniated intervertebral disc. *Spine Journal* **22**, 389–398 (2022). doi: 10.1016/j.spinee.2021.09.005.
20. Crump, K. B. *et al.* Cartilaginous endplates: A comprehensive review on a neglected structure in intervertebral disc research. *JOR Spine* **6**, e1294 (2023). doi: 10.1002/jsp2.1294.
21. Kuisma, M. *et al.* Modic changes in vertebral endplates: a comparison of MR imaging and multislice CT. *Skeletal Radiol* **38**, 141–147 (2009). doi: 10.1007/s00256-008-0590-9.
22. Heggli, I. *et al.* Modic type 2 changes are fibroinflammatory changes with complement system involvement adjacent to degenerated vertebral endplates. *JOR Spine* **6**, (2023). doi: 10.1002/jsp2.1237.
23. Rajasekaran, S. *et al.* The disc-endplate-bone-marrow complex classification: progress in our understanding of Modic vertebral endplate changes and their clinical relevance. *The Spine Journal* **24**, 34–45 (2024). doi: 10.1016/j.spinee.2023.09.002.
24. Moon, S. M. *et al.* Evaluation of intervertebral disc cartilaginous endplate structure using magnetic resonance imaging. *European Spine Journal* **22**, 1820–1828 (2013). doi: 10.1007/s00586-013-2798-1.
25. Kuchynsky, K. *et al.* Transcriptional profiling of human cartilage endplate cells identifies novel genes and cell clusters underlying degenerated and non-degenerated phenotypes. *Arthritis Res Ther* **26**, 12 (2024). doi: 10.1186/s13075-023-03220-6.
26. De Luca, P. *et al.* Intervertebral disc and endplate cell characterisation highlights annulus fibrosus cells as the most promising for tissue-specific disc degeneration therapy. *Eur Cell Mater* **39**, 156–170 (2020). doi: 10.22203/eCM.v039a10.
27. Klawitter, M. *et al.* Expression and regulation of toll-like receptors (TLRs) in human intervertebral disc cells. *European Spine Journal* **23**, 1878–1891 (2014). doi: 10.1007/s00586-014-3442-4.

28. Bisson, D. G., Mannarino, M., Racine, R. & Haglund, L. For whom the disc tolls: Intervertebral disc degeneration, back pain and toll-like receptors. *Eur Cell Mater* **41**, 355–369 (2021). doi: 10.22203/eCM.v041a23.
29. Krock, E. *et al.* Toll-like receptor activation induces degeneration of human intervertebral discs. *Sci Rep* **7**, (2017). doi: 10.1038/s41598-017-17472-1.
30. Teraguchi, M. *et al.* Detailed Subphenotyping of Lumbar Modic Changes and Their Association with Low Back Pain in a Large Population-Based Study: The Wakayama Spine Study. *Pain Ther* **11**, 57–71 (2022). doi: 10.1007/s40122-021-00337-x.
31. Teraguchi, M. *et al.* Prevalence and distribution of intervertebral disc degeneration over the entire spine in a population-based cohort: the Wakayama Spine Study. *Osteoarthritis Cartilage* **22**, 104–110 (2014). doi: 10.1016/j.joca.2013.10.019.
32. Abraham, E., Arcaroli, J., Carmody, A., Wang, H. & Tracey, K. J. Cutting edge: HMG-1 as a mediator of acute lung inflammation. *The Journal of Immunology* **165**, 2950–2954 (2000). doi: 10.4049/jimmunol.165.6.2950.
33. Andersson, U. & Erlandsson-Harris, H. HMGB1 is a potent trigger of arthritis. *J Intern Med* **255**, 344–350 (2004). doi: 10.1111/j.1365-2796.2003.01303.x.
34. Rice, J. W. *et al.* Small molecule inhibitors of Hsp90 potentially affect inflammatory disease pathways and exhibit activity in models of rheumatoid arthritis. *Arthritis & Rheumatism: Official Journal of the American College of Rheumatology* **58**, 3765–3775 (2008). doi: 10.1002/art.24047.
35. Tsung, A. *et al.* The nuclear factor HMGB1 mediates hepatic injury after murine liver ischemia-reperfusion. *J Exp Med* **201**, 1135–1143 (2005). doi: 10.1084/jem.20042614.
36. Koreckij, T. *et al.* Prospective, randomized, multicenter study of intraosseous basivertebral nerve ablation for the treatment of chronic low back pain: 24-Month treatment arm results. *North American Spine Society Journal (NASSJ)* **8**, (2021). doi: 10.1016/j.xnsj.2021.100089.
37. Mengis, T. *et al.* Bone marrow stromal cells in Modic type 1 changes promote neurite outgrowth. *Front Cell Dev Biol* **11**, (2023). doi: 10.3389/fcell.2023.1286280.



# Appendix

## Acknowledgments

This dissertation was made possible by the invaluable support of many individuals, both inside and outside the lab, and I would like to take a moment to acknowledge them here.

Foremost, I would like to thank Oliver Distler for granting me the opportunity to join the Center of Experimental Rheumatology already as a master's student, and subsequently enabling me to pursue my doctoral studies within the same environment. Oliver's contributions during lab and committee meetings consistently steered progress in the right direction.

I also extend sincere appreciation to the other committee members, Sibylle Grad and Christian Stockmann. Their guidance and perspectives from outside the group during the committee meetings each year were incredibly valuable. They played an important role in shaping the project and their input enhanced the quality of the work significantly.

My deepest gratitude goes to my supervisor, Stefan Dudli, who initially welcomed me into his research group for a short semester project as a master's student even though I did not possess any prior lab experience. Since then, he has been guiding me through this research journey, supporting my transition to a PhD, and now even offering me the opportunity to embark on my Post-Doc journey within his group. It is therefore clear that joining the Dudli Lab marked a pivotal moment in my academic journey, affirming that this is what I want to do and where I can thrive. Stefan's mentoring approach, characterized by openness to diverse ideas and guiding by asking just the right questions, nurtured my growth in basic research. His meticulous review of abstracts and papers, which (although sometimes scary to look at because of all the red markings), has been an invaluable source of learning, constantly shaping my understanding and improving my work. I am very grateful for his unwavering support and mentorship, which has exceeded all my expectations.

I am also truly thankful to Irina and Nick, with whom I formed a friendship I never thought possible. Irina, who was the sole PhD candidate when I arrived, welcomed me with such warmth and hospitality that I immediately felt at home at Balgrist. Without her encouragement to pursue a PhD and her knowing this was the right thing for me even before I realized it myself, I wouldn't be where I am today, doing what I love. But also, Nick was always there, ready to lend a hand whenever needed. Not only did he patiently teach me various lab techniques, but his unwavering support was a constant source of encouragement. I also want to thank Jan, with whom I'm excited to embark on several exciting projects in the coming year. Additionally, I extend my thanks to the entire Dudli Lab, including Danilo, Fritzi, Melina, Phelipe, but also all the students who were here throughout this time and contributed to making the lab such a vibrant and enjoyable environment to work in.

The work would also not have been possible without the spine surgeons at the Balgrist University Hospital including Prof. Mazda Farshad, Christoph Laux and many more making it possible for us to receive fresh discs, endplates and even bone marrow biopsies. Additionally, all the individuals working at the Balgrist Campus, including everyone from the Snedeker Lab, as well as our fellow colleagues in cell culture from the

Kispi, contributed to making each day unique and memorable here at Balgrist and I look forward to many more of those.

Besides the incredible support from everyone in the lab, I was fortunate to have unwavering and constant support at home. Philippe stood by me through thick and thin, providing me with the greatest support imaginable. Every evening, he took the time to listen to every detail of my projects, demonstrating such dedication that he could probably start researching Modic changes himself at this point.

Finally, I want to thank my parents and my sister, Sarah. Their unwavering belief in me, regardless of the path I chose, has been a constant source of strength and encouragement. Without their support, this entire academic journey would have been simply impossible.

# Curriculum Vitae



# TAMARA MENGIS

---

📅 12.07.1995 | ✉ tamara.mengis@usz.ch | 📞 +41 79 890 7355

---

## Personal information

Tamara Mengis  
Lärchenstrasse 6M  
8953 Dietikon  
Switzerland  
OrcID: 0009-0000-5595-5224

---

## Education

May 2021 – May 2024 | University of Zurich, Zürich, Switzerland  
PhD Candidate in Biomedicine

-----

September 2019 – April 2021 | ETH zurich, Zürich, Switzerland  
Master of Science in Health Science and Technology  
Specialization in Molecular Health Sciences

-----

September 2016 – September 2019 | ETH zurich, Zürich, Switzerland  
Bachelor of Science in Health Science and Technology

-----

August 2011- December 2015 | Gymnasium Münchenstein, Switzerland  
Eidgenössische Matura

-----

September 2012- June 2013 | Andover high school, USA  
High School Diploma

---

## Experience

May 2021- May 2024 | PhD candidate, University of Zurich

Center of Experimental Rheumatology | University Hospital Zurich and  
Balgrist University Hospital

Supervisor: Prof. Dr. Oliver Distler and PD Dr. Stefan Dudli

-----

September 2019 - April 2020 | Master thesis, University of Zurich  
Department of Pharmacology and Toxicology  
Supervisor: Prof. Dr. Schwank and Dr. Patrik Simmler

---

---

September 2019 - March 2020 | Lab internship

University of Zurich

Center of Experimental Rheumatology | University Hospital Zurich and  
Balgrist University Hospital

Supervisor: Prof. Dr. Oliver Distler and PD Dr. Stefan Dudli

---

Other work  
experience

2017 – 2020 | Temporary Bakery Sales Employee

2017 – 2020 | Teaching assistant

2014 – 2016 | Referee for the Swiss Football Association

2013 – 2018 | Waitress at TempStaff AG, Volkshaus Basel and Käfer AG

Personal skills

Software skills:

- Programming in Python, R, Java and Matlab

Laboratory skills:

- Mass spectrometry including N-Terminomics
- 2D & 3D cell culture
- Flow cytometry
- Histologic tissue processing
- Gene transduction and transfection
- Widefield microscopy

Languages (ILR scale):

- German (Native)
- English (Bilingual Proficiency)
- French (Elementary Proficiency)

---

Teaching

Teaching assistant | University of Zurich

Programming in Biology for 2<sup>nd</sup> year bachelor students

-----

Life science learning center instructor | University of Zürich

Matura student's lab introductory modules

-----

Block course teaching | University of Zurich

Block course teaching assistance and experiment preparation

-----

Teaching assistant | ETH Zurich

Introduction to programming

---

memberships in  
scientific  
committee

Orthopedic Research Society (ORS)

---

Conference  
participations

Conference attendance:

2022 ECM Conference | Davos, Switzerland – Poster presentation

2023 ORS Conference | Dallas, Texas, USA – Poster presentation, flash talk

---

---

2023 ISSLS Spine Week | Melbourne, Australia – Poster presentation

---

Awards

AO Poster Award | ECM Conference 2022

ISSLS Young Investigator Travel Grant | 2023

University of Zurich Biomed Travel Grant | 2023

Hartmann Müller Stiftung Travel Grant | 2023

---

Certificates

TRREE training program in research ethics evaluation

Introductory Course in animal laboratory science (LTK module 1)

---